Detecting the North Atlantic Right Whale using Satellite Imagery

Matus Hodul

Thesis submitted to the
University of Ottawa
in partial Fulfillment of the requirements for the
Doctorate in Philosophy

Department of Geography
Faculty of Arts
University of Ottawa

Abstract

The North Atlantic right whale (*Eubalaena glacialis*) is critically endangered, with only about 370 individuals remaining. Modern conservation efforts rely on accurate knowledge of their location and movements, and, while established surveying methods such as aerial survey flights produce high-quality data for this purpose, they can be costly and are unable to cover large areas. Satellite imaging has been proposed as an additional tool to aid in the detection and monitoring of the whales, allowing for much broader coverage at a lower cost, though at a reduced accuracy. This thesis describes the first attempts at observing the North Atlantic right whale in satellite imagery, and the development of an automated detector model, including a new form of training data.

On April 24$^{\text{th}}$, 2021, concurrent WorldView-3 satellite imagery and aerial photographs were acquired in Cape Cod Bay, Massachusetts. Ideal environmental conditions and an abundance of whales in the area resulted in 39 whale observations in the imagery, which were confirmed by the aerial survey. It was demonstrated that North Atlantic right whales were fairly easily visible in 30 cm and 15 cm satellite imagery, and that they were able to be identified on a species level due to visible markings unique to the right whale.

While right whales are often easily visible in such satellite imagery, visually identifying whales in a large number of images would be a very slow and tedious task. To develop an automated whale detector model, a large number of examples of right whales in satellite imagery are needed to allow the model to "understand" all the different ways a whale can look in such imagery However, at the time only the 39 observations mentioned above were available. Here, aerial photographs were modified to resemble satellite imagery using a deep learning approach called *Neural Style Transfer* (NST), in which the *style* of an existing satellite image of a right whale is transferred to the content of an aerial photograph. A unique set of satellite/aerial 'reference pairs' was developed, allowing for direct comparison between actual satellite imagery and the newly developed 'satellite-like' NST images using image similarity metrics. This demonstrated that the NST images were significantly more similar to satellite imagery than unmodified aerial photographs, and allowed for the immediate increase of examples of right whales in 'satellite imagery' from 39 to many thousands.

The NST images were directly compared to other types of training imagery, including unmodified aerial photographs, colour-normalized aerial photographs, and satellite imagery itself, by training a detector model using each of these

training data types and comparing detection accuracies between them. It was found that models trained on NST simulated images slightly outperformed those trained on colour normalized photographs, while both significantly outperformed unmodified aerial photographs. Models trained on satellite imagery had an excellent precision but rather poor recall, likely due to the small amount of training data relative to the other datasets. These results indicate that performing some type of preprocessing modification to aerial photographs before training is highly desirable, though the trade-off between a slight increase in accuracy with NST and the significantly lower preprocessing time with colour normalized photographs will be a decision point for the end user.

Acknowledgements

First and foremost, I would like to thank Dr. Anders Knudby for giving me the opportunity to complete my Ph.D. under his excellent guidance. Anders has always been extremely supportive of my academic efforts, and has been an invaluable help during my Ph.D. program, as well as before, during my M.Sc. and when I worked with him during my undergrad at Simon Fraser University.

I would also like to thank my thesis committee members Dr. Luke Copland and Dr. Michael Sawada for their advice and guidance in completing this project. I am grateful to Stephen Bird for putting together the SARDA crew and leading the effort to get us funding. Without his contributions, none of this work would have been possible. I also thank the Canadian Space Agency and Transport Canada for providing funding through their smartWhales program.

As always, thank you to Mr. Bolognese for being the best high school geography teacher on the planet, and for inspiring me to study geography in university.

Finally, I would like to thank Elizabeth and Lille. I love you both.

This thesis is dedicated to Helena Valachova and Jan Valach.

Contents

Chapter 1

Introduction

The North Atlantic right whale, *Eubalaena glacialis*, is Critically Endangered (Cooke 2020), with a global population that is declining and estimated at approximately 372 animals (Pettis and Hamilton 2025; count as of September 2024). Whaling, banned in US and Canadian waters in 1935, reduced the population from at least several thousand to probably less than 100 animals over a period spanning hundreds of years (Aguilar 1986; Reeves 2001). Human impacts on right whales continue today, directly through vessel strikes and entanglement in fishing gear, and indirectly through other causes such as climate-induced changes to prey distribution (Meyer-Gutbrod et al. 2021; Chust et al. 2013), increasing biotoxin loads in coastal waters (Doucette et al. 2006), and noise pollution (Parks et al. 2003).

Current conservation measures aim to balance the need for protecting right whales and maintaining commercial activities by creating dynamic protection zones, the locations and extents of which are modified based on whale movements (Davies and Brillant 2019; Hausner et al. 2021). The effectiveness of this approach relies crucially on the ability to detect right whales as quickly, completely and accurately as possible.

At present, right whales are detected based on visual observations from aircraft, boats, and occasionally drones, with additional detections from static and dynamic acoustic instruments (Baumgartner et al. 2020), but none of these solutions are ideal on their own. Aerial reconnaissance includes a level of risk (NARWC 2003), and it is difficult to search a large ocean for individual or small groups of whales, whose colour is similar to the ocean and who frequently dive beneath the surface (Brown et al. 2007). Acoustic detections rely on vocalization, do not indicate the exact location of the detected whale(s), and are not able to establish group size, limiting their use for introducing Dynamic Management Areas (DMAs). Telemetry tags are not typically used because they either cause trauma to the whale if implanted or are not sufficiently durable if attached externally (Moore et al. 2012). Satellite imagery may therefore complement other methods of right whale detection, covering large ocean areas relatively cheaply, with daily or near-daily revisit time. It is important to note

here that satellite data is intended as an *additional tool* in the toolbox of whale surveying and detection, and is not intended to replace any of the existing survey methods.

After Abileah (2002) initially demonstrated the potential to observe large marine mammals in high-resolution satellite imagery, Fretwell et al. (2014) identified 55 "probable" and 23 "possible" Southern right whales (*E. australis*) in a single WorldView-2 image covering part of Golfo Nuevo Bay, Argentina, based on visual image interpretation. Similarly, Cubaynes et al. (2019) visually identified a total of 211 whale-like objects in four WorldView-3 images from Hawaii, western Mexico, southern France, and Argentina. Further studies have been done since the beginning of work on this thesis, and are discussed in detail in the relevant chapters. These studies demonstrate the fundamental feasibility of space-based whale detection with high-resolution optical satellite imagery, but also illustrate some of the challenges.

Several whale species, including the Southern right whale, have a skin colour that is similar to the ocean background against which the whales must be detected (Cubaynes et al. 2019), and even slightly submerged whales therefore likely go undetected. While satellite-based detection of whale-like objects is clearly possible, species identification has not been demonstrated despite the existence of species-specific characteristics related to body size, shape and coloration; both of the above-mentioned studies relied on imagery from locations and times at which the presence of non-target species was unlikely. Importantly, neither study used coincident field observations to assess the identity of ambiguous whale-like objects.

This thesis presents work done beginning in the last few months of 2020, a time when the field of satellite detection of whales was still in its infancy. Our research group, along with two other groups which made up the 'smartWhales' initiative of the Canadian Space Agency, were tasked with performing preliminary research into, and developing automated detectors to find right whales in satellite imagery. Here, I present some of the results from that effort, the work from which contributed to my Ph.D. thesis.

Broadly, the thesis begins by presenting the first ever satellite observations of the North Atlantic right whale, and showing that species distinction is possible in the imagery. Next, the thesis tackles the problem faced by so many automated machine-learning approaches —not enough training data— by creating a simulated dataset of satellite observations from existing abundant aerial photographs. Finally, the thesis pits this new dataset in competition with the currently accepted methods of training whale detectors, to examine which method yields the most accurate detector models.

1.1 Research Objectives and Thesis Structure

The gaps in right whale survey capabilities outlined above motivate the following research objectives:

1.1.1 Research Objectives

1. **Identify and confirm North Atlantic Right Whales in satellite imagery:** Acquire satellite imagery at a location and time likely to contain right whales, manually locate the whales in the imagery, and confirm observations with field survey. Use these observations to determine to what extent it is possible to distinguish whales from other marine mammals, and right whales from other species of whales. Note that at the time when preliminary work began on this research, in early 2019, satellite observations of the Southern right whale had not yet been published, so our research objectives still included whether or not right whales could be observed using satellites at all.

2. **Solve the problem of a limited training data set for whale detection:** Due to the rarity of satellite observations of the North Atlantic right whale, there is a significant lack of data for training whale detector models. Develop a method for increasing the available training data by simulating satellite imagery from other sources.

3. **Compare the new training dataset to existing types of training data to determine which type yields the best results:** Using a standardized whale detection model, test several types of training data, including those currently used in the field and the new dataset developed here. Assess model performance for each dataset and compare them.

1.1.2 Outline of the Ph.D. Thesis

This thesis is written in an article format with three papers, preceded by a literature review on the North Atlantic right whale, focusing on the biology and natural history of the whale. Because each of the three main papers/chapters will contain literature reviews relevant to satellite detection of whales, this topic will be kept brief in the main literature review.

The three papers correspond to the three research objectives outlined above:

1. **Paper 1:** *Individual North Atlantic Right Whales Identified From Space* uses coincident field survey data and satellite imagery of Cape Cod Bay on April 24^{th}, 2001 to confirm that right whales are visible from satellite imagery, and distinguishable on a species level from other whales. The paper also presents some ground-breaking findings on the capability of satellite imagery for individual-level identification in special circumstances. This paper was published in Marine Mammal Science in 2022.

2. **Paper 2:** *Simulating Satellite Imagery from Aerial Photographs using Neural Style Transfer* details the novel application of an existing machine learning algorithm to simulate satellite imagery from aerial photographs of right whales. Given the extreme rarity of satellite observations of right whales, but the relative ubiquity of aerial photographs of them, a method

to simulate satellite imagery from these abundant photographs is developed here. Image similarity metrics are used to demonstrate the success of the simulation procedure. This paper has been accepted in Marine Mammal Science and is currently undergoing revisions.

3. **Paper 3:** *Comparison of Training Imagery Types for Satellite Detections of North Atlantic Right Whales* performs an experiment in which types of data commonly used in the field for training whale detectors, and the novel dataset developed in Paper 2, are compared. The performance of each model is assessed, and the benefits and drawbacks of each type of training dataset are discussed in detail. This paper has not yet been submitted for publication.

The conclusion has been written in a more free-flowing story format, describing our research from a personal point of view, though still including major findings. Because an article-format thesis can be quite repetitive, I decided that such a format would bring a fresh point of view not yet exhaustively covered by the many abstracts, introductions, and paper conclusions herein.

1.2 Funding and the smartWhales Program

The research within this thesis is part of, and funded by, a broader research program called "smartWhales", which was run by the Canadian Space Agency, and supported by Transport Canada and the Department of Fisheries and Oceans (DFO). The smartWhales program provided a total of $5.3 million to five industry-academic partner groups for the purposes of developing novel right whale monitoring strategies, divided into two streams: detection and monitoring, and prediction and modelling.

Our team, headed by Fluvial Systems Research Inc. (Surrey, BC), and including University of Ottawa (Ottawa, ON), Canadian Whale Institute (Welshpool, NB), and INSARSAT Inc. (Dunham, QC), was awarded $1.2 million in the *Detection and Monitoring* stream to develop a method for right whale detection using satellite imagery. Our collective team name was SARDA, or the "Satellite Acquisition and Right Whale Detection Algorithm", which is also the name given to right whales by the 11th century Basque whalers (Figure 1.1) who helped hunt the whale nearly to extinction.

1.3 A Note on Terminology

A note on terminology used throughout the thesis:

Unless otherwise explicitly stated, "right whale" will refer to the North Atlantic right whale, *Eubalaena glacialis*. If the Southern right whale or North Pacific right whale are mentioned, their names will always be written out in full. None of the geographic ranges of the three varieties of right whale overlap.

Generally, "imagery" will be used to refer to satellite imagery, and "photographs" will be used to refer to aerial photographs. "Images" will be used to refer to a more generic concept describing pictures in general as well as products derived from aerial photographs, such as the "satellite-like" simulated images created using the NST method.

1.4 References

Abileah, R. 2002. Marine mammal census using space satellite imagery. U.S. Navy Journal of Underwater Acoustics, 52(3), 709-724.

Aguilar, A. 1986 A review of old Basque whaling and its effect on the right whales of the North Atlantic. Report International Whaling Commission, 10, 191-199

Baumgartner, M. F., Bonnell, J., Corkeron, P. J., Van Parijs, S. M., Hotchkin, C., Hodges, B. A., Thornton, J. B., Mensi, B. L., and Bruner, S. M. 2020. Slocum gliders provide accurate near real-time estimates of baleen whale presence from human-reviewed passive acoustic detection information. Frontiers in Marine Science, 7, 100. https://doi.org/10.3389/fmars.2020.00100

Brown, M.W., Kraus, S.D., Slay, C.K., and Garrison, L.P. 2007. Surveying for Discovery, Science, and Management. The Urban Whale: North Atlantic Right Whales at the Crossroads, ch4. Harvard University Press, Cambridge, MA.

Chust, G., Castellani, C., Licandro, P., Ibaibarriaga, L., Sagarminaga, Y., and Irigoien, X. 2013. Are Calanusspp. shifting poleward in the North Atlantic? A habitat modelling approach. ICES Journal of Marine Science, 71(2), 241-253. https://doi.org/10.1093/icesjms/fst147

Cooke, J.G. 2020. Eubalaena glacialis (errata version published in 2020). The IUCN Red List of Threatened Species 2020: e.T41712A178589687. https://dx.doi.org/10.2305/IUCN.UK.2020-2.RLTS.T41712A178589687.en

Cubaynes, H.C., Fretwell, P.T., Bamford, C., Gerrish, L., and Jackson, J.A. 2019. Whales from space: Four mysticete species described using new VHR satellite imagery. Marine Mammal Science, 35(2), 466-491. https://doi.org/10.1111/mms.12544

Davies, K.T.A., and Brillant, S.W. 2019. Mass human-caused mortality spurs federal action to protect endangered North Atlantic right whales in Canada. Marine Policy, 104, 157-162. https://doi.org/10.1016/j.marpol.2019.02.019

Doucette, G.J., Cembella, A.D., Martin, J.L., Michaud, J., Cole, T.V.N., and Rolland, R.M. 2006. Paralytic shellfish poisoning (PSP) toxins in North Atlantic right whales Eubalaena glacialis and their zooplankton prey in the Bay of Fundy, Canada. Marine Ecology Progress Series, 306, 303-313. doi:10.3354/meps306303

Figure 1.1: Basque whaling of the "sarda". Pierre-Jacob Guéroult du Pas, 1710.

Fretwell, P.T., Staniland, I.J., and Forcada, J. 2014. Whales from Space: Counting Southern Right Whales by Satellite. PLoS ONE, 9(2). https://doi.org/10.1371/journal.pone.0088655

Hausner, A., Samhouri, J.F., Hazen, E.L., Delgerjargal, D., and Abrahms, B. 2021. Dynamic strategies offer potential to reduce lethal ship collisions with large whales under changing climate conditions. Marine Policy, 130, 104565. https://doi.org/10.1016/j.marpol.2021.104565

Meyer-Gutbrod, E.L., Greene, C.H., Davies, K.T.A., and Johns, D.G. 2021. Ocean regime shift is driving collapse of the north atlantic right whale population. Oceanography, 34(3), 22-31. https://doi.org/10.5670/oceanog.2021.308

NARWC. 2003. Tragedy. Right Whale News, 10(1), 1-3. https://www.narwc.org/uploads/1/1/6/6/116623219/rwfeb03.pdf

Moore, M., Andrews, R., Austin, T. Bailey, J., Costidis, A., George, C., Jackson, K., Pitchford, T., Landry, S., Ligon, A., McLellan, W., Morin, D., Smith, J., Rotstein, D., Rowels, T., Slay, C., and Walsh, M. 2012. Rope trauma, sedation, disentanglement, and monitoring-tag associated lesions in a terminally entangled North Atlantic right whale (Eubalaena glacialis). Marine Mammal Science, 29(2). DOI:10.1111/j.1748-7692.2012.00591.x

Parks, S.E. 2003. Acoustic communication in the North Atlantic right whale (Eubalaena glacialis). Thesis: Massachusetts Institute of Technology. https://hdl.handle.net/1912/2453

Pettis, H.M., and Hamilton, P.K. 2025. North Atlantic Right Whale Consortium 2024 Annual Report Card. Report to the North Atlantic Right Whale Consortium. https://www.narwc.org/uploads/1/1/6/6/116623219/2024reportcardfinal.pdf, accessed 2025-08-16.

Reeves, R.R. 2001. Overview of catch history, historic abundance and distribution of right whales in the western North Atlantic and in Cintra Bay, West Africa. J. Cetacean Res. Manage., 2, 187-192.

Chapter 2

The North Atlantic Right Whale

Figure 2.1: The North Atlantic Right Whale. Image: NOAA Fisheries.

2.1 Biology

This section provides a brief overview of the North Atlantic right whale's appearance, life cycle, and behaviour. For greater detail, I suggest reading the excellent book *The Urban Whale*, written by many of the authors cited below. While interesting in its own right, the whale's biology is necessary to consider while attempting to develop novel detection methods. For instance, what does a right whale look like, and how can we distinguish it from other whales in the area? What visual features of a right whale might be visible in satellite imagery? Where are right whales likely to be at any given time during the year? What whale behaviour is most likely to lead to a successful survey detection?

2.1.1 Appearance

The North Atlantic right whale is among the largest whales; adults weigh approximately 36,000 kg and have a body length of 13 m to 14 m. Adult males tend to be slightly smaller than adult females (Fortune et al. 2021), and calves are born at around 5 m long (Patrician et al. 2009). Modern right whales appear to be smaller than their pre-1980s counterparts by about 7%, or 1 m of length, likely due to modern environmental stressors. This reduced size is especially notable for individuals who experienced entanglement early in life (Stewart et al. 2021).

Their bodies (Figure 2.1, above) are black or very dark grey in colour, and quite wide relative to their length, giving them an almost oval appearance. They notably lack a dorsal fin, which is unique among whale species in their geographic range. The most prominent visible markings are white patches on the top of the head, above the eyes, and on the chin and lips. In these areas, named callosities, rough spikes of skin tissue are infested with white or cream-coloured whale lice, or cyamids (Kaliszewska et al. 2005), giving them their contrasting colour (Figure 2.2). Newborn calves have callosities upon birth, but they are not yet populated by cyamids (Foley et al. 2011) and thus have no white markings. They gain cyamids over the first several months of life, beginning at the lips within 6 to 15 days after birth (Patrician et al. 2009), receiving them directly through physical contact with their mothers (Kaliszewska et al. 2005).

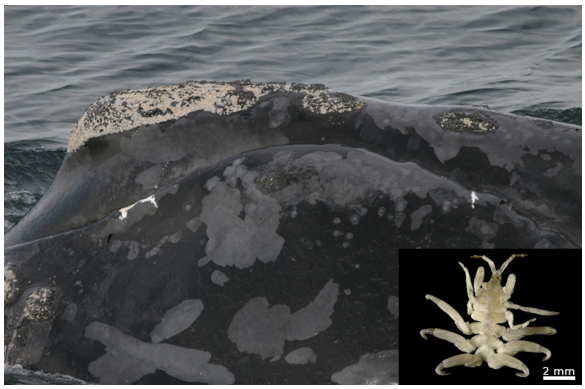

Figure 2.2: Callosities are visible on this right whale's head as the rough, columnar structures of hardened black skin that are populated by white or cream-coloured whale cyamids (inset), each of which are about the size of a pinkie fingernail (5-12 mm). Whale image from NOAA Photo Library, cyamid inset © Hans Hillewaert under Creative Commons.

The particular shape and pattern of these callosities are unique to each individual whale and stable over time, allowing for individual identification (Figure 2.3a). Scars from boat impacts and entanglements will heal white, allowing an additional level of unique patterning that allows for individual identification (Figure 2.3b). These two unique patterns, callosities and scars, are the primary methods used to identify individual whales in the North Atlantic Right Whale Catalog (https://rwcatalog.neaq.org).

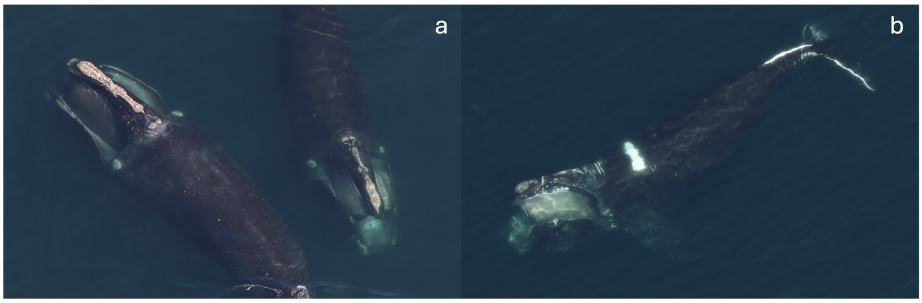

Figure 2.3: Callosities, (a) the patterns of rough patches of skin around a right whale's head, which are infested with white whale lice, are unique to each whale, allowing for individual identification of whales from photographs. Notice the difference in callosity pattern between these two whales. (b) Scars heal white, and often result in unique patterns, helping with individual identification. Center for Coastal Studies NOAA federal permit #19315–01.

2.1.2 Life Cycle and Range

Right whale calves are born in the coastal waters between Brunswick, Georgia and Cape Canaveral, Florida (Figure 2.4) between December and March, with births peaking in January and February (Zani et al. 2008). Here, the mothers nurse the calves by converting stored blubber into milk, allowing calves to grow very rapidly (Fortune et al. 2012) while the mothers eat nothing themselves (Hamilton and Cooper 2010). In the early spring, once the calves are strong enough for prolonged swimming, the mother/calf pairs travel north, keeping within 30 nautical miles of the coast (Firestone et al. 2008).

Their destination is Cape Cod Bay or the Great South Channel, where their primary food, the copepod *Calanus finmarchicus*, is abundant at the surface and easy to catch (Mayo et al. 2018). Here, the mothers will feed for the first time since giving birth and teach the calves the technique of skim-feeding by opening their mouths and gliding along the surface to gather the tiny zooplankton, though they will not be weaned for several more months or possibly up to a year (Hamilton and Cooper 2010). They then move farther north into the Bay of Fundy and Roseway Basin, and more recently into the Gulf of St. Lawrence, following the copepods into the summer feeding grounds, where they stay during the summer and fall months (Baumgartner and Mate 2005; Meyer-Gutbrod et al. 2023).

About one-third of the whale population do not go to the Bay of Fundy and Roseway Basin, and are thus referred to as the "Non-Fundy Right Whales", though it is not known where exactly they go (Schaeff et al. 1993; Cole et al. 2013). The divide appears to be familial, thus a whale brought to Fundy as a calf will in turn bring her calves to Fundy as well.

Approaching winter, pregnant whales travel back south to the calving grounds off Florida and Georgia to begin the cycle again; higher ocean temperatures farther south prevent them from traveling much past this region (Keller et al. 2006). However, the majority of the whales don't travel to the calving grounds, and until recently it was not known where this portion of the population went in

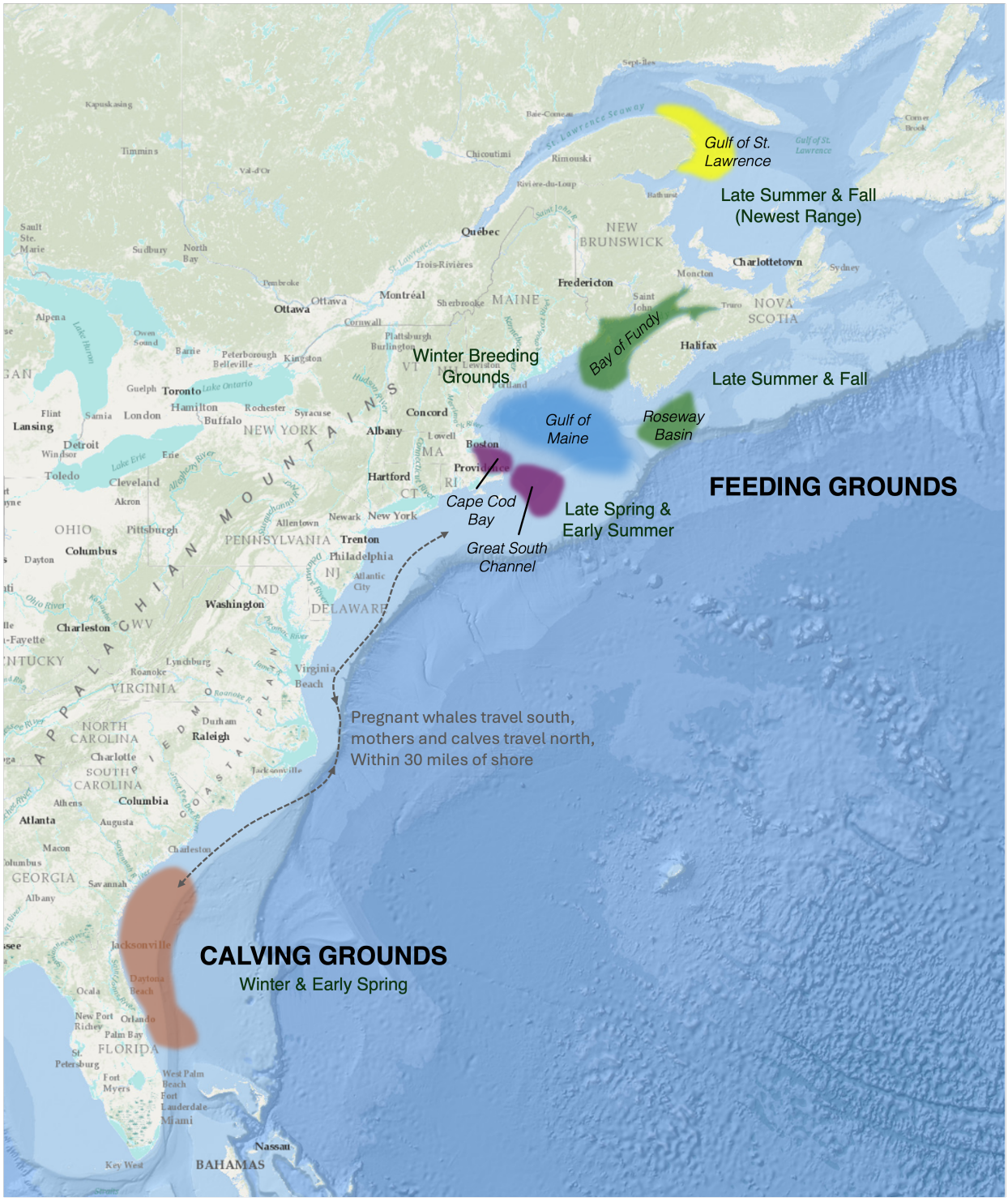

Figure 2.4: Map of the North Atlantic right whale's movements within its primary range on the east coast of North America. *Right whale movement sources described in text below. Basemap sources: Esri, GEBCO, NOAA, National Geographic, DeLorme, HERE, Geonames.org, and other contributors.*

the winter (Kraus and Rolland 2007). This was of great concern to conservation efforts, since it was thought that mating occurred during this period, making it important to protect the mating grounds. Recent evidence strongly suggests that the wintering ground is in the Gulf of Maine, and it appears that mating does indeed occur here (Cole et al. 2013).

2.1.3 Food and Feeding Behaviour

The primary food source for the North Atlantic right whale is the zooplankton *Calanus finmarchicus* (Figure 2.5), a tiny (2-3 mm long) zooplankton (Baumgartner et al. 2007), though other species of Calanus are also eaten (Sorochan et al. 2021). To capture their prey, right whales open their mouths while swimming slowly forward, exposing large baleen strips which are used to filter the copepods from the water. Because of the large surface area exposed when feeding, requiring a significant amount of force to drive through the water, the whales swim very slowly while feeding, thus limiting their prey to very small zooplankton; larger species are able to swim away before being captured. The life-cycle of *C. finmarchicus* informs the feeding behaviour of the whales: in late winter and early spring, the copepods come to the surface to feed on phytoplankton blooms, where right whales skim-feed along the surface, then as phytoplankton supplies diminish, the copepods sink back down to the relative safety of deeper waters, where right whales dive to feed on them, having been observed diving up to 200 m (Baumgartner and Mate 2003).

Figure 2.5: The right whale's primary source of food: Calanus finmarchicus. Photo: "Calanus finmarchicus" by Michael Bok, CC BY-NC-SA 2.0

2.2 Human Interaction

While the hunting of the North Atlantic right whale was banned internationally in 1935 and whaling is no longer a serious threat to the species, the thousand-year history of the practice nearly caused the extinction of these whales. From

their lowest numbers of less than 100 individuals just before the whaling ban took effect (Reeves 2001), right whales have since struggled to recover their numbers due to a host of modern mortality issues, primarily ship strikes and entanglement.

2.2.1 Whaling

North Atlantic right whales are known to have been hunted as far back as 1059 by Basque fishermen operating from small, open-top boats after spotting the whales from shore (Aguilar 1986). As the Basque whaling boats got larger, operations extended farther from shore, especially once processing of the catch was being done onboard, allowing for multiple (perhaps up to seven) whales to be caught, processed, and stored in one voyage.

In the 1700s, whaling for the right whale peaked along the North American coast, where it first acquired its name, purportedly for being the "right" whale to catch because its rich blubber content made it extremely lucrative to hunt, its docile nature and slow surface swimming made it relatively easy to kill, and its propensity to remain afloat once killed allowing for easy processing. While quite a tidy explanation for the "right" name, it is equally as likely that the term "right" was used at the time in a way similar to "typical", as these were considered ordinary, common whales. The true origin of the name has been lost to time (Dolin 2007).

The last North Atlantic right whale was hunted in the United States on 31 March 1935 and the population had reached its lowest point, after which the International Convention for the Regulation of Whaling was signed into effect, banning whaling of the species. It is debated exactly how many right whales were left at this time, but it is generally considered to be less than 300, and possibly less than 100 (Reeves 2001).

Today, while deliberate hunting of the right whale has stopped, their population is still in peril, now due to the complexities of living in some of the busiest waterways in the world: the Eastern Seaboard of North America. Here, they encounter pollution, disruptive noise, numerous shipping lanes, and dense fisheries.

2.2.2 Modern Mortality

The major mortality sources for right whales in the modern day are ship strikes and entanglement in fishing gear; of the two, entanglement is the slightly more frequent killer. For instance, Knowlton and Krauss (2001) found that between 1970 and 1999, 55.4% of necropsied whales were found to have been killed by entanglement, and 44.6% by ship strikes; similarly, Sharp et al. (2019) found that between 2003 and 2018, 57.9% were killed by entanglement and 42.1% by ship strikes. Entanglement, when not immediately fatal, is also known to cause severe stress on the whale involved, resulting in a range of detrimental outcomes, such as emaciation due to the physical effort of dragging the attached fishing gear for months or even years (Moore et al. 2021).

The fishing gear of most concern are types which extend a vertical line from a float on the surface to a weight on the sea floor, multiple of which are typically arrayed in a small area, causing the whale to become entangled (Hamilton and Krauss 2019). Upon initial entanglement, the whale may begin to thrash about or roll, further wrapping the line around themselves (Howle et al. 2013). The whale then begins to drag the entangled line (Figure 2.6), often with the float and trap still attached at either end and often for months, and eventually dies from emaciation (van der Hoop et al. 2016) due to the effort. Even whales which are freed from entanglement by rescue crews may die days later due to stress and emaciation (Moore et al. 2013).

Figure 2.6: An entangled right whale. Image from the Kaggle right whale dataset (Image: Khan and Shashank 2015).

Though ship strikes are a common threat to most large whales, right whales are particularly susceptible due to their large body size, slow swimming speed, tendency to swim close to the surface for feeding, and presence in areas with a high vessel traffic (Wiley et al. 2016). Vessel speed and size contribute to the potential lethality of a ship strike (Conn and Silber 2013).

Indirect contributors to right whale mortality act as stressors on the whales, affecting their reproduction, growth, and ability to recover from injury. These include noise pollution and toxins in the water caused by their proximity to the industry-heavy eastern seaboard, and climate-induced shifts in the distribution and behaviour of their prey.

Noise pollution can mask the low-frequency noises produced by right whales to communicate and attract mates: the frequency of the under-water sound of a large motorized vessel is remarkably similar to the frequency of right and other baleen whale calls, meaning that a passing vessel will obscure or distort a right whale's calling sound, preventing it from maintaining the long-distance (up to 20 km) communications the whales use to find and keep track of each other while traveling (Clark et al. 2009). Louder, more sudden noises may lead to temporary or permanent hearing loss (Southall et al. 2019), further hindering communication activities, and the overall anthropogenic noise background has

been shown to increase stress for right whales, leading to behavioral changes (Rolland et al. 2012).

Climate change, the warming of ocean waters, is having an effect on the distribution of *Calanus finmarchicus*, which in turn exerts an effect on the movements of right whales seeking their tiny copepod prey. Changing sea surface temperatures, having warmed about 1°C between 1970 and 2004, have led to a poleward shift of *C. finmarchicus* by about 8 km per decade (Chust et al. 2014). Following their food, right whales have also moved poleward. This northward shift in species distribution, bringing them into areas where conservation measures hadn't yet been implemented, is thought to have contributed to the unprecedented mortality event in the summer of 2017, where 12 right whales died in the span of a few months in the Gulf of St. Lawrence (Meyer-Gutbrod et al. 2018). Of the seven whales that underwent necropsies from this event, four were found to have been killed by ship strikes, and two by entanglement in snow crab fishing gear (Daoust et al. 2017).

Right whales are also extremely susceptible to waterborne biotoxins and pollutants; even if the pollutants don't cause mortality directly, they can contribute to the general decline in health and calving rates seen in the population (Doucette et al. 2006). Sources of harmful materials ingested by the whales include neurotoxins produced by the prey of *C. finmarchicus*, which bioaccumulate in the whales through their feeding on the copepods (Leandro et al. 2010). Bioaccumulation of harmful materials can also come from ingestion of anthropogenically created pollutants, such as organochlorides originating from pesticides (Weisbrod et al. 2000).

2.2.3 Conservation Strategies

Conservation strategies to mitigate the two major mortality causes center primarily on identifying specific zones of conflict between human activity and right whales, and applying special rules in those zones depending on the specific nature of the conflict (Davies and Brillant 2019). These zones are typically referred to as Dynamic Management Areas (DMAs) in the United States (Cole and Crowe 2019) and Marine Protected Areas (MPAs) in Canada (Hinch and Santo 2011).

Importantly, these zones must be dynamic to adapt to changes in whale movements throughout their annual migration cycle, but also adapt yearly to broader changes in whale movement caused by climate change (DFO 2018; Crespo et al. 2020; Hausner et al. 2021). For instance, to reduce the risk of vessel strikes, the Government of Canada has implemented seasonal vessel speed restrictions, requiring large vessels to reduce their speed to 10 knots from April to November in the Gulf of St. Lawrence (GSL), where many right whales are found in the summer months (TC 2021). In parts of the GSL vessel speeds are restricted throughout this period, but in other areas they are only triggered for a period of 15 days after a right whale has been detected. Similarly, to reduce the risk of entanglement, a right whale detection can trigger a 15-day closure of fishing with non-tended fixed gear (e.g. for lobster and crab), covering an area

of approximately 2000 km^2 around the position of the detection (DFO 2021). Similar speed and fishery restrictions exist in United States waters, where they are triggered if three or more right whales are within three miles of each other (Cole and Crowe 2019).

2.3 Detection and Monitoring

It thus follows that to successfully implement these protected zones, it is critical to know where right whales are at any given moment — *"In part, migratory critical habitat has not been designated because wildlife managers do not understand exactly when right whales migrate, and through which exact pathways."* (Mullen et al. 2013). To do that, we must be able to find them!

Unlike many other animals whose position is of interest to scientists, radio-tagging is not typically used on right whales, since it has been found to be particularly detrimental to their health (Moore et al. 2013). As a result, non-invasive surveying techniques must be used.

2.3.1 Conventional Survey Methods

Conventional survey methods can be divided into three groups: Shipborne, Aerial, and Acoustic. A fourth method to gather positional data on the whales exists, opportunistic sightings, where a whale is spotted by mariners or even sometimes people on land who aren't otherwise engaged in an organized right whale survey (Lawson et al. 2025). However, due to the limited metadata surrounding such observations, they can be of limited use in organized right whale research (Kenney 2019), and aren't considered an important source of whale location data, except where they reveal a whale to be in an unusual location (Brown et al. 2007).

Both vessel and aerial surveys are conducted by following regular tracklines across the study area, with trained spotters, with or without binoculars, scanning the water for whales (Brown et al. 2007). Once a whale is spotted, the survey craft will typically break away from the trackline in order to approach the whale and take detailed photographs. In the case of shipborne surveys, biological samples may also be taken (Gillett et al. 2010). The right whale's distinct callosity patterns and scars (Figure 2.3), which allow them to be individually identified from photographs, make for a unique opportunity to conduct mark-recapture style population estimates from aerial surveys without needing to interact with or tag the animals, like traditional mark-recapture analysis (Crowe et al. 2021). Observations are generally compiled with the North Atlantic Right Whale Consortium, which also maintains the Right Whale Identification Catalog at https://rwcatalog.neaq.org (Johnson et al. 2021).

Though a large variety of airplanes have been used for right whale surveying, most popular is the Cessna 337 Skymaster; designed specifically for aerial reconnaissance, its ability to fly slowly lends itself to spotting and photographing

Figure 2.7: The Cessna 337 Skymaster used by the Center for Coastal Studies to conduct aerial surveys in Cape Cod Bay in 2021. Note the distinct twin tail design. Photo from CCS Facebook page accessed 29 August 2025.

whales (Brown et al. 2007). Its distinct twin-tail design (Figure 2.7) is notable, and would be reasonably visible in satellite imagery.

More recently, acoustic monitoring has been used to locate right whales, using either stationary (Clark et al. 2010) or mobile hydrophones on submersible autonomous gliders (Baumgartner et al. 2020). Right whales are detected by hearing their distinct calls, which can be automatically identified using software, and can typically be heard from up to about 30 km away from a glider or 15 km from a stationary buoy (Johnson et al. 2022).

2.3.2 Satellite Detection

While these conventional survey methods are extremely accurate, they can be costly, and may not cover as much ocean area as researchers would ideally prefer. Satellite imaging has been used in many research fields to significantly increase the amount of available data to scientists, though due to technological limits in spatial resolution, has only been proposed for wildlife detection somewhat recently. Abileah (2001) published the first observations of whales, possible for the first time due to the newly-launched IKONOS-2 sensor with 1 m panchromatic spatial resolution. Cleverly, they imaged a whale at a SeaWorld park to obtain a confirmed whale observation and also observed some suspected whales in the wild near Hawaii.

The more recent surge of satellite whale observation studies, begun by Fretwell et al. (2014), were made possible thanks to 50 cm WorldView-2 imagery, and continued on with 30 cm WorldView-3 imagery (Cubaynes et al. 2019). Other species, such as polar bears, have also been surveyed using satellite imagery (La Rue et al. 2015). A more detailed review of satellite whale observations is included in the following three chapters. The next chapter demonstrates how a satellite survey of right whales might be conducted, and presents the first ever successful observations of the North Atlantic right whale in satellite imagery, among other exciting firsts in the field of satellite whale detection. Make special note of the airplane shown above in Figure 2.7 —you'll be seeing a satellite

image of it very soon.

2.4 References

Abileah, R. 2001. Marine Mammal Census using Space Satellite Imagery. US Navy Journal of Underwater Acoustics, 52(3), 709-724.

Aguilar, A. 1986. A review of old Basque whaling and its effect on the right whales of the North Atlantic. Report International Whaling Commission, 10, 191-199

Baumgartner, M.F., Mate, B.R., 2005. Summer and fall habitat of North Atlantic right whales (Eubalaena glacialis) inferred from satellite telemetry. Can. J. Fish. Aquat. Sci. 62, 527–543. https://doi.org/10.1139/f04-238

Baumgartner, M.F., Mayo, C.A., and Kenney, R.D. (2007). Enormous Carnivores, Microscopic Food, and a Restaurant That's Hard To Find. In S. D. Kraus and R. M. Rolland (Eds.), The urban whale: North Atlantic right whales at the crossroads (pp. 138-171). Harvard University Press.

Baumgartner, M.F., Bonnell, J., Corkeron, P.J., Van Parijs, S.M., Hotchkin, C., Hodges, B.A., Bort Thornton, J., Mensi, B.L., Bruner, S.M., 2020. Slocum Gliders Provide Accurate Near Real-Time Estimates of Baleen Whale Presence From Human-Reviewed Passive Acoustic Detection Information. Front. Mar. Sci. 7, 100. https://doi.org/10.3389/fmars.2020.00100

Chust, G., Castellani, C., Licandro, P., Ibaibarriaga, L., Sagarminaga, Y., and Irigoien, X. 2013. Are Calanusspp. shifting poleward in the North Atlantic? A habitat modelling approach. ICES Journal of Marine Science, 71(2), 241-253. https://doi.org/10.1093/icesjms/fst147

Clark, C., Ellison, W., Southall, B., Hatch, L., Van Parijs, S., Frankel, A., Ponirakis, D., 2009. Acoustic masking in marine ecosystems: intuitions, analysis, and implication. Mar. Ecol. Prog. Ser. 395, 201–222. https://doi.org/10.3354/meps08402

Clark, C.W., Brown, M.W., Corkeron, P., 2010. Visual and acoustic surveys for North Atlantic right whales, Eubalaena glacialis, in Cape Cod Bay, Massachusetts, 2001-2005: Management implications. Marine Mammal Science 26, 837–854. https://doi.org/10.1111/j.1748-7692.2010.00376.x

Cole, T., Hamilton, P., Henry, A., Duley, P., Pace, R., White, B., Frasier, T., 2013. Evidence of a North Atlantic right whale Eubalaena glacialis mating ground. Endang. Species. Res. 21, 55–64. https://doi.org/10.3354/esr00507

Cole, T., and Crowe, L. 2019. An analysis of dynamic management areas, January 2010 - August 2019, in support of the U.S. take reduction team. Interactive Monthly DMA Analyses, NOAA Fisheries. https://apps-nefsc.fisheries.noaa.gov/psb/surveys/interactive-monthly-dma-analyses/

Conn, P.B., Silber, G.K., 2013. Vessel speed restrictions reduce risk of collision-related mortality for North Atlantic right whales. Ecosphere 4, art43. https://doi.org/10.1890/ES13-00004.1

Crespo, O.G., Mossop, J., Dunn, D., Gjerde, K., Hazen, E., Reygondeau, G., Warner, R., Tittensor, D., Halpin, P., 2020. Beyond static spatial management: Scientific and legal considerations for dynamic management in the high seas. Marine Policy 122, 104102. https://doi.org/10.1016/j.marpol.2020.104102

Cubaynes, H.C., Fretwell, P.T., Bamford, C., Gerrish, L., Jackson, J.A., 2019. Whales from space: Four mysticete species described using new VHR satellite imagery. Marine Mammal Science 35, 466–491. https://doi.org/10.1111/mms.12544

Pace, R.M., Corkeron, P.J., Kraus, S.D., 2017. State–space mark–recapture estimates reveal a recent decline in abundance of North Atlantic right whales. Ecology and Evolution 7, 8730–8741. https://doi.org/10.1002/ece3.3406

Daoust, P.-Y., Couture, E.L., Wimmer, T., and Bourque, L. 2018. Incident Report: North Atlantic Right Whale Mortality Event in the Gulf of St. Lawrence, 2017. Collaborative Report Produced by: Canadian Wildlife Health Cooperative, Marine Animal Response Society, and Fisheries and Oceans Canada. 256 pp.

Davies, K.T.A., Brillant, S.W., 2019. Mass human-caused mortality spurs federal action to protect endangered North Atlantic right whales in Canada. Marine Policy 104, 157–162. https://doi.org/10.1016/j.marpol.2019.02.019

DFO. 2018. Science Advice on Timing of the Mandatory Slow-down Zone for Shipping Traffic in the Gulf of St. Lawrence to Protect the North Atlantic Right Whale. DFO Can. Sci. Advis. Sec. Sci. Resp. 2017/042.

DFO. 2021. 2021 fishery management measures: North Atlantic right whales. Department of Fisheries and Oceans, https://www.dfo-mpo.gc.ca/fisheries-peches/commercial-commerciale/atl-arc/narw-bnan/management-gestion-eng.html, accessed 2021-07-21.

Dolin, E.J. 2007. Leviathan: The History of Whaling in America. WW Norton and Co., New York. 373pp.

Doucette, G.J., Cembella, A.D., Martin, J.L., Michaud, J., Cole, T.V.N., and Rolland, R.M. 2006. Paralytic shellfish poisoning (PSP) toxins in North Atlantic right whales Eubalaena glacialis and their zooplankton prey in the Bay of Fundy, Canada. Marine Ecology Progress Series, 306, 303-313. doi:10.3354/meps306303

Firestone, J., Lyons, S.B., Wang, C., Corbett, J.J., 2008. Statistical modeling of North Atlantic right whale migration along the mid-Atlantic region of the eastern seaboard of the United States. Biological Conservation 141, 221–232. https://doi.org/10.1016/j.biocon.2007.09.024

Foley, H.J., Holt, R.C., Hardee, R.E., Nilsson, P.B., Jackson, K.A., Read, A.J., Pabst, D.A., McLellan, W.A., 2011. Observations of a western North Atlantic right whale (Eubalaena glacialis) birth offshore of the protected southeast U.S. critical habitat. Marine Mammal Science 27, E234–E240. https://doi.org/10.1111/j.1748-7692.2010.00452.x

Fortune, S.M.E., Trites, A.W., Perryman, W.L., Moore, M.J., Pettis, H.M., Lynn, M.S., 2012. Growth and rapid early development of North Atlantic right whales (Eubalaena glacialis). J Mammal 93, 1342–1354. https://doi.org/10.1644/11-MAMM-A-297.1

Fortune, S.M.E., Moore, M.J., Perryman, W.L., Trites, A.W., 2021. Body growth of North Atlantic right whales (Eubalaena glacialis) revisited. Marine Mammal Science 37, 433–447. https://doi.org/10.1111/mms.12753

Fretwell, P.T., Staniland, I.J., Forcada, J., 2014. Whales from Space: Counting Southern Right Whales by Satellite. PLoS ONE 9, e88655. https://doi.org/10.1371/ journal.pone.0088655

Gillett, R.M., Frasier, T.R., Rolland, R.M., White, B.N., 2010. Molecular identification of individual North Atlantic right whales (Eubalaena glacialis) using free-floating feces. Marine Mammal Science 26, 917–936. https://doi.org/10.1111/j.1748-7692.2010.00380.x

Hamilton, P.K., Cooper, L.A., 2010. Changes in North Atlantic right whale (Eubalaena glacialis) cow-calf association times and use of the calving ground: 1993-2005. Marine Mammal Science 26, 896–916. https://doi.org/10.1111/j.1748-7692.2010.00378.x

Hamilton, P., Kraus, S., 2019. Frequent encounters with the seafloor increase right whales' risk of entanglement in fishing groundlines. Endang. Species. Res. 39, 235–246. https://doi.org/10.3354/esr00963

Hausner, A., Samhouri, J. F., Hazen, E. L., Delgerjargal, D., and Abrahms, B. 2021. Dynamic strategies offer potential to reduce lethal ship collisions with large whales under changing climate conditions. Marine Policy, 130, Article 104565. https:// doi.org/10.1016/j.marpol.2021.104565

Hinch, P.R., De Santo, E.M., 2011. Factors to consider in evaluating the management and conservation effectiveness of a whale sanctuary to protect and conserve the North Atlantic right whale (Eubalaena glacialis). Marine Policy 35, 163–180. https://doi.org/10.1016/j.marpol.2010.09.002

Howle, L.E., Kraus, S.D., Werner, T.B., Nowacek, D.P., 2019. Simulation of the entanglement of a North Atlantic right whale (Eubalaena glacialis) with fixed fishing gear. Marine Mammal Science 35, 760–778. https://doi.org/10.1111/mms.12562

Johnson, H., Morrison, D., Taggart, C., 2021. WhaleMap: a tool to collate and display whale survey results in near real-time. JOSS 6, 3094. https://doi.org/10.21105/joss.03094

Johnson, H.D., Taggart, C.T., Newhall, A.E., Lin, Y.-T., Baumgartner, M.F., 2022. Acoustic detection range of right whale upcalls identified in near-real time from a moored buoy

and a Slocum glider. The Journal of the Acoustical Society of America 151, 2558–2575. https://doi.org/10.1121/10.0010124

Kaliszewska, Z.A., Seger, J., Rowntree, V.J., Barco, S.G., Benegas, R., Best, P.B., Brown, M.W., Brownell, R.L., Carribero, A., Harcourt, R., Knowlton, A.R., Marshall-Tilas, K., Patenaude, N.J., Rivarola, M., Schaeff, C.M., Sironi, M., Smith, W.A., Yamada, T.K., 2005. Population histories of right whales (Cetacea: Eubalaena) inferred from mitochondrial sequence diversities and divergences of their whale lice (Amphipoda: Cyamus). Mol Ecol 14, 3439–3456. https://doi.org/10.1111/j.1365-294X.2005.02664.x

Keller, C.A., Ward-Geiger, L.I., Brooks, W.B., Slay, C.K., Taylor, C.R., Zoodsma, B.J., 2006. North atlantic right whale distribution in relation to sea-surface temperature in the southeastern united states calving grounds. Marine Mammal Sci 22, 426–445. https://doi.org/10.1111/j.1748-7692.2006.00033.x

Kenney, R.D. 2019. The North Atlantic Right Whale Consortium Database: A guide for Users and Contributors. Version 6. North Atlantic Right Whale Consortium Reference Document 2019-02.

Khan, C.B., Shashank, W.K. (2015). Right Whale Recognition. https://kaggle.com/competitions/noaa-right-whale-recognition

Knowlton, A.R., Kraus, S.D., 2020. Mortality and serious injury of northern right whales (Eubalaena glacialis) in the western North Atlantic Ocean. JCRM 193–208. https://doi.org/10.47536/jcrm.vi.288

Kraus, S.D., and Rolland, R.M. (2007). Right Whales in the Urban Ocean. In S. D. Kraus and R. M. Rolland (Eds.), The urban whale: North Atlantic right whales at the crossroads (pp. 1-38). Harvard University Press.

LaRue, M.A., Stapleton, S., Porter, C., Atkinson, S., Atwood, T., Dyck, M., Lecomte, N., 2015. Testing methods for using high-resolution satellite imagery to monitor polar bear abundance and distribution. Wildlife Society Bulletin 39, 772–779. https://doi.org/10.1002/wsb.596

Lawson, J.W., Sheppard, G.L., Comeau, S., and Murphy, A.J. 2025. North Atlantic Right Whales in Newfoundland and Labrador Waters, Based on Calls and Opportunistic Sightings. DFO Can. Sci. Advis. Sec. Res. Doc. 2025/018. iv + 27 p.

Leandro, L., Rolland, R., Roth, P., Lundholm, N., Wang, Z., Doucette, G., 2010. Exposure of the North Atlantic right whale Eubalaena glacialis to the marine algal biotoxin, domoic acid. Mar. Ecol. Prog. Ser. 398, 287–303. https://doi.org/10.3354/meps08321

Mayo, C.A., Ganley, L., Hudak, C.A., Brault, S., Marx, M.K., Burke, E., Brown, M.W., 2018. Distribution, demography, and behavior of North Atlantic right whales (Eubalaena glacialis) in Cape Cod Bay, Massachusetts, 1998-2013: Right Whales in Cape Cod Bay. Mar Mam Sci 34, 979–996. https://doi.org/10.1111/mms.12511

Meyer-Gutbrod, E., Greene, C., Davies, K., 2018. Marine Species Range Shifts Necessitate Advanced Policy Planning: The Case of the North Atlantic Right Whale. Oceanog 31. https://doi.org/10.5670/oceanog.2018.209

Meyer-Gutbrod, E.L., Davies, K.T.A., Johnson, C.L., Plourde, S., Sorochan, K.A., Kenney, R.D., Ramp, C., Gosselin, J., Lawson, J.W., Greene, C.H., 2023. Redefining North Atlantic right whale habitat-use patterns under climate change. Limnology and Oceanography 68. https://doi.org/10.1002/lno.12242

Moore, M., Andrews, R., Austin, T., Bailey, J., Costidis, A., George, C., Jackson, K., Pitchford, T., Landry, S., Ligon, A., McLellan, W., Morin, D., Smith, J., Rotstein, D., Rowles, T., Slay, C., Walsh, M., 2013. Rope trauma, sedation, disentanglement, and monitoring-tag associated lesions in a terminally entangled North Atlantic right whale (Eubalaena glacialis). Mar Mam Sci 29. https://doi.org/10.1111/j.1748-7692.2012.00591.x

Moore, M., Rowles, T., Fauquier, D., Baker, J., Biedron, I., Durban, J., Hamilton, P., Henry, A., Knowlton, A., McLellan, W., Miller, C., Pace, R., Pettis, H., Raverty, S., Rolland, R., Schick, R., Sharp, S., Smith, C., Thomas, L., van der Hoop, J., Ziccardi, M., 2021. REVIEW Assessing North Atlantic right whale health: threats, and development of tools critical for conservation of the species. Dis. Aquat. Org. 143, 205–226. https://doi.org/10.3354/dao03578

Mullen, K.A., Peterson, M.L., Todd, S.K., 2013. Has designating and protecting critical habitat had an impact on endangered North Atlantic right whale ship strike mortality? Marine Policy 42, 293–304. https://doi.org/10.1016/j.marpol.2013.03.021

Patrician, M.R., Biedron, I.S., Esch, H.C., Wenzel, F.W., Cooper, L.A., Hamilton, P.K., Glass, A.H., Baumgartner, M.F., 2009. Evidence of a North Atlantic right whale calf (Eubalaena glacialis) born in northeastern U.S. waters. Marine Mammal Science 25, 462–477. https://doi.org/10.1111/j.1748-7692.2008.00261.x

Reeves, R.R. 2001. Overview of catch history, historic abundance and distribution of right whales in the western North Atlantic and in Cintra Bay, West Africa. J. Cetacean Res. Manage., 2, 187-192.

Rolland, R.M., Parks, S.E., Hunt, K.E., Castellote, M., Corkeron, P.J., Nowacek, D.P., Wasser, S.K., and Kraus, S.D. 2012. Evidence that ship noise increases stress in right whales. Proc Biol Sci, 279(1737), 2363-8. doi:10.1098/rspb.2011.2429

Schaeff, C.M., Kraus, S.D., Brown, M.W., White, B.N., 1993. Assessment of the population structure of western North Atlantic right whales (Eubalaena glacialis) based on sighting and mtDNA data. Can. J. Zool. 71, 339–345. https://doi.org/10.1139/z93-047

Sharp, S., McLellan, W., Rotstein, D., Costidis, A., Barco, S., Durham, K., Pitchford, T., Jackson, K., Daoust, P., Wimmer, T., Couture, E., Bourque, L., Frasier, T., Frasier, B., Fauquier, D., Rowles, T., Hamilton, P., Pettis, H., Moore, M., 2019. Gross and histopathologic diagnoses from North Atlantic right whale Eubalaena glacialis mortalities between 2003 and 2018. Dis. Aquat. Org. 135, 1–31. https://doi.org/10.3354/dao03376

Sorochan, K.A., Plourde, S., Baumgartner, M.F., Johnson, C.L., 2021. Availability, supply, and aggregation of prey (Calanus spp.) in foraging areas of the North Atlantic right whale (Eubalaena glacialis). ICES Journal of Marine Science 78, 3498–3520. https://doi.org/10.1093/icesjms/fsab200

Southall, B.L., Finneran, J.J., Reichmuth, C., Nachtigall, P.E., Ketten, D.R., Bowles, A.E., Ellison, W.T., Nowacek, D.P., Tyack, P.L., 2019. Marine Mammal Noise Exposure Criteria: Updated Scientific Recommendations for Residual Hearing Effects. Aquat Mamm 45, 125–232. https://doi.org/10.1578/AM.45.2.2019.125

Stewart, J.D., Durban, J.W., Knowlton, A.R., Lynn, M.S., Fearnbach, H., Barbaro, J., Perryman, W.L., Miller, C.A., Moore, M.J., 2021. Decreasing body lengths in North Atlantic right whales. Current Biology 31, 3174-3179.e3. https://doi.org/10.1016/j.cub.2021.04.067

TC. 2021. Protecting North Atlantic right whales from collisions with vessels in the Gulf of St. Lawrence. Transport Canada, https://tc.canada.ca/en/marine-transportation/navigation-marine-conditions/protecting-north-atlantic-right-whales-collisions-vessels-gulf-st-lawrence, accessed 2021-07-21.

Van Der Hoop, J.M., Corkeron, P., Kenney, J., Landry, S., Morin, D., Smith, J., Moore, M.J., 2016. Drag from fishing gear entangling North Atlantic right whales. Mar Mam Sci 32, 619–642. https://doi.org/10.1111/mms.12292

Weisbrod, A.V., Shea, D., Moore, M.J., Stegeman, J.J., 2000. Organochlorine exposure and bioaccumulation in the endangered Northwest Atlantic right whale (Eubalaena glacialis) population. Environmental Toxicology and Chemistry 19, 654–666. https://doi.org/10.1002/etc.5620190318

Wiley, D.N., Mayo, C.A., Maloney, E.M., Moore, M.J., 2016. Vessel strike mitigation lessons from direct observations involving two collisions between noncommercial vessels and North Atlantic right whales (Eubalaena glacialis). Marine Mammal Science 32, 1501–1509. https://doi.org/10.1111/mms.12326

Zani, M.A., Taylor, J.K.D., Kraus, S.D., 2008. Observation of a Right Whale (¡I¿Eubalaena glacialis¡/I¿) Birth in the Coastal Waters of the Southeast United States. aquatic mammals 34, 21–24. https://doi.org/10.1578/AM.34.1.2008.21

Chapter 3

Individual North Atlantic Right Whales Identified From Space

Matus Hodul[1], Anders Knudby[1], Brigid McKenna[2], Amy James[2], Charles Mayo[2], Moira Brown[3], Delphine Durette-Morin[3], Stephen Bird[4]

[1] University of Ottawa, Department of Geography, Environment, and Geomatics. Ottawa, Ontario, Canada
[2] Center for Coastal Studies, Right Whale Ecology Program. Provincetown, Massachusetts, United States of America
[3] Canadian Whale Institute, Welshpool, New Brunswick, Canada
[4] Fluvial Systems Research Inc., Surrey, British Columbia, Canada

(2022) *Marine Mammal Science, 39(1)*, 221-231

This paper addresses the first research objective outlined in Section 1.1.1

> **Identify and confirm North Atlantic Right Whales in satellite imagery:** Acquire satellite imagery at a location and time likely to contain right whales, manually locate the whales in the imagery, and confirm observations with field survey. Use these observations to determine to what extent it is possible to distinguish whales from other marine mammals, and right whales from other species of whales.

Notably, this work represents the *first time* that North Atlantic right whales have been observed in satellite imagery, the *first* example of a whale being observed in satellite imagery and aerial photography within seconds of each other ("Halo"), and the *first* known example of an individual named animal being identified from satellite imagery alone based on visible body markings ("Ruffian"). It was also likely the first study to be published using Maxar's new (at the time) 15 cm imagery product.

This research has been done in collaboration with the Right Whale Ecology Program at the Center for Coastal Studies (CCS) in Provincetown, Massachusetts, who supplied the aerial photographs of right whales. It has been published in the journal Marine Mammal Science, where it received the *F.G. Wood Memorial Scholarship Award*, given to the first author of the best student paper each biennium.

A short *Postscript* follows the references for this paper, showing newly available results relevant to the topic of this paper which were not available at the time of its publication.

Author attributions: MH conceptualized the study, performed the work, and wrote the manuscript. AK assisted in conceptualization, provided feedback, and helped with editing. BM, AJ, and CM conducted the aerial survey and provided the data. MB and DDM provided scientific assistance with biology aspects of the research. SB was the principle investigator and helped secure funding.

Abstract

The population of the critically endangered North Atlantic right whale, *Eubalaena glacialis*, numbers approximately 336 individuals, and continues to decline. Current development and implementation of protection measures and monitoring of right whale presence relies on visual surveys from vessel and aerial platforms, and passive acoustic monitoring, which contribute to location data. Here we demonstrate that satellite imagery can be used to detect and confirm the North Atlantic right whales at a species level using newly-available imaging methods, providing another tool to inform conservation efforts. Using optical satellite imagery with 15 cm resolution, 25 right whales were observed in Cape Cod Bay on April 24$^{\text{th}}$, 2021. Species confirmation was possible due to clearly visible callosity patterns indicative of their species within this range. Although the variations in callosity patterns commonly used to identify individuals were too small to be resolved at this image resolution, one whale with large distinctive markings visible on his body was identified at an individual level from satellite imagery alone. Although visual and acoustic survey methods can be combined for monitoring this species in critical habitats, satellite-based monitoring can be especially helpful to understand whale presence outside the areas monitored with existing visual and acoustic detection methods.

3.1 Introduction

The North Atlantic right whale (*Eubalaena glacialis*; henceforth "right whale"), was recently uplisted to "critically endangered" by the International Union for the Conservation of Nature (Cooke, 2020). The species has been in decline since 2010 (Pace et al. 2017) and was estimated to number approximately 356 in 2019 (Pettis et al. 2021) and 336 in 2020 (Pettis et al. 2022). Over a period spanning hundreds of years, the species was heavily exploited by commercial whaling, reducing the population from at least several thousands to probably less than 100 animals (Reeves 2001). Although the commercial hunting of right whales has been banned worldwide since 1935, anthropogenic threats to right whales continue today, with vessel strikes and entanglements in fishing gear being the predominant known human-caused mortality in the population (Bourque et al. 2020; Daoust et al. 2017; Knowlton and Kraus 2001; Moore et al. 2004; Sharp et al. 2019).

To mitigate acute anthropogenic threats to right whales, the governments of Canada and the United States have implemented various protection measures to reduce the impacts of vessel strike and entanglement in fishing gear. These conservation measures were designed to balance the need for protecting right whales while maintaining commercial activities, and have been met with varying levels of compliance, and regional success and failure (van der Hoop et al. 2012, 2015). Dynamic protection measures are a management strategy where the locations and extent of human marine activities, notably vessel speed and fishery activities, are modified based on whale presence and movements in real time or near-real time (Davies and Brillant 2019; Hausner et al. 2021). Dynamic measures have been implemented in both Canada (Department of Fisheries and Oceans 2021; Transport Canada 2021) and the United States (Cole and Crowe 2019). The effectiveness of these measures relies on the ability to accurately detect the presence of right whales to modify the location and timing of zones restricting human activity.

At present, right whales are detected using visual observation and acoustic detections from a variety of platforms. Visual observations are obtained from trained marine mammal observers on aircraft and vessels (Brown et al. 2007), while acoustic detections are obtained from fixed and mobile hydrophones (Baumgartner et al. 2020). Satellite-monitored telemetry tags are not typically used on right whales because they can cause trauma to the whale if implanted and are not sufficiently durable if attached externally (Moore et al., 2012). Although visual and acoustic monitoring methods can detect right whales accurately, they are difficult to scale up to cover the whale's entire known distribution range. The scope of aerial surveys are limited by the cost of the necessary skilled labour —both pilot and observer— for extended periods of time, as well as the practical limit on the range of an aircraft and safe operating conditions. Acoustic surveys are limited by the cost and complexity of deploying the many platforms needed to cover a large area, as well as the cost of skilled labour for analysis of the recieved data.

Satellite imaging techniques offer the ability to acquire data across very

large spatial scales, potentially covering entire ocean basins on a daily or near-daily basis (Martellato et al. 2022). Such imaging can provide another tool for remote detection of right whales in areas where aerial and acoustic surveys are not currently conducted. Very-high-resolution (VHR) optical satellite imaging provides imagery with a spatial resolution on the order of tens of centimeters, depending on the sensing platform (Airbus 2021; Maxar 2020; Planet 2022). allowing for right whales to be resolved as discrete objects.

The potential to observe large marine mammals in VHR imagery was initially demonstrated by Abileah (2002), after which Fretwell et al. (2014) identified 55 "probable" and 23 "possible" southern right whales (*E. australis*) in a single 50 cm resolution image covering part of Golfo Nuevo, Argentina, based on visual image interpretation. Similarly, Cubaynes et al. (2019) visually identified a total of 211 whale-like objects in four 30 cm resolution images from Hawaii, western Mexico, southern France, and Argentina. Bamford et al. (2020) also used 30 cm VHR imagery along with a shipborne visual survey to confirm the presence of humpback and fin whales off the coast of Antarctica, and Corrêa et al. (2022) used an aerial survey to confirm observations of southern right whales using a variety of satellite sensors, including 50 cm Pleiades imagery.

These studies demonstrate the fundamental feasibility of space-based whale detection with high-resolution optical satellite imagery, but also demonstrate some of the challenges. Several whale species, including the southern right whale, have a skin color that is similar to the ocean background against which the whales must be detected (Cubaynes et al. 2019), and therefore even slightly submerged whales likely go undetected. Imagery resolution also plays a significant role in the ability to detect whales, with a higher spatial resolution, in general, resulting in a higher degree of confidence in whale observations (Corrêa et al. 2022).

At a spatial resolution of 50 cm, available in WorldView-2 imagery and other VHR imaging platforms, an adult right whale with a typical length of 12.5 m (Stewart et al. 2021) would be covered by 25 pixels lengthwise. This would allow for the basic shape of a marine mammal to be distinguished from that of other marine objects, but species distinction would be difficult. However, in WorldView-3 imagery, at a resolution of 30 cm, a right whale would be covered by 42 pixels, allowing large color patterns to be more apparent.

Here, we use Maxar's newly available 15 cm resolution HD image product, which is derived from the 30 cm resolution WorldView-3 platform (Formeller 2020), and costs about 10% more than the base 30 cm imagery. This is the highest resolution satellite imagery yet used to observe marine mammals. At this resolution, an adult right whale would be covered by 83 pixels lengthwise, potentially allowing for distinct color patterns of the whales to be seen. Using satellite imagery from Cape Cod Bay, Massachusetts, along with coincident aerial photography, we confirm detection and species identification of right whales observed in the 15 cm resolution imagery, and explore the potential to use callosity and scarring patterns visible in this imagery to identify individual right whales.

3.2 Materials and Methods

3.2.1 Satellite Imagery

This study took place in Cape Cod Bay, where right whales are known to aggregate to feed during late winter and early spring (Charif et al. 2019; Mayo et al. 2018). In the spring, the whales' prey, which includes the copepods *Calanus finmarchicus*, *Pseudocalanus spp.*, and *Centropages spp.*, aggregates in patches near the surface (Mayo and Marx 1990; Pendleton et al. 2009; Sorochan et al. 2021; Watkins and Schevill 1976). The whales sometimes feed on these patches by skim-feeding, a behavior where the whales swim at or near the surface with part of the upper jaw above the water surface while the rest of the body is only slightly submerged (Baumgartner et al. 2007; Watkins and Schevill 1976). The prevalence of this feeding behavior, where the whales are at the surface and entirely visible from above the water, was a determining factor in selecting this habitat area for an attempt at whale detection with satellite imagery.

Once field observations confirmed that right whales had entered the study area and were skim-feeding, in April 2021, WorldView-3 imagery acquisition was tasked in the area of the bay where they had been observed. A cloud-free image with ideal ocean conditions, wave height approximately 10 cm (NOAA 2021) and minimal sun glint, was acquired on 24$^{\text{th}}$ April 2021, 11:40 EDT (Figure 3.1) covering 200 km^2 in two swaths, including an eastern swath (Catalog ID 1040010067D36B00) and a western swath (10400100674B2100). The imagery was preprocessed to 15 cm resolution by the data provider using a proprietary process (Formeller 2020) before being delivered; no other spatial or atmospheric corrections were performed.

The imagery was systematically scanned using QGIS by a trained observer familiar with marine satellite imagery and whale identification, who did not have prior knowledge of the location of the whales as observed in the aerial survey. Objects identified as potential whales were flagged, and then further classified as "unambiguous" when species was able to be determined by observing callosities, or "ambiguous" when callosities were not clearly distinguishable. Imagery tiles containing the whales, like those in Figure 3.3, were created and sent to four marine biologists specializing in right whale observation, who confirmed that the objects were correctly identified as right whales. The observations were then matched to the locations of observations in the aerial survey for further confirmation.

3.2.2 Field Observations

Seasonal aerial surveys for monitoring of the right whale population are conducted in Cape Cod Bay by the Right Whale Ecology Program at the *Center for Coastal Studies* (CCS) in Provincetown, MA. Survey lines are flown in a Cessna Skymaster 337 in an east-west direction across the bay with a 1.5 nautical mile spacing at an altitude of 1,000 feet altitude and aircraft speed of 100 knots (Brown et al. 2007; Mayo et al. 2018). On April 24$^{\text{th}}$ 2021, the aerial

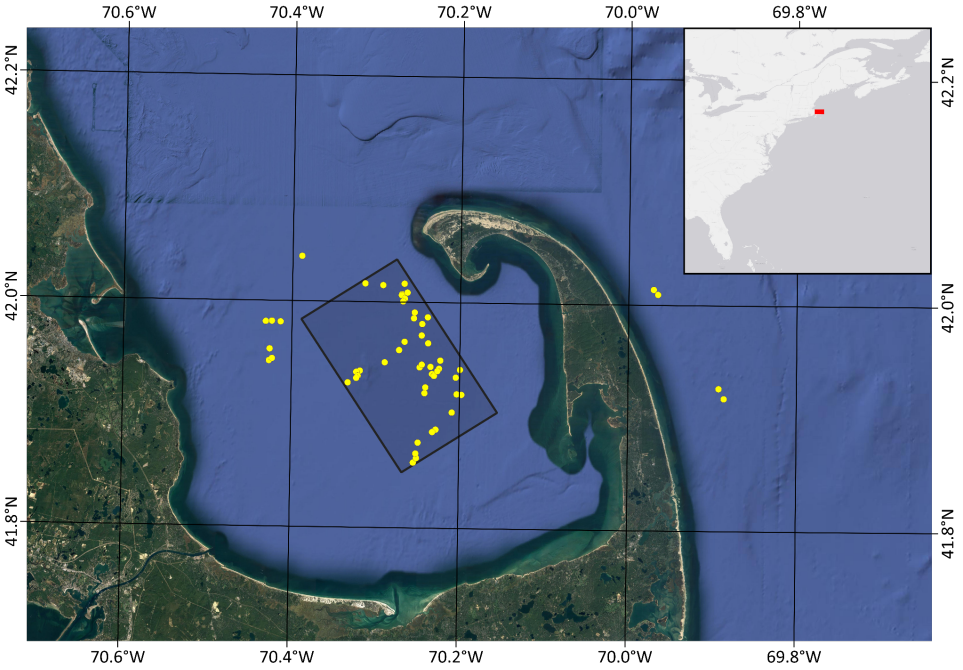

Figure 3.1: Overview of the Cape Cod Bay study area. The black shaded rectangle indicates the coverage of the 15 cm WorldView-3 imagery from 24 April, 2021 (Catalog IDs 1040010067D36B00 and 10400100674B2100). The yellow dots indicate the location of right whales observed in the field by the Center for Coastal Studies aerial survey team.

survey team flew between the hours of 9:23 and 16:30 EDT, during which time they observed 72 right whales, as well as 14 whales of other species, and 202 dolphins. The approximately 1,100 aerial photographs taken during the survey and the geo-location data obtained from the GPS navigation device in the aircraft were used to validate satellite-based right whale observations. For consistency, *imagery* will be used to refer to the WorldView-3 satellite imagery, and *photographs* will refer to the aerial field photography acquired by CCS.

3.3 Results

3.3.1 Identifying Whale Species in Imagery

The observer flagged 31 whale-like objects in the satellite imagery, of which 25 could be unambiguously identified as right whales due to the clear presence of whitish head callosities, the uniquely-identifiable patterns of raised and roughened skin patches with whitish colored whale lice on the surface of each whale's head (Hamilton et al. 2007). Table 3.1 lists the latitude and longitude of each whale observation in the imagery, while Figure 3.2 maps the observations relative to observations made by the aerial survey team.

Table 3.1: List of coordinates for the 31 whale observations, divided into 25 unambiguously identified right whales, and 6 ambiguously identified whales. * indicates the location of Ruffian (Figure 3.4) and ** indicates the location of Halo (Figure 3.5). Letter superscripts correspond to locations of whales shown in Figure 3.3.

Unambiguous		**Unambiguous**	
41.93285710	-70.3152045 [a]	41.93291142	-70.2259382 [d]
41.93950956	-70.3112931 [e]	41.93257456	-70.2249384 [g]
41.94123800	-70.2860575	41.93270798	-70.2245800 [f]
41.97683733	-70.2588551	41.92876091	-70.2017034
41.97918626	-70.2565542	41.91908892	-70.2347800
41.97936659	-70.2540829 [c]	41.91380847	-70.2481208
41.97986158	-70.2536904 [b]	41.90950988	-70.2028676
41.97887902	-70.2263361	41.88744892	-70.2245133 [a]
41.97582371	-70.2263347		
41.96968514	-70.2321683	**Ambiguous**	
41.97117875	-70.2266444	41.97529146	-70.2474413
41.95616554	-70.2245144	41.97077528	-70.2412951
41.94678000	-70.2138914 *	41.93861738	-70.2421223
41.93718148	-70.2336107	41.92227144	-70.2451779
41.88587746	-70.2303011 **	41.91225554	-70.2026960
41.86840123	-70.2502868	41.91120772	-70.2013629
41.86875255	-70.2502709		

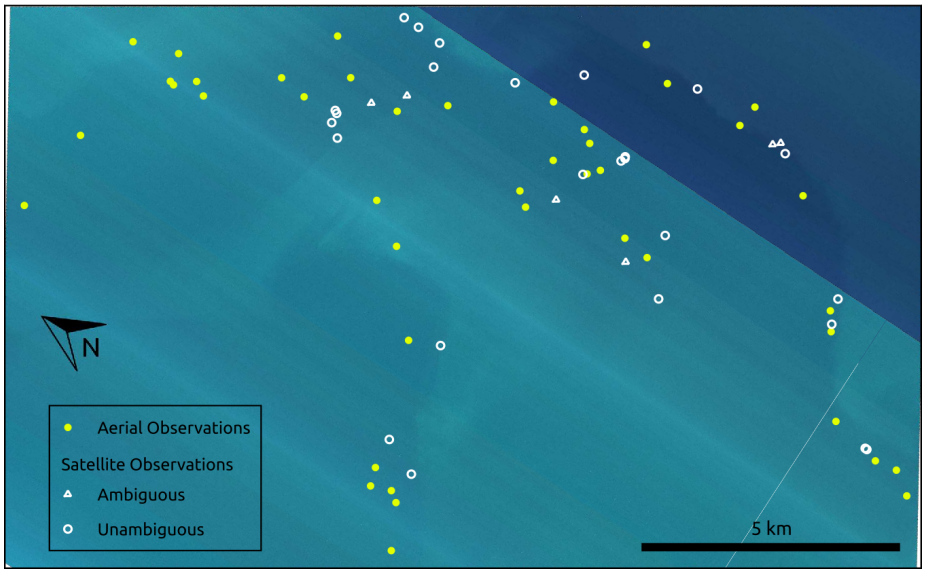

Figure 3.2: Locations of right whales observed in the aerial survey (yellow dots) and satellite observations (white outlines) over the Cape Cod Bay study area. The full extent of the map in this figure corresponds to the shaded rectangle in Figure 1, which has been rotated here for visualization purposes. Satellite image © 2022 Maxar Technologies.

At a spatial resolution of 15 cm, the whitish callosities along the top of their heads are visible (Figure 3.3). There are no other large whale species with callosity-like markings on the tops of their heads whose range overlaps with North Atlantic right whales; observing these callosities thus allows positive species identification. The remaining six whales whose species could not be identified were either rotated such that their callosities were not visible in the imagery, or had waves obscuring the part of the head where callosities are found.

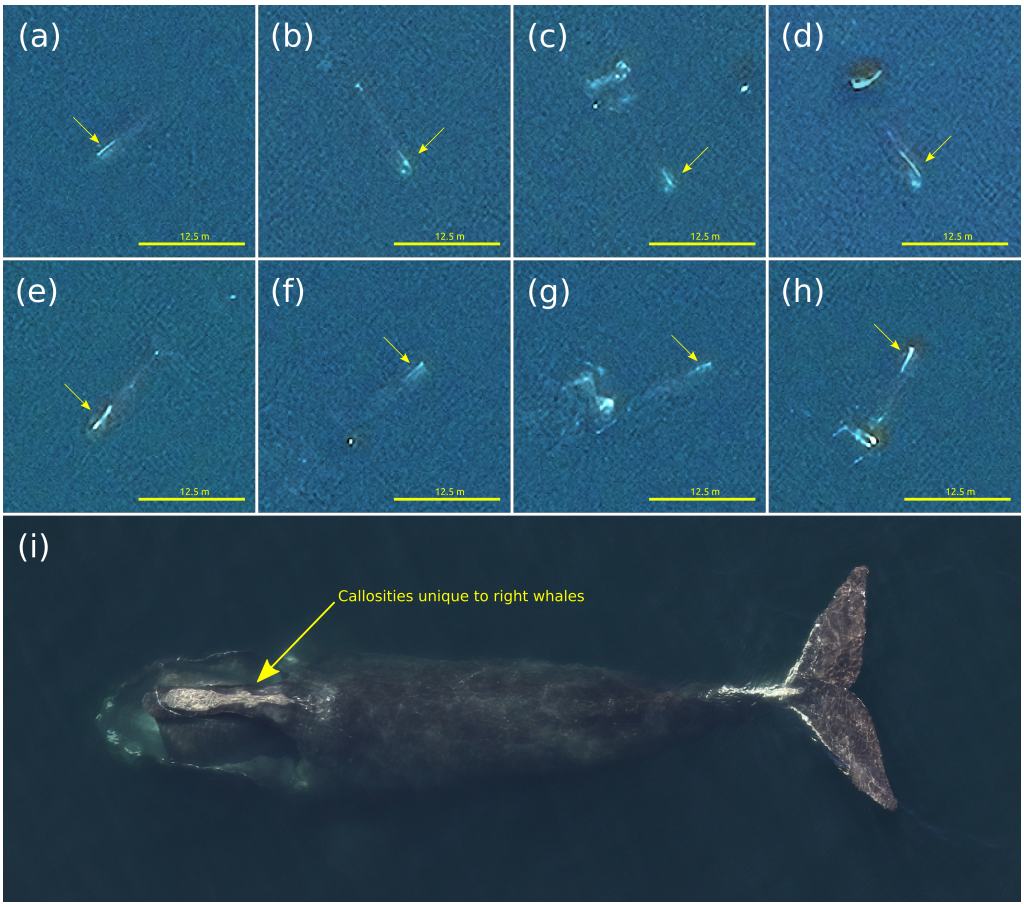

Figure 3.3: Examples of North Atlantic right whale observations in 15 cm resolution imagery, clearly showing the presence of callosities (indicated by yellow arrows), allowing for positive species identification (a-h). For reference, (i) is an aerial photograph of "Twister" (Catalog #3510) showing similar callosities. Based on the location of the callosity patterns on their bodies, we can determine that whales (b,c) are facing southeast, (f-h) are facing roughly northeast, and (a,e) are facing southwest. A scale bar of 12.5 m was used in this and other figures to correspond to the typical size of modern adult right whales (Stewart et al. 2021). Center for Coastal Studies NOAA federal permit #19315-01. Satellite image © 2022 Maxar Technologies.

Except for when the timing of the imagery capture overlapped with the field survey, there was no direct spatial match between satellite and field whale observations. This is because satellite imagery is captured near-simultaneously over the entire study area while the field survey takes several hours to complete and the whales move during this time. However, all whale observations in the satellite imagery were made within 1.6 km of field observations of right whales. Furthermore, the field survey did not detect any other whale species within the area covered by the satellite imagery around the time of imaging. This allowed species confirmation in the satellite observations. Several fin (*Balaenoptera physalus*), sei (*Balaenoptera borealis*), humpback (*Megaptera novaeangliae*), and minke (*Balaenoptera acutorostrata*) whales were spotted outside of the area covered by imagery.

3.3.2 Identifying Individual Right Whales

Individual right whales are routinely identified in aerial photographs using the small variations in the shape of callosity patterns which are unique to each whale (Hamilton et al. 2007). Though this study has demonstrated that these callosities are visible enough for species identification, a spatial resolution of 15 cm is not sufficient for resolving the small pattern variations necessary for individual identification. However, some right whales possess larger white markings caused by scarring; these, if distinctive enough, may allow for unique individual identification. One such example is the right whale named "Ruffian" (Catalog #3530), whose distinctive dorsum scar makes his identification using only the satellite imagery possible (Figure 3.4). This identification of Ruffian is the first known example of identification of an individual animal directly from satellite imagery.

In most cases, a whale's scarring patterns will not be large or distinctive enough to provide positive individual identification from the 15 cm satellite imagery alone, but may aid in narrowing down individuals in a group given prior knowledge of group locations. A right whale named "Halo" (Catalog #3546), who has a scar along the left leading edge of her fluke, as well as a prominent continuous head callosity that extends from her nares to the anterior rostrum, is shown in Figure 3.5. By a fortunate coincidence, at the exact moment that the satellite imagery was captured, the aerial survey team was logging the observation of Halo, making the survey aircraft visible in the imagery directly overhead of the whale. While such a fluke scar is not unique to Halo, and likely not enough to allow for unique identification, it is clearly visible in the imagery and may be useful in identifying Halo in a group of known right whales or while tracking Halo in successive daily imagery.

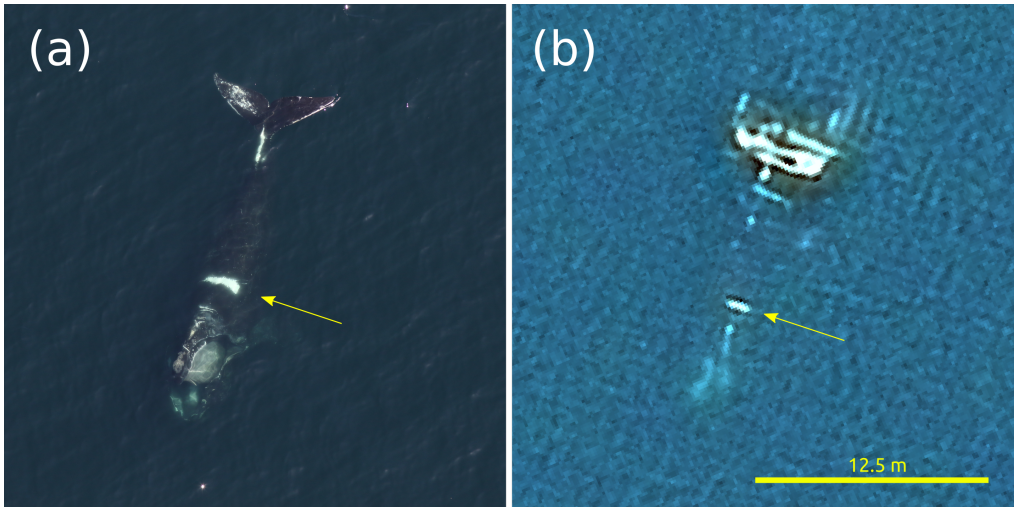

Figure 3.4: North Atlantic right whale "Ruffian" (Catalog #3530), observed on April 24th, 2021, in (a) aerial photography at 12:32 EDT at 41.94863°N, 70.22321°W; and (b) WorldView-3 satellite imagery at 11:40 EDT at 41.94678°N, 70.21389°W (800 m away from a). The distinctive white marking on Ruffian's dorsum behind his head can clearly be seen in the satellite imagery (yellow arrow), allowing for easy identification of this individual. Center for Coastal Studies NOAA federal permit #19315-01. Satellite image © 2022 Maxar Technologies.

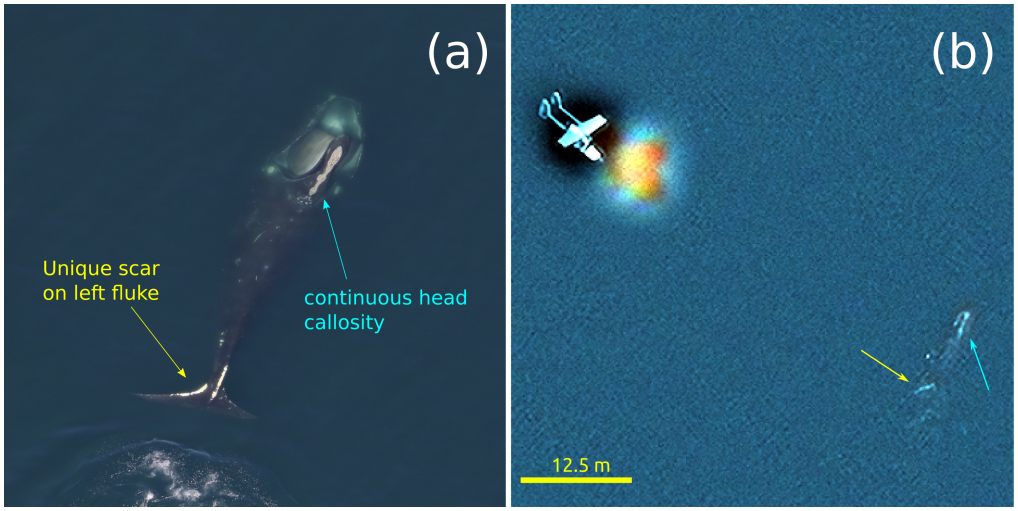

Figure 3.5: North Atlantic right whale "Halo" (Catalog #3546) observed on April 24th, 2021, in (a) aerial photography; and (b) WorldView-3 satellite imagery, both at 11:40 EDT at 41.88587°N, 70.23030°W. The white scars along the leading edge of Halo's left fluke and her continuous head callosity can be seen in the satellite imagery. The survey aircraft, a Cessna Skymaster 337 with its characteristic twin tails, can also be seen northwest of the whale. Center for Coastal Studies NOAA federal permit #19315-01. Satellite image © 2022 Maxar Technologies.

3.3.3 Comparison Between 30 cm and 15 cm Imagery

Since the 15 cm WorldView-3 imagery is derived from the base 30 cm imagery, it is useful to compare the two directly; Figure 3.6 shows a comparison between the two forms of imagery for Ruffian, Halo, and four other right whales. Though callosities and scars are discernable in the 30 cm imagery, they appear less sharp, and with less of a defined shape, potentially making them more difficult to differentiate from waves. The shape of larger patterns, especially scarring, may not be accurately represented in the 30 cm imagery due to pixelation. For instance, Ruffian's (Figure 3.6a) dorsum scar, which in reality takes roughly the shape of a rectangle (Figure 3.4), appears in the 30 cm imagery to have a "V" shape, while in the 15 cm imagery, appears as its actual rectangle shape. Such distortions due to pixelation would make it difficult to identify individual whales based on scarring patterns in the 30 cm imagery.

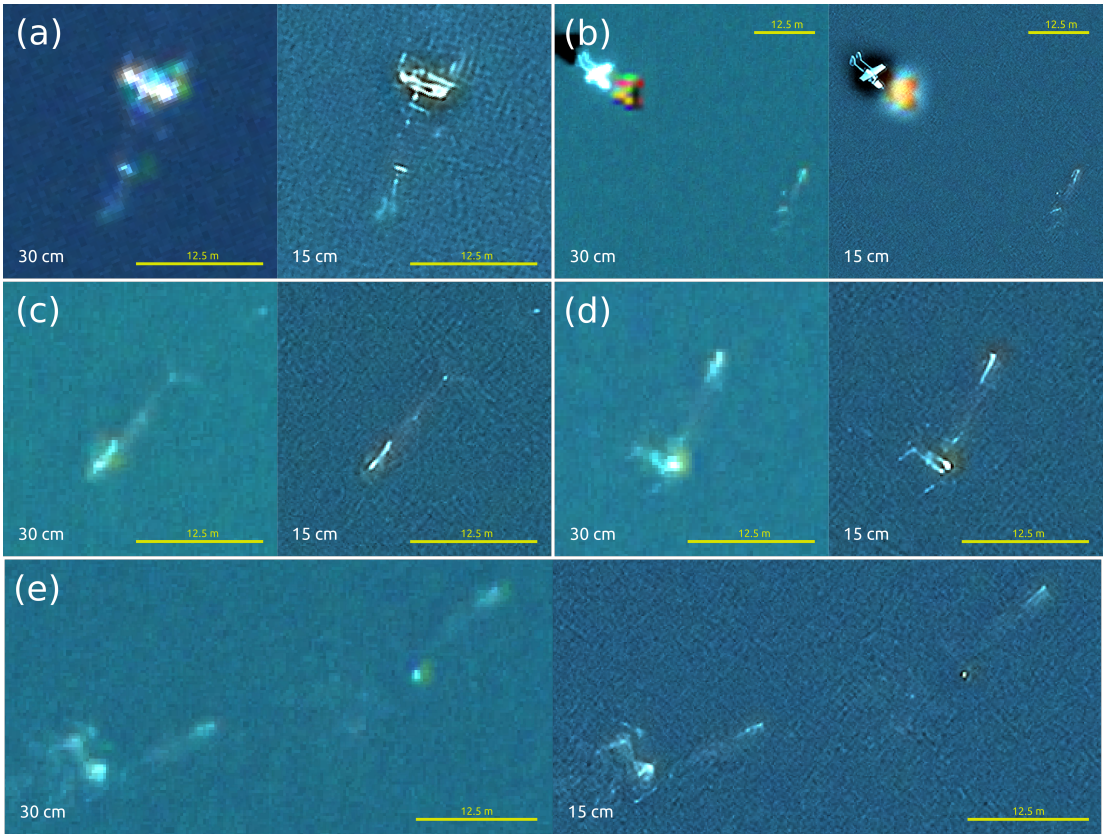

Figure 3.6: Comparison of the 30 cm WorldView-3 pansharpened base imagery to the new 15 cm imagery. (a) shows Ruffian (as in Figure 4) while (b) shows Halo (as in Figure 3.5). (c) and (d) here correspond to tiles (e) and (h) respectively in Figure 3 and Table 1, and (e) here shows two whales in close proximity, which correspond to those in Figure 3.3 and Table 3.1 labelled as (g) (here, left individual) and (f) (right individual). Satellite image © 2022 Maxar Technologies.

3.4 Discussion and Conclusion

This study has demonstrated the ability to use the newly-available 15 cm WorldView-3 HD satellite imagery to identify the species of a North Atlantic right whale based on the presence of visible callosity patterns. This represents a key development in the field of space-based whale detection, as it is the first example of the North Atlantic right whale being observed in satellite imagery, the first to use the 15 cm imagery, and the first to identify a named individual based on scarring patterns.

A promising application of this identification capability will be to assist in management and conservation efforts for right whales in Canadian and US waters, by adding detection capability alongside that of visual surveys and acoustic monitoring, as well as helping to detect right whales outside of areas typically covered by these traditional survey methods. Specifically, the Government of Canada has expressed interest in using satellite imagery to help detect and monitor right whale presence and predict their movements in the Bay of Fundy and Gulf of St. Lawrence to aid in developing and updating shipping restrictions and fishery management zones (Canadian Space Agency 2021). More important to a broader characterization of right whale distribution, this identification capability has the potential to assist in finding the over 50% of the right whale population which has not been documented in the Gulf of St. Lawrence or other known critical habitats along the Atlantic coast of North America during summer and fall months, and whose whereabouts are currently unknown (Crowe et al. 2021), a task not suited to the smaller-scale capabilities of visual surveys.

While identifying right whales from satellite imagery certainly promises benefits for conservation efforts, it is important to be mindful of technological and environmental limitations. The WorldView-3 imagery used here was acquired under excellent conditions for whale detection; the imagery is free of clouds and glint, wave height is low at around 10 cm, and a high density of whales are found swimming horizontally near the surface. The environment and right whale behavior in Cape Cod Bay are generally conducive to space-based whale detection, as the bay is sheltered and the whales congregate and often skim-feed at the surface or socialize in Surface Active Groups (Kraus et al. 2007) here. However, most other parts of the whales' migratory range are less sheltered, the whales are found in lower densities, and spend less time at the surface where they can be observed (Sorochan et al. 2021). The potential for more widespread and systematic space-based right whale monitoring thus depends on the ability to detect the whales in these less optimal conditions, an ability which will likely be directly improved by an increase in available spatial resolution such that it becomes easier to differentiate whales from waves and other marine objects.

As demonstrated here, 15 cm resolution imagery, the best currently available, enabled species-level identification of right whales. Individual whales with unique scarring patterns may also be identified, given that these patterns can be resolved at the spatial resolution of the imagery. These patterns must be large and distinctive, such as the scar on Ruffian. In principle, even the smaller variations in callosity patterns that are traditionally used to identify individ-

ual whales may become visible in satellite imagery as the spatial resolution of imagery continues to improve. For instance, an upcoming imaging satellite called "Albedo" has been recently approved by the United States Government to provide commercial imagery at a 10 cm native resolution (Werner 2021), which should be operational by 2024. Whether such imagery will be capable of resolving callosity patterns to an individual level remains to be seen.

The use of satellite imagery for right whale detection and monitoring appears to be a promising technique for whale conservation efforts, but it is necessary to be mindful that this is only a single tool in a broad toolbox of monitoring methods, each with their strengths and weaknesses. Satellite detection and monitoring may allow for the locating of new or as-yet undiscovered habitats, and the monitoring of overlaps with existing and emerging human activities. However, it will be unlikely to be useful for monitoring individual whale size, health, or behaviours, given the technological constraints of the method. Thus, a combination of acoustic monitoring, visual surveys, and satellite detection will be critical to the effective and long term conservation of the North Atlantic right whale. Determining exactly how satellite detection and monitoring will fit into the range of existing conservation tools remains an area of research.

3.5 Acknowledgements

This project was undertaken with the financial support of the Canadian Space Agency and the Department of Fisheries and Oceans in collaboration with Transport Canada, as part of the Canadian Space Agency 'smartWhales' initiative to explore improved methods for the detection and modelling of North Atlantic right whales using space-based data sources. Data provided by the North Atlantic right whale programs through projects at the Center for Coastal Studies funded by Massachusetts Division of Marine Fisheries through a grant from NOAA. Data were collected under NOAA federal permit #19315-01. The participation of the University of Ottawa in this project has been undertaken as a team member led by Fluvial Systems Research Inc.

3.6 References

Abileah, R. (2002). Marine mammal census using space satellite imagery. U.S. Navy Journal of Underwater Acoustics, 52(3), 709–724.

Airbus. (2021). Pléiades Neo [Brochure]. https://www.intelligence-airbusds.com/imagery/constellation/pleiades-neo/ Bamford, C. C. G., Kelly, N., Dalla Rosa, L., Cade, D. E., Fretwell, P. T., Trathan, P. N., Cubaynes, H. C., Mesquita, A. F. C.,

Gerrish, L., Friedlaender, A. S., and Jackson, J. A., (2020). A comparison of baleen whale density estimates derived from overlapping satellite imagery and a shipborne survey. Scientific Reports, 10, 1–12. https://doi.org/10.1038/s41598-020- 69887-y

Baumgartner, M. F., Bonnell, J., Corkeron, P. J., Van Parijs, S. M., Hotchkin, C., Hodges, B. A., Thornton, J. B., Mensi, B. L., and Bruner, S. M. (2020). Slocum gliders provide accurate near real-time estimates of baleen whale presence from human- reviewed passive acoustic detection information. Frontiers in Marine Science, 7, Article 100. https://doi.org/10.3389/ fmars.2020.00100

Baumgartner, M. F., Mayo, C. A., and Kenney, R. D. (2007). Enormous carnivores, microscopic food, and a restaurant that's hard to find. In S. D. Kraus and R. M. Rolland (Eds.), The urban whale: North Atlantic right whales at the crossroads (pp. 138– 171). Harvard University Press.

Bourque, L., Wimmer, T., Lair, S., Jones, M., and Daoust, P.-Y. (2020). Incident report: North Atlantic right whale mortality event in Eastern Canada, 2019. Collaborative report produced by Canadian Wildlife Health Cooperative and Marine Animal Response Society.

Brown, M. W., Kraus, S. D., Slay, C. K., and Garrison, L.P. (2007). Surveying for discovery, science, and management. In S. D. Kraus and R. M. Rolland (Eds.), The urban whale: North Atlantic right whales at the crossroads (pp. 105–137). Harvard University Press.

Canadian Space Agency. (2021). Data from space could help protect the endangered North Atlantic right whale [News release]. https://www.canada.ca/en/space-agency/news/2021/01/data-from-space-could-help-protect-the-endangered-north- atlantic-right-whale.html

Charif, R. A., Shiu, Y., Muirhead, C. A., Clark, C. W., Parks, S. E., and Rice, A. N. (2019). Phenological changes in North Atlantic right whale habitat use in Massachusetts Bay. Global Change Biology, 26(2), 734–745. https://doi.org/10.1111/ gcb.14867

Cole, T., and Crowe, L. (2019). An analysis of dynamic management areas, January 2010–August 2019, in support of the U.S. take reduction team. Interactive Monthly DMA Analyses, NOAA Fisheries. https://apps-nefsc.fisheries.noaa.gov/psb/ surveys/interactive-monthly-dma-analyses/

Cooke, J. G. (2020). Eubalaena glacialis (errata version published in 2020). IUCN Red List of Threatened Species, e.T41712A178589687. https://doi.org/10.2305/IUCN.UK.2020-2.RLTS.T41712A178589687.en

Corrêa, A. A., Quoos, J. H., Barreto, A. S., Groch, K. R., and Eichler, P. P. B. (2022). Use of satellite imagery to identify southern right whales (Eubalaena australis) on a Southwest Atlantic Ocean breeding ground. Marine Mammal Science, 38(1), 87–101. https://doi.org/10.1111/mms.12847

Crowe, L. M., Brown, M. W., Corkerton, P. J., Hamilton, P. K., Ramp, C., Ratelle, S., Vanderlaan, A. S. M., and Cole, T. V. N. (2021). In plane sight: a mark-recapture analysis of North Atlantic right whales in the Gulf of St. Lawrence. Endangered Species Research, 46, 227–251. https://doi.org/10.3354/esr01156

Cubaynes, H. C., Fretwell, P. T., Bamford, C., Gerrish, L., and Jackson, J. A. (2019). Whales from space: Four mysticete species described using new VHR satellite imagery. Marine Mammal Science, 35(2), 466–491. https://doi.org/10.1111/ mms.12544

Daoust, P.-Y., Couture, E. L., Wimmer, T., and Bourque, L. (2017). Incident report: North Atlantic right whale mortality event in the Gulf of St. Lawrence, 2017. Collaborative report produced by Canadian Wildlife Health Cooperative, Marine Animal Response Society, and Fisheries and Oceans Canada.

Davies, K. T. A., and Brillant, S. W. (2019). Mass human-caused mortality spurs federal action to protect endangered North Atlantic right whales in Canada. Marine Policy, 104, 157–162. https://doi.org/10.1016/j.marpol.2019.02.019

Department of Fisheries and Oceans. (2021). 2021 fishery management measures: North Atlantic right whales. https:// www.dfo-mpo.gc.ca/fisheries-peches/commercial-commerciale/atl-arc/narw-bnan/management-gestion-eng.html

Formeller, C. (2020). Introducing 15 cm HD: The highest clarity from commercial satellite imagery [Blog]. https:// blog.maxar.com/earth-intelligence/2020/introducing-15-cm-hd-the-highest-clarity-from-commercial-satellite-imagery

Fretwell, P. T., Staniland, I. J., and Forcada, J. (2014). Whales from space: Counting southern right whales by satellite. PLoS ONE, 9(2), Article e88655. https://doi.org/10.1371/journal.pone.0088655

Hamilton, P. K., Knowlton, A. R., and Marx, M. K. (2007). Right whales tell their own stories: The photo-identification catalog. In S. D. Kraus and R. M. Rolland (Eds.), The urban whale: North Atlantic right whales at the crossroads (pp. 75–104). Harvard University Press.

Hausner, A., Samhouri, J. F., Hazen, E. L., Delgerjargal, D., and Abrahms, B. (2021). Dynamic strategies offer potential to reduce lethal ship collisions with large whales under

changing climate conditions. Marine Policy, 130, Article 104565. https:// doi.org/10.1016/ j.marpol.2021.104565

Knowlton, A. R., and Kraus, S. D. (2001). Mortality and serious injury of northern right whales (Eubalaena glacialis) in the west- ern North Atlantic Ocean. Journal of Cetacean Research and Management, 2, 193–208. https://doi.org/10.47536/ jcrm.vi.288

Kraus, S. D., Pace, R. M., and Frasier, T. R. (2007). High investment, low return: The strange case of reproduction in Eubalaena glacialis. In S. D. Kraus and R. M. Rolland (Eds.), The urban whale: North Atlantic right whales at the crossroads (pp. 172–199). Harvard University Press.

Martellato, E., Piccirillo, A. M., Ferraioli, G., Rotundi, A., Della Corte, V., Palumbo, P., Alcaras, E., Appolloni, L., Aulicino, G., Bertini, I., Capozzi, V., Catucci, E., Dionnet, Z., Di Palma, P., Esposito, F., Ferrentino, E., Innac, A., Inno, L., Pennino, S., ... Zambianchi, E. (2022). A new orbiting deployable system for small satellite observations for ecology and earth observa- tion. Remote Sensing, 14(9), Article 2066. https://doi.org/10.3390/rs14092066

Maxar. (2020). WorldView-3 data sheet. https://resources.maxar.com/data-sheets/worldview-3

Mayo, C. A., and Marx, M. A. (1990). Surface foraging behavior of the North Atlantic right whale, Eubalaena glacialis, and associated zooplankton characteristics. Canadian Journal of Zoology, 68(10), 2214–2220. https://doi.org/10.1139/ z90-308

Mayo, C. A., Ganley, L., Hudak, C. A., Brault, S., Marx, M. K., Burke, E., and Brown, M. W. (2018). Distribution, demography, and behavior of North Atlantic right whales (Eubalaena glacialis) in Cape Cod Bay, Massachusetts, 1998–2013. Marine Mammal Science, 34(4), 979–996. https://doi.org/10.1111/mms.12511

Moore M. J., Knowlton A. R., Kraus, S. D., McLellan W. A., and Bonde R. K. (2004). Morphometry, gross morphology and avail- able histopathology in North Atlantic right whale (Eubalaena glacialis) mortalities (1970–2002). Journal of Cetacean Research and Management, 6(3), 199–214.

Moore, M., Andrews, R., Austin, T. Bailey, J., Costidis, A., George, C., Jackson, K., Pitchford, T., Landry, S., Ligon, A., McLellan, W., Morin, D., Smith, J., Rotstein, D., Rowels, T., Slay, C., and Walsh, M. (2012). Rope trauma, sedation, disentan- glement, and monitoring-tag associated lesions in a terminally entangled North Atlantic right whale (Eubalaena glacialis). Marine Mammal Science, 29(2), E98–E113. https://doi.org/10.1111/ j.1748-7692.2012.00591.x

NOAA. (2021). Historical data. National Data Buoy Center. https://www.ndbc.noaa.gov/ station_page.php?station=44090

Pace, R. M., Corkeron, P. J., and Kraus, S. D. (2017). State–space mark–recapture estimates reveal a recent decline in abun- dance of North Atlantic right whales. Ecology and Evolution, 7(21), 8730–8741. https://doi.org/10.1002/ece3.3406 Pendelton, D. E., Pershing, A. J., Brown, M. W., Mayo, C. A., Kenney, R. D., Record, N. R., and Cole, T. V. N. (2009). Regional- scale mean copepod concentration indicates relative abundance of North Atlantic right whales. Marine Ecology Progress Series, 278, 211–225. https://doi.org/10.3354/meps07832

Pettis, H. M., Pace, R. M., III, and Hamilton, P. K. (2021). North Atlantic Right Whale Consortium 2020 Annual Report Card. Report to the North Atlantic Right Whale Consortium. https://www.narwc.org/report-cards.html

Pettis, H. M., Pace, R. M., III, and Hamilton, P. K. (2022). North Atlantic Right Whale Consortium 2021 Annual Report Card. Report to the North Atlantic Right Whale Consortium. https://www.narwc.org/report-cards.html

Planet. (2022). Planet imagery product specifications. https://assets.planet.com/docs/ Planet_Combined_Imagery_Product_ Specs_letter_screen.pdf

Reeves, R. R. (2001). Overview of catch history, historic abundance and distribution of right whales in the western North Atlantic and in Cintra Bay, West Africa. Journal of Cetacean Research and Management, 2, 187–192.

Sharp, S. M., McLellan, W. A., Rotstein, D. S., Costidis, A. M., Barco, S. G., Durham, K., Pitchford, T. D., Jackson, K. A., Daoust, P.-Y., Wimmer, T., Couture, E. L., Bourque, L., Frasier, T., Frasier, B., Fauquier, D., Rowles, T. K., Hamilton, P. K., Pettis, H.,

and Moore, M. J. (2019). Gross and histopathologic diagnoses from North Atlantic right whale Eubalaena glacialis mortalities between 2003 and 2018. Diseases of Aquatic Organisms, 135, 1–31. https://doi.org/10.3354/dao03376

Sorochan, K. A., Plourde, S., Baumgartner, M. F., and Johnson, C. L. (2021). Availability, supply, and aggregation of prey (Cala- nus spp.) in foraging areas of the North Atlantic right whale (Eubalaena glacialis). ICES Journal of Marine Science, 78(10), 3498–3520. https://doi.org/10.1093/icesjms/fsab200

Stewart, J. D., Durban, J. W., Knowlton, A. R., Lynn, M. S., Fearnbach, H., Barbaro, J., Perryman, W. L., Miller, C. A., and Moore, M. J. (2021). Decreasing body lengths in North Atlantic right whales. Current Biology, 31, 3174–3179. https:// doi.org/10.1016/j.cub.2021.04.067

Transport Canada. (2021). Protecting North Atlantic right whales from collisions with vessels in the Gulf of St. Lawrence. https://tc.canada.ca/en/marine-transportation/navigation-marine-conditions/protecting-north-atlantic-right-whales- collisions-vessels-gulf-st-lawrence

van der Hoop, J. M., Moore, M. J., Barco, S. G., Cole, T. V. N., Daoust, P.-Y., Henry, A. G., McAlpine, D. F., McLellan, W. A., Wimmer, T., and Solow, A. R. (2012). Assessment of management to mitigate anthropogenic effects on large whales. Conservation Biology, 27(1), 121–133. https://doi.org/10.1111/j.1523-1739.2012.01934.x

van der Hoop, J. M., Vanderlaan, A. S. M., Cole, T. V. N., Henry, A. G., Hall, L., Mase-Guthrie, B., Wimmer, T., and Moore, M. J. (2015). Vessel strikes to large whales before and after the 2008 ship strike rule. Conservation Letters, 8(1), 24–32. https://doi.org/10.1111/conl.12105

Watkins, W. A., and Schevill, W. E. (1976). Right whale feeding and baleen rattle. Journal of Mammalogy, 57(1), 58–66. https:// doi.org/10.2307/1379512

Werner, D. (2021). Albedo wins license to sell 10-centimeter imagery. Space News. https:// spacenews.com/albedo-wins- license-to-sell-10-centimeter-imagery/

Chapter 4

Simulating Satellite Imagery from Aerial Photographs using Neural Style Transfer

Matus Hodul[1], Anders Knudby[1], Amy James[2], Stephen Bird[3]

[1] University of Ottawa, Department of Geography, Environment, and Geomatics. Ottawa, Ontario, Canada
[2] Center for Coastal Studies, Right Whale Ecology Program. Provincetown, Massachusetts, United States of America
[3] Fluvial Systems Research Inc., Surrey, British Columbia, Canada

Marine Mammal Science, Accepted pending revisions.

This paper addresses the second research objective outlined in Section 1.1.1

> **Solve the problem of a limited training data set for whale detection:** Due to the rarity of satellite observations of the North Atlantic right whale, there is a significant lack of data for training whale detector models. Develop a method for increasing the available training data by simulating satellite imagery from other sources.

The novelty and significance of this study come, in part, from the fact that we were able to use near-concurrent examples of aerial photographs and satellite imagery of right whales, allowing us to create the extremely unique image pairs of nearly-identical observations of whale in both satellite imagery and aerial photograph, something no other study has been able to do owing to the extreme rarity of the targets and the difficulty in coordinating aerial and satellite observations so closely.

This research has been done with the permission of the Right Whale Ecology Program at the Center for Coastal Studies (CCS) in Provincetown, Massachusetts, who supplied the aerial photographs of right whales. It has been submitted to the journal Marine Mammal Science, where it is currently under review.

Author attributions: MH conceptualized the study, performed the work, and wrote the manuscript. AK assisted in conceptualization, provided feedback, and helped with editing. AJ provided the data on behalf of the Center for Coastal Studies. SB was the principle investigator and helped secure funding.

Abstract

Convolutional Neural Network models are routinely being used to detect objects of interest in satellite imagery, and are typically trained on tens or hundreds of thousands of examples of the target object. Where target objects are rare in satellite imagery, a training dataset of sufficient size may not exist; often aerial photographs of the target are more abundant as they are easier to collect. This work proposes a Neural Style Transfer (NST) approach to simulate satellite imagery from aerial photographs in order to increase the number of "satellite-like" examples of a rare target. As a case-study application of this procedure, we show the simulation as applied to whales. Satellites are increasingly being used to detect and monitor large cetacean species, including the critically endangered North Atlantic right whale (*Eubalaena glacialis*). While rarely observed in satellite imagery, a large number of aerial photographs exist of these whales, allowing for a very substantial increase in available training data through this simulation technique. Image similarity metrics, commonly used in other forms of image synthesis, are used here to show that NST-simulated images strongly resemble actual satellite images of visually similar whales, both in color and structure.

4.1 Introduction

The North Atlantic right whale (*Eubalaena glacialis*, henceforth 'right whale') is a critically endangered baleen whale (Cooke 2020) with declining population numbers estimated at 340 individuals as of August 2022 (Pettis et al. 2023). Though historical right whale population decline was caused by commercial whaling (Reeves 2001), modern mortality events primarily occur due to ship strikes and entanglement in fishing gear (Knowlton and Kraus 2001; Pace et al. 2021). To mitigate these anthropogenic threats while balancing the need to maintain commercial activities, dynamic protection measures have been implemented to limit vessel speed and fisheries activities (Davies and Brillant 2019; Hausner et al. 2021). The implementation of these measures is informed by an understanding of whale location and movements, which in turn relies on accurate methods of whale detection and monitoring.

It is now well established that Very High Resolution (VHR) satellite imagery can be used to observe large whales (Abileah 2002; Fretwell et al. 2014; Cubaynes et al. 2019; Bamford et al. 2020; Corrêa et al. 2022; Khan et al. 2023), including right whales (Hodul et al. 2022, Davies et al. 2025). Most studies to date have used a manual scanning approach to find whales in the imagery, which is accurate but time-consuming. Automated detection approaches using Convolutional Neural Networks (CNNs) have also been developed, though their accuracy and broad application is currently limited by the lack of a large, robust training dataset of target whales (Höschle et al. 2021, Davies et al. 2025).

Guirado et al. (2019) and Borowicz et al. (2019) both trained detector CNNs using aerial photographs, with only Borowicz having downsampled them first, with 945 and 690 whale examples respectively. Using satellite imagery of whales directly to train detectors is still a challenge, due simply to the limited number of available images. Cubaynes and Fretwell (2022) have compiled a dataset of 633 annotated whale examples in WorldView-2, -3, GeoEye-1, and QuickBird-1 imagery. These include 463 southern right whales (*Eubalaena australis*), 56 humpback whales (*Megaptera novaeangliae*), 34 fin whales (*Balaenoptera physalus*), and 80 grey whales (*Eschrichtius robustus*). Davies et al. (2025) used a dataset of 428 large whales of various species in WorldView-2, -3, Pleiades Neo, and GeoEye-1 to train a two-step human-in-the-loop detector. However, Guirado et al. (2019), Browicz et al. (2019), Höschle et al. (2021), Cubaynes and Fretwell (2022), and Davies et al. (2025) all suggest that further increasing the number of available training images of whales will be important to improve the performance of detector models and better generalizing them to more study areas, different species, and varying sea conditions.

Green et al. (2023) trained a gray whale detector model using satellite whale observations and tested to see whether including non-downsampled aerial photographs in addition to the satellite observations for training would improve the model, finding no substantial improvement when training with the additional aerial photographs. They concluded that since preprocessing aerial photographs to a sufficient degree to make them resemble satellite imagery is difficult, it would be better to focus on building a larger database of satellite observations.

Other fields employing CNN classification in computer vision applications have begun training models using synthetic or simulated images (Tremblay et al. 2018), including in remote sensing applications (Zhang et al. 2022), allowing the creation of larger training datasets than would otherwise be available. This paper proposes a simple method to simulate satellite imagery from aerial photographs using a Neural Style Transfer (NST) model to transform aerial photographs of whales into simulated satellite imagery by applying the style of a satellite image to the content of an aerial photo. Using publicly available databases of aerial photographs of whales, this allows very quick production of a much larger dataset for training detector models; for instance, the Kaggle Right Whale Recognition aerial photograph database (Khan and Shashank 2015) contains 11,470 aerial photographs of right whales, which, if used to simulate satellite imagery, would create a training database with a similar size as used for ship detection (for example Kızılkaya et al. 2022). This is useful because the number of available aerial photographs of right whales is at least an order of magnitude larger than the available number of satellite imagery detection of right whales.

4.2 Data and Methods

4.3 Data

WorldView-3 imagery and aerial photography were acquired concurrently on April 24$^{\text{th}}$, 2021 in Cape Cod Bay. The satellite imagery was captured at 11:40 EDT (local time), covering 200 km^2 in two swaths (Catalog IDs 1040010067D36B00 and 10400100674B2100) as Standard 2A imagery, and preprocessed from the original 30 cm panchromatic and 2 m multispectral to a 15 cm resolution RGB image by Maxar, the imagery provider (Formeller 2020), through a proprietary process not revealed to the public. This imagery was chosen because it was the best commercially available resolution at the time of the study; while right whales are large animals, they are still relatively small objects when viewed from space. Corrêa et al. (2022) and Hodul et al. (2022) examined varying resolutions for satellite whale observation, and both concluded that higher resolution is generally best for whale detection. Aerial photography was acquired as part of a regular aerial survey effort by the Center for Coastal Studies (CCS) between the hours of 9:23 and 16:30 EDT using a standard RGB DSLR camera. See Hodul et al. (2022) for further details on the imagery and survey methods.

For the purpose of visual and quantitative comparison of simulated and actual satellite imagery, a set of 39 image *reference pairs* were compiled. Figure 4.1 shows an example of four such reference pairs; the full set of 39 can be found as supplementary material. These four pairs were specifically chosen to cover most of the typical whale behaviors/signatures visible in satellite imagery, as identified by Cubaynes et al. (2019) including wake, contour, blow, flukeprint.

It is important to note that the matched photographs do not necessarily show the *exact* whale observed in the satellite imagery, but rather have been

Figure 4.1: Four representative examples of aerial photograph and satellite imagery pairs of right whales, the reference pairs. Pairs do not necessarily contain the same exact whale, rather they have been chosen from near-concurrent imagery to very closely resemble each other. Panels are labelled as a) through d) to allow easier comparison to the corresponding whales across other figures. Center for Coastal Studies NOAA federal permit #19315–01. Satellite image © 2022 Maxar Technologies.

chosen because they very closely resemble the satellite observations, allowing for the closest possible comparison. Nevertheless, pairs come from the same date and location, meaning that water quality, sea state, and atmospheric conditions are as close to identical as practically possible.

4.3.1 Neural Style Transfer

NST is an application of a Convolutional Neural Network (CNN) that is designed to blend two or more images together (Singh et al. 2021; Cai et al. 2023), introduced by Gatys et al. (2015). The concept of NST is likely more familiar to readers in the form of online tools meant for amusement, which can be used to make regular photos resemble paintings, as in Figure 4.2. By providing a "content" image, typically a photo, and a "style" image, typically a painting, the NST is able to blend them together to make the content of the photo seem like it was painted in the style of painting.

The NST works by using the intermediate layers of a pretrained CNN to extract the textural and color components ("features") from the style image, and the positional (shape) components of the content image. The model then iteratively creates an output image which satisfies both the textural and color elements of the style image and the positional elements of the content image, working toward a predetermined (assigned) balance between the two inputs. The output of an NST can thus be tuned to more closely resemble the texture and color of the style image, or more preserve the spatial coherence of the content image.

NST may be suitable for simulating satellite imagery from aerial photographs for the purpose of using the simulated imagery as training input to a whale-detection CNN, because CNNs detect whales not primarily from the spectral

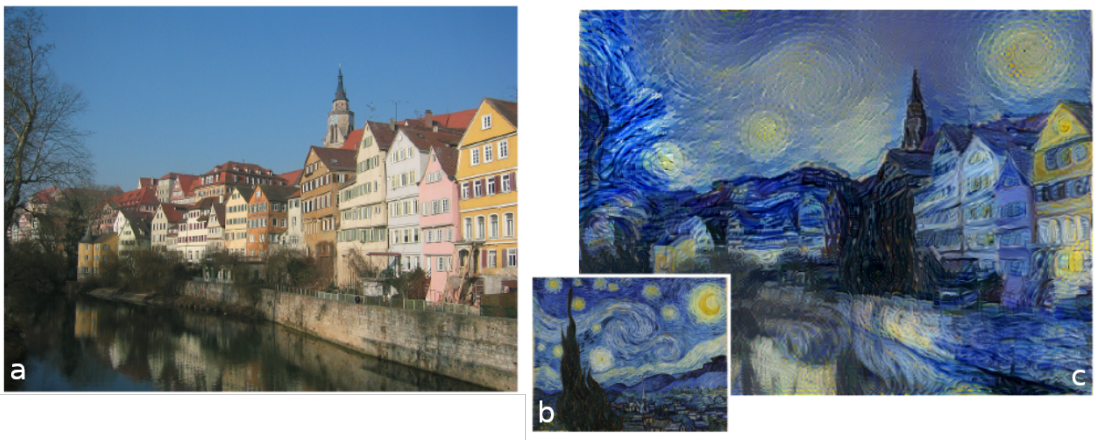

Figure 4.2: An example of the typical application of an NST model (adapted from Gatys et al. (2015)), showing the content image (a) of a row of houses, the style image (b) of Starry Night, and the resulting NST output (c) where the content image has been made to resemble the style of the painting.

properties of individual pixels but rather based on the shape and texture of image sections. Here, we use the aerial photographs as content images, and an actual satellite image of a whale as the style image. The goal is to create simulated images in the *style* of satellite imagery, using the *content* of the aerial photographs.

We adapted code from Chollet (2020), who based his code on Gatys et al. (2015), which uses the ubiquitous VGG19 model pretrained on the ImageNet database for feature extraction. There are three model parameters which, by assigning weights to each, can be used to tune the simulated image: *Style Loss* determines how much of the "style" of the style image ends up in the simulated image; *Content Loss* determines how much of the content image remains; and *Total Variation Loss* maintains local coherence of objects in the output. Additional details on these three parameters can be found in Gatys et al. (2015). Here, their values were determined experimentally by examining results from a set parameter space and selecting the parameters which yielded the best visual results; in general, the model required high *style* weight, to force the output to look like a satellite image, a low *content* weight, to not require that the output look much like the original aerial photograph, and a very high *total variation* weight, to ensure that the shape of the whales would remain true to the aerial photo. Since whales and water texture appear different in imagery acquired by different satellite sensors due to spatial resolution, spectral properties, and blur/noise, simulated imagery must be produced separately for each sensor. In this demonstration we use 15 cm WorldView-3 imagery, but the process can, in principle, be used with any sensor with a sufficiently high spatial resolution, provided that at least one example of a whale observation exists for that sensor, to be used as a style image.

To create a dataset of simulated 15 cm WorldView-3 images, the model is

Figure 4.3: The style image used to simulate 15 cm WorldView-3 imagery from aerial photographs, showing North Atlantic right whale Halo as seen in Cape Cod Bay on 24 April, 2021. Satellite image © 2022 Maxar Technologies.

run on each aerial photograph (the content images), with a single style image, Figure 4.3, being kept constant: the satellite image of Halo from the 24 April 2021 Cape Cod Bay imagery in Hodul et al. (2022). This image was chosen because it is an example of a right whale in satellite imagery of which we are certain because the aerial survey observation was near-simultaneous and concurrent to the satellite acquisition; it is also a representative example of a right whale seen in 15 cm WorldView-3 imagery, with fins and callosities visible.

The scale of each aerial photograph is estimated by assuming that the whale in each photograph is 12.5 m long, the average length of a modern adult right whale (Stewart et al. 2021). Whale length, in photo pixels, is measured manually for each photograph (Cubaynes et al. 2023), and thus a resolution for each photograph is estimated. This value is then used to calculate the output size of the simulated image to achieve a desired target resolution, in this case 15 cm.

4.3.2 Image Similarity Metrics

Image similarity metrics are used in computer vision tasks to directly compare two images to each other, and calculate a quantitative assessment of how similar the two images are. Consider comparing the same image to itself: this comparison would yield a "perfect" similarity score. Modifying one of the images slightly would yield a slightly worse similarity score, and comparing two extremely different images would yield a poor similarity score. Many similarity metrics have been developed for various uses.

Here, to quantitatively assess the quality of the simulation method, two image similarity metrics were used to compare the simulated images to their reference pairs (Figure 4.1), one to measure the accuracy of the simulated colors, and the other to measure the accuracy of the simulated structure. Relative Globale Adimensionnelle de Synthèse (ERGAS) directly compares pixel values between two images (Wald 2002), and was chosen as an indicator of the quality of the color simulation, while the Structural Similarity Index Measure (SSIM) compares pixel intensities within a sliding window (Wang 2004), and was chosen as an indicator of the quality of the structural component (Zhang 2022).

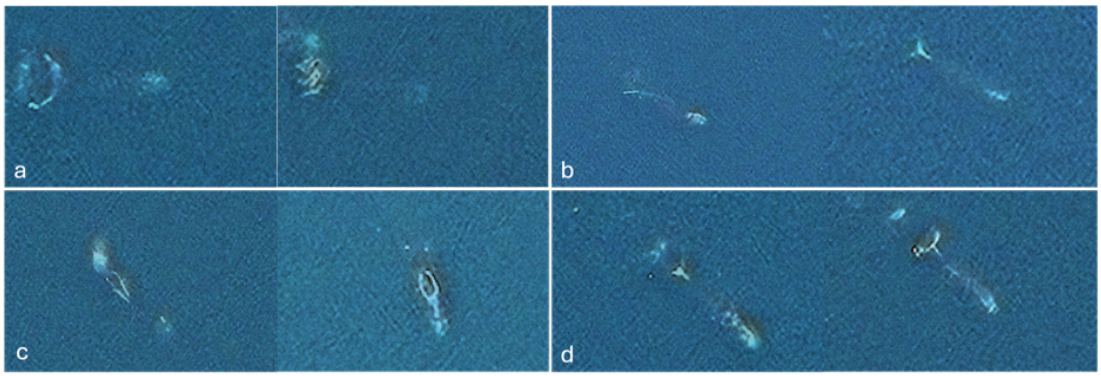

Figure 4.4: Visually similar satellite whale observations, used to create a baseline value for the similarity metrics, indicating what a "perfectly" simulated image might score. Panels are labelled as a) through d) to allow easier comparison to the corresponding whales across other figures. Satellite image 2022 Maxar Technologies.

Since the simulation is an iterative process, we can calculate the similarity metrics for each successive iteration, producing a curve illustrating the increasing similarity between the simulated and reference image as the simulation proceeds. Here, we run the simulation through 4000 iterations, a value arrived at experimentally, having observed that little to no change in the simulated imagery occurs with additional iterations.

In addition to the reference pairs discussed above, a further set of similar imagery observations of the whales is needed to create a baseline of similarity scores against which to judge the performance of the simulation model (Figure 4.4). We would not expect even perfectly simulated imagery to be identical to the satellite image in its reference pair, due to slight differences in whale position, splashing, depth, etc. However, we would expect perfectly simulated imagery to be about as similar to its reference image as that reference image is similar to another visually similar satellite image of a whale, because this image would have the same degree of difference in whale position, splashing, etc. In other words, we would expect that a perfectly simulated image would achieve the same score on a given similarity metric as a similar satellite image, when both are compared to the reference image. This allows us to define a target similarity metric score that will quantify how successful the simulation has been.

To assess the image similarity scores of the entire 39-image dataset, a "success" value is calculated using Equation 4.1 separately fro ERGAS and SSIM for each image i.

$$success_i = \frac{A - S}{A - T} \tag{4.1}$$

where A is the similarity between the aerial photograph and its reference image, S is the similarity metric between the final simulated image and its reference image, and T is the similarity metric between the "similar" satellite image and

its reference image. This score measures how far the simulation moved each similarity metric from the original photo towards the similarity expected of a perfectly simulated image.

4.4 Results

Figure 4.5 shows the simulated imagery results for the four example aerial photos used throughout this paper; the full set of 39 aerial/satellite image pairs can be found in Appendix A. Visually, the simulation appears to have been successful, especially regarding water texture and color.

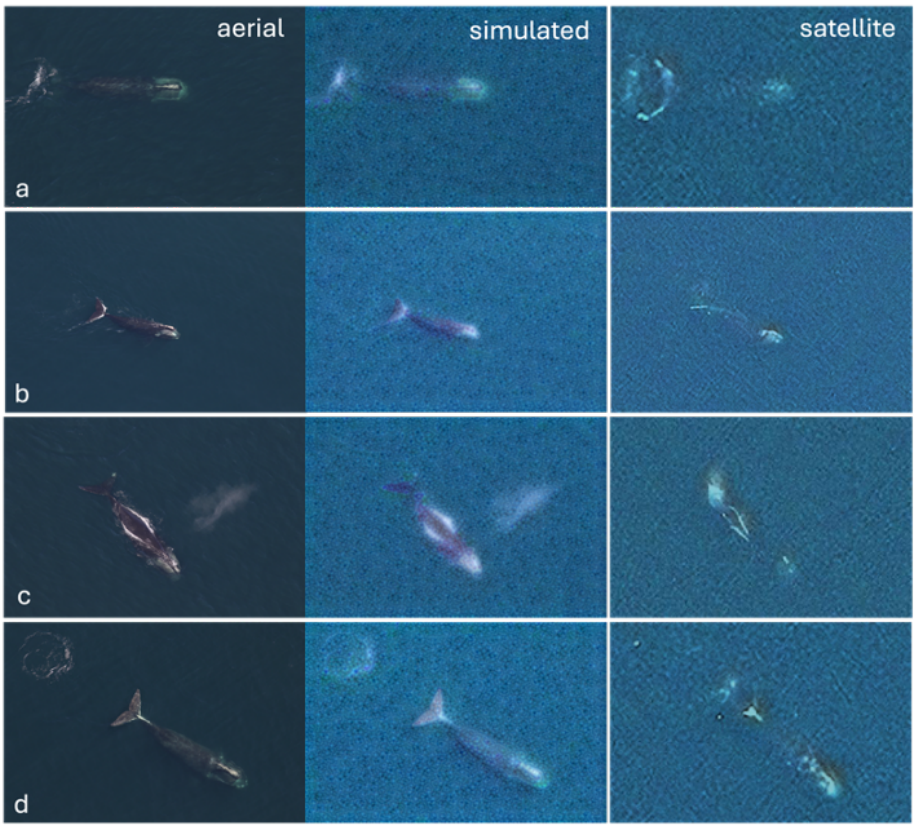

Figure 4.5: Simulated imagery (center column) from the four example photographs (left column), alongside satellite imagery reference pairs (right column). Panels are labelled as a) through d) to allow easier comparison to the corresponding whales across other figures. Center for Coastal Studies NOAA federal permit #19315–01. Satellite image © 2022 Maxar Technologies.

Figure 4.6 shows the ERGAS and SSIM similarity metric values for each image, as a function of the iteration number from 1 to 4000, as well as similarity metric values for raw photo/imagery pairs (as in Figure 4.1) and similar pairs

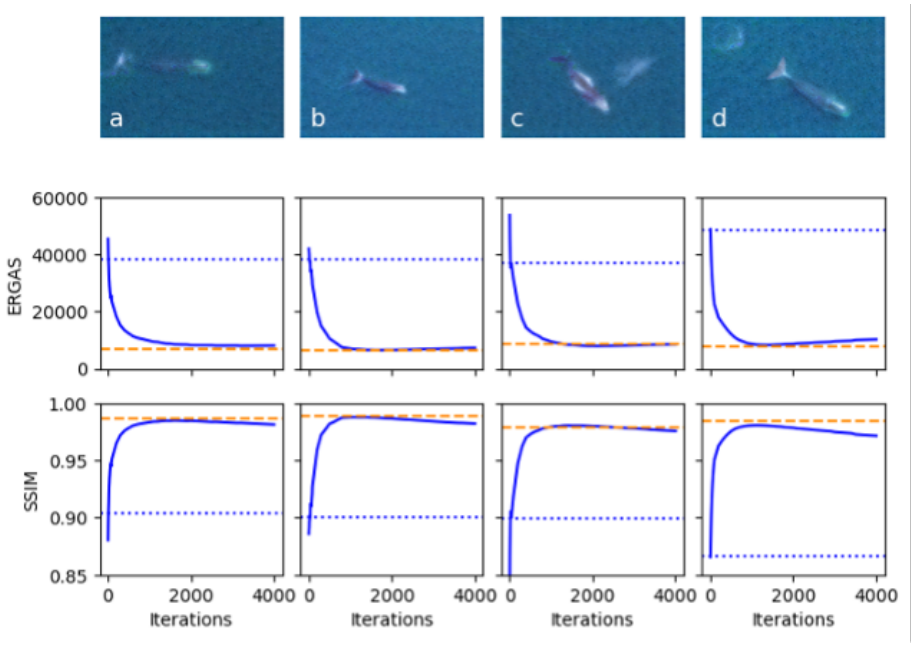

Figure 4.6: Similarity metrics for the four example images, showing similarity between: simulated imagery and reference pair (solid blue curve) as the simulation progresses through 4000 iterations; the raw aerial photograph and satellite reference pair, as in Figure 4.1 (blue dotted horizontal line); and the two "similar" satellite observations, as in Figure 4.4 (orange dashed line). Panels are labelled as a) through d) to allow easier comparison to the corresponding whales across other figures.

(as in Figure 4.4). Note that a perfect ERGAS score (in which the two images being compared are exactly identical) would be 0, and a perfect SSIM score would be 1; for both metrics, the scores for the simulated images get closer to the corresponding perfect score as the simulation progresses, and the simulated index scores stabilize at, or very close to, the metric values for the similar pairs, indicating that the simulated imagery is about as similar to its reference image as that reference image is to a similar satellite image.

In all examples, the simulated images are an improvement over the raw aerial photographs in terms of how similar they look to satellite imagery, and resemble satellite imagery more than the originals, both visually and according to ERGAS and SSIM.

Figure 4.7 summarizes the calculated success values for the 39 images; the complete table can be found in the supplementary information. ERGAS had a mean success value of 79.8% and median of 84.2%, while SSIM had a mean of 73% and median of 78%. In general, simulated photos with good ERGAS success values also had good SSIM success values (for instance, the ERGAS success value of 182% and the SSIM success value of 145% are from the same image). Success values higher than 100% can occur when the similarity metric of the simulated imagery ends up being better than the corresponding metric

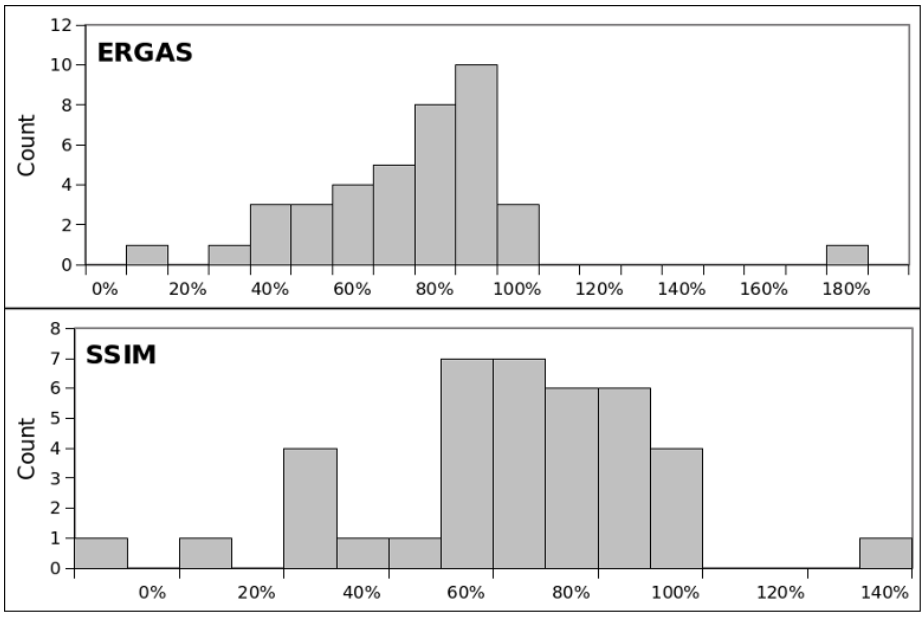

Figure 4.7: Histograms summarizing the ERGAS and SSIM success scores for all 39 images.

between the "similar" satellite image and reference image. The single negative success value for SSIM resulted from the simulated image getting a worse SSIM metric score than the "similar"-reference SSIM metric for that photo. These extreme values are likely caused due to the similarity of the "similar"-reference satellite image pairs not being of high quality, which is a limitation of the satellite imagery used in this study.

It appears that no further improvement to simulation quality, and indeed in some cases a decrease in simulation quality, is seen after about 1500 iterations, notably in examples (b) and (d). Since NST simulations are computationally slow, practical application of this method could be limited to around 1500 iterations in order to save processing time while maintaining simulation quality. Running on a NVIDIA *GeForce GTX 1660 Super GPU*, a simulation of a 5472 x 3648 pixel aerial photograph takes 9.5 minutes to reach 4000 iterations; smaller images take significantly less time.

Since only one style image is used for the NST modeling, it is necessary to examine what effect the choice of style image has on the results. Figure 4.8 presents a grid of style images and content images, showing the variation in simulation output for each of the four aerial photos shown in Figures 4.5 and 4.6, combined with style images showing various whale behaviours.

Visually, the simulated images don't appear to be very sensitive to the choice of style image. Calculating the success scores for the complete 39-image dataset for each style image (Table 4.1) reveals small differences in the overall quality of the simulations, with the large splash style image (Figure 4.8b) having a significantly worse score than the original style image, while the obscured whale

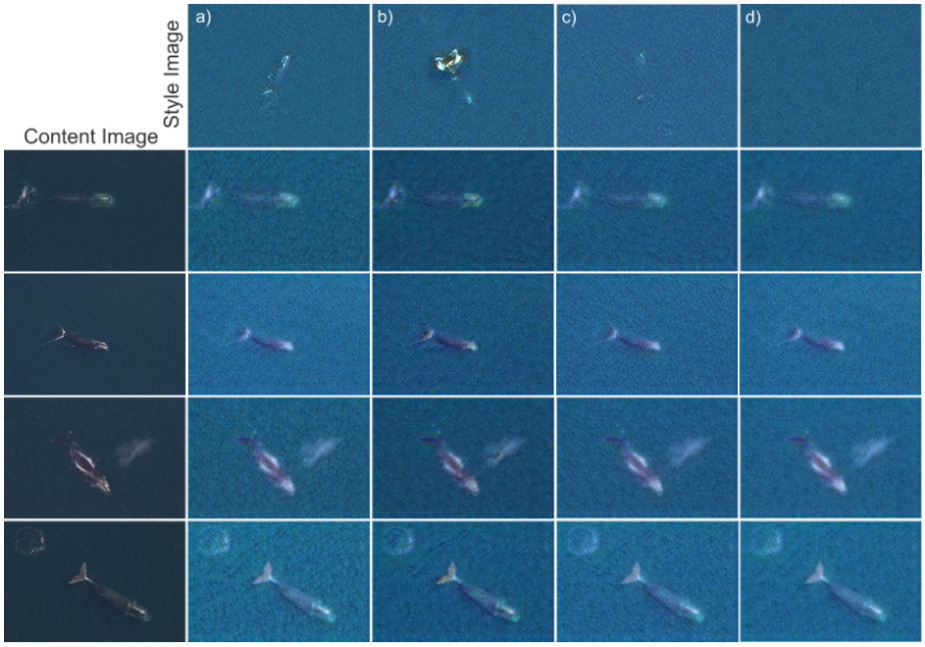

Figure 4.8: An example of different style images used during the NST process: a) the original style image, chosen to show a representative amount of wake, body visibility, and fluke pattern; b) showing a very large amount of splash pattern; c) showing the whale almost completely obscured; and d) plain water. Center for Coastal Studies NOAA federal permit #19315–01. Satellite image 2022 Maxar Technologies.

and plain water (Figures 4.8c and 4.8d) had slightly better scores. This seems to suggest that it is possible to run an NST simulation for a sensor, for the purposes of developing training data for whale detection, without having an example of the target whale species in imagery from that sensor.

4.5 Discussion

The field of satellite whale detection broadly agrees that the current bottleneck to development of a robust whale detector is the lack of training data needed

Table 4.1: Results of the success scores for the full 39-image dataset when simulated using a) the original style image, chosen to show a representative amount of wake, body visibility, and fluke pattern; b) showing a very large amount of splash pattern; c) showing the whale almost completely obscured; and d) plain water.

	a) original	b) large splash	c) obscured whale	d) plain water
ERGAS mean	79.8%	67.4%	81.5%	83.3%
ERGAS median	84.2%	68.0%	85.6%	89.8%
SSIM mean	73.8%	56.8%	77.1%	77.0%
SSIM median	78.0%	56.7%	81.9%	79.4%

to train models over a wide range of whale species, poses, environmental conditions, and locations. The most obvious method to generate more training data is simply to gather more satellite imagery of whales, and this is indeed being done, albeit at a very slow pace: Whale observations are rare, especially those of the North Atlantic right whale, and to build a detector which might more quickly gather such observations itself requires training data. Instead, researchers have looked to other data sources for model training, traditionally aerial photographs. While directly using aerial photographs, or downsampling them first, has been done in previous studies with moderate success, we believe that modifying them to more closely resemble satellite imagery before training can increase model performance. This is inherently intuitive: if the model is to detect whales in imagery acquired by a given sensor, it must learn what whales look like *in imagery acquired by that sensor*. Here we demonstrate that NST can be used to convert aerial photography into simulated satellite imagery, and that this simulated satellite imagery is more similar to actual satellite imagery (according to image similarity metrics) than the aerial photos themselves. This study is unique because of the aerial/satellite image pairs used to calculate image similarity metrics. To be able to use image such metrics to examine how "close" an NST simulation has gotten to an actual satellite image, concurrent observations of a whale in satellite and aerial are needed; the whale and water conditions need to look the same in both. No other study to date has been able to achieve sufficiently concurrent observations.

Other methods of training data preparation, development, or generation may also be possible, and further research into these would be a valuable undertaking. From simple methods such as colour-normalization or histogram-matching of aerial photos, to more complex undertakings such as using a Generative Adversarial Network (GAN) or even 3D modelling to generate images, many possibilities exist and should be explored. Here, we presented one such option, NST-based modification of aerial photos. Another benefit of using NST simulations is the ease of transferring the simulation to a different sensor: the NST need only be run using a different style image, one from the desired sensor, to create a new simulated dataset for that sensor. Indeed, it this study shows that it may not even be necessary to have a whale observation in the new sensor to run the simulation, a feature which would be extremely useful when modelling for brand new sensors for which we do not yet have whale observations.

In the next chapter, a larger, more detailed comparison of methods will be conducted, comparing detector models trained on a variety of different training data types, including the NST proposed here, downsampled aerial photos, and actual satellite observations.

4.6 Conclusion

The use of CNNs to detect whales in satellite imagery is a promising development in the whale conservation field, but the need for large training datasets is complicated by the relative rarity of whale observations in satellite imagery. To

better train whale-detector CNNs, this paper presents a novel method of simulating satellite imagery of whales using a Neural Style Transfer model applied to abundant aerial photographs of whales, increasing the available bank of training imagery of rare, endangered whales by more than an order of magnitude. Importantly, the method presented here does not rely on aerial photo metadata (camera used, flying altitude, atmospheric conditions, etc.), significantly simplifying its application.

The current best effort to compile actual satellite images of whales contains 633 satellite observations of a variety of whale species (Cubaynes et al. 2022), acquired with four different satellite sensors. In comparison, our method can immediately expand the available training imagery by 11,470 observations of the right whale alone, by applying our simulation procedure to the publicly available Kaggle *Right Whale Recognition* aerial photograph database (Khan and ShaShank 2015). Results presented here demonstrate that simulation of satellite imagery from aerial photographs improves image similarity metrics. A full applied comparison of training data types in a detector model will be presented in the next chapter.

4.7 Acknowledgements

This project was undertaken with the financial support of the Canadian Space Agency and the Department of Fisheries and Oceans in collaboration with Transport Canada, as part of the Canadian Space Agency "smartWhales" initiative to explore improved methods for the detection and modeling of North Atlantic right whales using space-based data sources. Data provided by the North Atlantic right whale programs through projects at the Center for Coastal Studies (CCS) funded by Massachusetts Division of Marine Fisheries through a grant from NOAA. Data were collected under NOAA federal permit #19315-01. Specific thanks to Brigid McKenna, Christy Hudak, and Charles Mayo at the CCS for support on this project. The participation of the University of Ottawa in this project has been undertaken as a team member led by Fluvial Systems Research Inc.

4.8 References

Abileah, R. 2002. Marine mammal census using space satellite imagery. U.S. Navy Journal of Underwater Acoustics, 52(3), 709-724.

Bamford, C.C.G., Kelly, N., Dalla Rosa, L., Cade, D.E., Fretwell, P.T., Trathan, P.N., Cubaynes, H.C., Mesquita, A.F.C., Gerrish, L., Friedlaender, A.S., Jackson, J.A., 2020. A comparison of baleen whale density estimates derived from overlapping satellite imagery and a shipborne survey. Sci. Rep. 10, 1–12. https://doi.org/10.1038/s41598-020-69887-y

Borowicz, A., Le, H., Humphries, G., Nehls, G., Höschle, C., Kosarev, V., Lynch, H.J., 2019. Aerial-trained deep learning networks for surveying cetaceans from satellite imagery. PLoS ONE 14, e0212532. https://doi.org/10.1371/journal.pone.0212532

Cai, Q., Ma, M., Wang, C., and Li, H. Image neural style transfer: A review. 2023. Computers and Electrical Engineering, 108. https://doi.org/10.1016/j.compeleceng.2023.108723

Chollet, F. 2020. Neural style transfer. Keras Code Examples. https://keras.io/examples/generative/neural_style_transfer/ accessed: 15 March 2023.

Cooke, J.G. 2020. Eubalaena glacialis (errata version published in 2020). The IUCN Red List of Threatened Species 2020: e.T41712A178589687. https://dx.doi.org/10.2305/IUCN.UK.2020-2.RLTS.T41712A178589687.en

Corrêa, A.A., Quoos, J.H., Barreto, A.S., Groch, K.R., Eichler, P.P.B., 2022. Use of satellite imagery to identify southern right whales (Eubalaena australis) on a Southwest Atlantic Ocean breeding ground. Mar. Mammal Sci. 38, 87–101. https://doi.org/10.1111/mms.12847

Cubaynes, H.C., Fretwell, P.T., Bamford, C., Gerrish, L., and Jackson, J.A. 2019. Whales from space: Four mysticete species described using new VHR satellite imagery. Marine Mammal Science, 35(2), 466-491. https://doi.org/10.1111/mms.12544

Cubaynes, H.C., Fretwell, P.T., 2022. Whales from space dataset, an annotated satellite image dataset of whales for training machine learning models. Sci Data 9, 245. https://doi.org/10.1038/s41597-022-01377-4

Cubaynes, H. C., Clarke, P. J., Goetz, K. T., Aldrich, T., Fretwell, P. T., Leonard, K. E., and Khan, C. B. 2023. Annotating very high-resolution satellite imagery: a whale case study. MethodsX, 10. https://doi.org/10.1016/j.mex.2023.102040

Davies, K.T.A., and Brillant, S.W. 2019. Mass human-caused mortality spurs federal action to protect endangered North Atlantic right whales in Canada. Marine Policy, 104, 157-162. https://doi.org/10.1016/j.marpol.2019.02.019

Davies, K.T.A., Webster, A., Babu, V., Brillant, S.W., Carlyle, C.G., Lonati, G.L., Sharma, H., and Tsui, O.W. 2025. Semi-automated detection of right whales (Eubalaena spp.) in very high-resolution satellite imagery. Marine Mammal Science, (early preview version). https://doi.org/10.1111/mms.70024

Formeller, C. 2020. Introducing 15 cm HD: The Highest Clarity From Commercial Satellite Imagery. Blog: https://blog.maxar.com/earth-intelligence/2020/introducing-15-cm-hd-the-highest-clarity-from-commercial-satellite-imagery, accessed 2021-10-04.

Fretwell, P.T., Staniland, I.J., and Forcada, J. 2014. Whales from Space: Counting Southern Right Whales by Satellite. PLoS ONE, 9(2). https://doi.org/10.1371/journal.pone.0088655

Gatys, L.A., Ecker, A.S., Bethge, M., 2015. A Neural Algorithm of Artistic Style. Journal of Vision, 16(12). https://doi.org/10.1167/16.12.326

Green, K.M., Virdee, M.K., Cubaynes, H.C., Aviles-Rivero, A.I., Fretwell, P.T., Gray, P.C., Johnston, D.W., Schönlieb, C., Torres, L.G., Jackson, J.A., 2023. Gray whale detection in satellite imagery using deep learning. Remote Sens Ecol Conserv 9, 829–840. https://doi.org/10.1002/rse2.352

Guirado, E., Tabik, S., Rivas, M.L., Alcaraz-Segura, D., Herrera, F., 2019. Whale counting in satellite and aerial images with deep learning. Sci Rep 9, 14259. https://doi.org/10.1038/s41598-019-50795-9

Hausner, A., Samhouri, J.F., Hazen, E.L., Delgerjargal, D., and Abrahms, B. 2021. Dynamic strategies offer potential to reduce lethal ship collisions with large whales under changing climate conditions. Marine Policy, 130, 104565. https://doi.org/10.1016/j.marpol.2021.104565

Hodul, M., Knudby, A., McKenna, B., James, A., Mayo, C., Brown, M., Durette-Morin, D., and Bird, S. 2022. Individual North Atlantic right whales identified from space. Marine Mammal Science, 39 (1), 220-231. https://doi.org/10.1111/mms.12971

Höschle, C., Cubaynes, H.C., Clarke, P.J., Humphries, G., and Borowicz, A. 2021, The potential for satellite imagery for surveying whales. Sensors, 21, 963. https://doi.org/10.3390/s21030963

Khan, C.B., Shashank, W.K. (2015). Right Whale Recognition. https://kaggle.com/competitions/noaa-right-whale-recognition

Khan, C.B., Goetz, K.T., Cubaynes, H.C., Robinson, C., Murnane, E., Aldrich, T., Sackett, M., Clarke, P.J., LaRue, M.A., White, T., Leonard, K., Ortiz, A., and Ferres, J.M.L. 2023. A Biologist's Guide to the Galaxy: Leveraging Artificial Intelligence and Very High-Resolution Satellite Imagery to Monitor Marine Mammals from Space. J. Mar. Sci. Eng. 11, 595. https://doi.org/10.3390/jmse11030595

Kızılkaya, S., Alganci, U., Sertel, E. 2022. VHRShips: An Extensive Benchmark Dataset for Scalable Deep Learning-Based Ship Detection Applications. International Journal of Geo-Information, 11, 445. https://doi.org/10.3390/ijgi11080445

Knowlton, A.R., and Kraus, S.D. 2001. Mortality and serious injury of northern right whales (Eubalaena glacialis) in the western North Atlantic Ocean. Journal of Cetacean Research and Management, 2, 193-208. https://doi.org/10.47536/jcrm.vi.288

Pace III, R.M., Williams, S., Kraus, S.D., Knowlton, A.R., and Pettis, H.M. 2021. Cryptic mortality of North Atlantic right whales. Conservation Science and Practice, 3(2). https://doi.org/10.1111/csp2.346

Pettis, H.M., Pace, R.M. III, Hamilton, P.K. 2023. North Atlantic Right Whale Consortium 2022 Annual Report Card. Report to the North Atlantic Right Whale Consortium.

Reeves, R.R. 2001. Overview of catch history, historic abundance and distribution of right whales in the western North Atlantic and in Cintra Bay, West Africa. J. Cetacean Res. Manage., 2, 187-192.

Singh, A., Jaiswal, V., Joshi, G., Sanjeeve, A., Gite, S., Kotecha, K., 2021. Neural Style Transfer: A Critical Review. IEEE Access 9, 131583–131613. https://doi.org/10.1109/ACCESS.2021.3112996

Stewart, J.D., Durban, J.W., Knowlton, A.R., Lynn, M.S., Fearnbach, H., Barbaro, J., Perryman, W.L., Miller, C.A., and Moore, M.J. (2021). Decreasing body lengths in North Atlantic right whales. Current Biology, 31, 3174-3197. https://doi.org/10.1016/j.cub.2021.04.067

Tremblay, J., Prakash, A., Acuna, D., Brophy, M., Jampani, V., Anil, C., To, T., Cameracci, E., Boochon, S., and Birchfield, S. 2018. Training deep networks with synthetic data: Bridging the reality gap by domain randomization. IEEE/CVF Conference on Computer Vision and Pattern Recognition Workshops (CVPRW), 1082-10828. https://doi.org/10.1109/CVPRW.2018.00143

Wald, L. 2002. Data Fusion. Definitions and Architectures - Fusion of images of different spatial resolutions. Presses de l'Ecole, Ecole des Mines de Paris, Paris, France, pp.200, 2002, ISBN 2-911762-38-X. Ffhal-00464703f

Wang Z., Bovik A.C., Sheik H., Simoncelli E. (2004). Image quality assessment: from error visibility to structural similarity. IEEE Transactions on Image Processing, 13 (4): 600-612. doi: http://dx.doi.org/10.1109/TIP.2003.819861

Zhang, R., Isola, P., Efros, A.A., Shechtman, E., and Wang, O. 2018. The unreasonable effeciveness of deep features as a perceptual metric. IEEE/CVF Conference on Computer Vision and Pattern Recognition, Salt Lake City, UT, USA, 2018, pp. 586-595, doi:10.1109/CVPR.2018.00068

Zhang, C., Wang, Y., Liu, H., Sun, Y., Hu, L., 2022. SAR Target Recognition Using Only Simulated Data for Training by Hierarchically Combining CNN and Image Similarity. IEEE Geosci. Remote Sensing Lett. 19, 1–5. https://doi.org/10.1109/LGRS.2022.3141389

Chapter 5

Comparison of Training Imagery Types for Satellite Detections of North Atlantic Right Whales

Matus Hodul[1], Anders Knudby[1], Stephen Bird[2]

[1] University of Ottawa, Department of Geography, Environment, and Geomatics. Ottawa, Ontario, Canada
[2] Fluvial Systems Research Inc., Surrey, British Columbia, Canada

---

This paper addresses the third research objective outlined in Section 1.1.1

> **Compare the new training dataset to existing types of training data to determine which type yields the best results:** Using a standardized whale detection model, test several types of training data, including those currently used in the field and the new dataset developed here. Assess model performance for each dataset and compare them.

Author attributions: MH conceptualized the study, performed the work, and wrote the manuscript. AK assisted in conceptualization, provided feedback, and helped with editing. SB was the principle investigator and helped secure funding.

Abstract

Automated detectors are beginning to see use for North Atlantic right whale detection in satellite imagery in an academic setting, and conservation efforts will likely benefit greatly from their continued improvement and ultimately their operational implementation. Current detector models are trained with either downsampled aerial photographs or satellite imagery chips, though both methods have shortcomings: downsampled aerial photographs don't look much like satellite imagery, and actual satellite imagery of these whales is rare. This work compares satellite right whale detector models trained on these two currently used training data types, as well as two newly proposed types: simulated imagery created using Neural Style Transfer (NST), and colour-normalized aerial photographs. Detectors trained using NST prove to be slightly more accurate than those trained using colour-normalized photos, both of which are significantly more accurate than those trained on downsampled aerial photos. Models trained on satellite imagery are limited by the lack of variability in training data. Unless the researcher has access to a very large, high-quality satellite dataset of their target whale, it is recommended that they train detector models with aerial photographs that have undergone some form of preprocessing; whether NST or colour-normalization is used can be a decision balancing the need for accuracy versus the available processing time and resources, NST simulation being significantly more processing-intensive than colour-normalization.

5.1 Introduction

The North Atlantic right whale (*Eubalaena glacialis*), is a critically endangered baleen whale with population numbers estimated at 372 individuals as of September 2024 (Pettis and Hamilton 2025). Understanding whale movements is critical for conservation efforts (Davies and Brillant 2019; Hausner et al. 2021), and while aerial and acoustic survey methods produce high-quality data, they can be costly and difficult to scale. In the past few years, satellite detection of right whales has become established as a promising addition to the toolkit of whale detection and monitoring (Höschle et al. 2021), allowing for surveying on a much larger spatial scale, albeit not as accurately as traditional survey methods.

Beginning with Ablieah (2002), who demonstrated the first known instance of whales in satellite imagery, many studies have now been put forth exploring various aspects of whale detection in satellite imagery (Fretwell et al. 2014; Borowizc et al. 2019; Cubaynes et al. 2019; Guirado et al. 2019; Bamford et al. 2020; Corrêa et al. 2021; Hodul et al. 2022; Rodofili et al. 2024; and Davies et al. 2025).

Borowizc et al. (2019) was the first to demonstrate a machine learning-based automated detector, using CNN models trained on aerial photographs downsampled to the same resolution as their target satellite imagery (WorldView-3 at 0.3 m), based on known flight and camera parameters. Guirado et al. (2019) furthered the CNN detection concept by introducing a two-step approach, where a CNN model first classifies imagery tiles as containing or not containing whales. Tiles in which whales were classified as present are then sent to a second CNN which applies bounding boxes around the whales. These models were also trained on an annotated set of aerial photographs. Guirado et al. (2019) did not downsample the aerial photographs during preprocessing. Davies et al. (2025) used satellite observations of whales directly to train their two-step model, with 428 observations of large whales including North Atlantic and Southern right, gray, and fin whales.

All three of the abovementioned CNN detector studies used a *pretrained* model, where the CNN is first trained on an unrelated extremely large dataset —in all three cases the ImageNet dataset (Deng et al. 2009) was used— then subsequently trained on the (relatively) much smaller target dataset, leading to greater accuracy than if the model was trained solely on the target dataset; a technique known as *Transfer Learning* (Brodzicki et al. 2020).

It is difficult to directly compare model accuracy between these three studies, since each used a different set and size of training data, different CNN architectures, and different target imagery. Nevertheless, all three studies, and other similar ones (Höschle et al. 2021; Cubaynes and Fretwell 2022), stress the need for expanding the available training data in order to improve model accuracies, and increase the applicability to different species, locations, and environmental conditions.

These studies have used two main sources of training data: aerial photographs, downsampled, as a proxy for satellite imagery, and actual satellite

imagery. While aerial photographs don't directly resemble satellite imagery, there is a much greater amount of it available for training data-hungry detector models. In Chapter 4, we introduced another form of training data: "satellite-like" imagery, derived from aerial photographs using a Neural Style Transfer algorithm. This, in theory, would provide the benefits of the training/target matching of satellite imagery, along with the abundance of aerial photographs.

Other training data treatments also exist, including simple colour-matching of downsampled aerial photos, and fully synthetic images. This paper will compare a number of training data types in training a whale detector, and will then discuss the advantages and disadvantages of each data type.

5.2 Data and Methods

Experiment design consisted of four identical CNN image classification models, each trained with a different type of training data. These models were then used to classify image chips from a unique test satellite image as either containing or not containing whales, and the performance of each model was assessed and compared using standard metrics.

5.2.1 Training Datasets

Here, we propose the categorization of training data into three broad types: Aerial, Satellite, and Synthetic. The **aerial** category includes raw aerial imagery, which is not typically used directly, as well as products derived from aerial photographs. Such products can include downsampled aerial photographs, which are commonly used; photographs with some sort of colour-matching to satellite imagery; and the previously mentioned NST "satellite-like" aerial images. The **satellite** category is simply satellite image chips (Cubaynes and Fretwell 2022). The fully **synthetic** category can include images generated using machine-learning algorithms such as Generative Adversarial Networks (GANs), or perhaps 3D rendered models.

This study will compare the use of four of the above-mentioned types of training data: 1) Downsampled aerial, 2) Downsampled aerial with colour matching, 3) NST, and 4) Satellite imagery.

Notably, we chose not to include GAN in our testing: we were unable to find a GAN model that seemed to create results suitable for use as training data. Several existing GAN models were investigated, including a version of Stable Diffusion specifically pretrained for satellite imagery, however all available models were suited for synthesizing satellite imagery of *land*, and failed to produce satisfactory results for marine environments and especially for producing convincing examples of right whales. Training a new GAN for production of whale imagery was considered, however due to the fact that GANs typically need significantly larger datasets to train than our limited number of satellite whale observations (Karras et al. 2020), creation of a custom GAN was not undertaken.

Non-downsampled aerial imagery was not included as one of the training data types, because Green et al. (2023) had demonstrated that little improvement is gained when including such imagery.

A final aspect of training data creation is that of the negative data: images without whales. For satellite imagery, such imagery is easy to come by as the vast majority of a given satellite image will be open water providing copious amounts of negative data. For aerial imagery, this is somewhat more challenging as survey crews specifically take photos of the whales they locate. Here, we use satellite imagery of open water.

Aerial Preprocessing and Downsampled Aerial

Aerial photographs were acquired from two sources: the aerial photographs provided by CCS used in Hodul et al. (2022); and the Kaggle right whale identification dataset (Khan and Shashank 2015). Photographs were manually annotated in a manner similar to Cubaynes et al. (2023), with the important addition of "whale framing", which describes whether framing is "complete", or only "partial" (i.e. whether or not the entire body of the whale is visible within the photograph). For photographs where the whale was completely in frame, whale length was measured from the tip of the lower jaw to the notch of the fluke (Christiansen et al. 2020). In instances where the fluke was difficult to see in the photograph due to being deeply submerged, a best estimate of length was given. A rotated bounding box was also drawn around the whales using the annotation software SuperAnnotate, to be used in later processing.

Only photographs where the whale is fully in frame were retained. Further filtering was done to remove photographs taken at extremely oblique angles, an observation geometry which doesn't occur in satellite imagery, and photographs with extreme levels of glint in which the whale is mostly obscured. Figure 5.1 shows an example of an acceptable photo (a), and non-acceptable photos (b-d).

Because the metadata for the aerial photographs from the Kaggle dataset were not available, photograph scale was estimated by assuming a whale size of 12.5 m (Stewart et al. 2021). For confirmation of the 12.5 m assumption, we checked the sizes of the whales seen in the imagery in Hodul et al. (2022), finding a mean whale length of 12.96 m with a standard deviation of 1.04 m. A photograph scale factor S was then calculated using Equation 5.1,

$$S = \frac{A}{LR} \tag{5.1}$$

where A is the assumed whale length of 12.5 m, L is the length of the whale in the photograph in pixels, and R is the target imagery resolution (0.3 m in the case of WorldView-3). In the case of two or more whales in the same photograph, the largest one was used as the basis for the scale calculation. Photographs were then downsampled using OpenCV with a bit-exact bilinear interpolation. Other downsampling methods were also investigated, including an area averaging method, but yielded worse results.

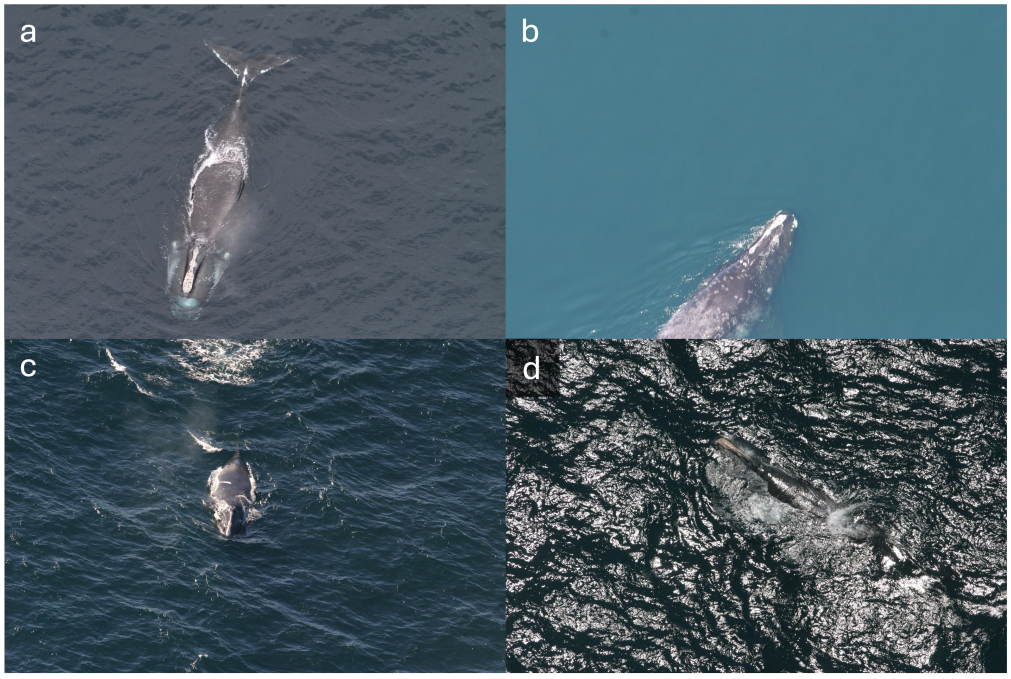

Figure 5.1: Examples of acceptable and non-acceptable aerial photographs from the Kaggle dataset. A) Acceptable; and non-acceptable because of: B) partial framing, C) oblique observation, and D) excessive glint. (Images: Khan and Shashank 2015)

Finally, a *padding* step was applied: The input images entering into a CNN are almost always square, with the exact dimensions determined by the particular architecture of the model; typically, if an input image doesn't conform to these dimensions, a preprocessing step is applied to scale/distort the image to match. Instead of applying such a distortion, we chose to pad the images out to the correct dimension by mirroring areas of open water in the aerial photographs, using the rotated bounding boxes. Figure 5.2 illustrates the padding process.

All aerial-derived methods used the same preprocessing procedure, ensuring that the datasets would be identical except for the specific image manipulation method intended to be applied.

Colour-Normalized Aerial

Colour normalization is performed using a histogram-matching technique, where the aerial photographs are modified such that the histogram of each colour band matches that of a reference image, in this case a satellite whale observation (the same image used as a style reference for the NST). This is performed using the Scikit-Image's *exposure* library, and is performed prior to downsampling; Figure 5.3d shows an example.

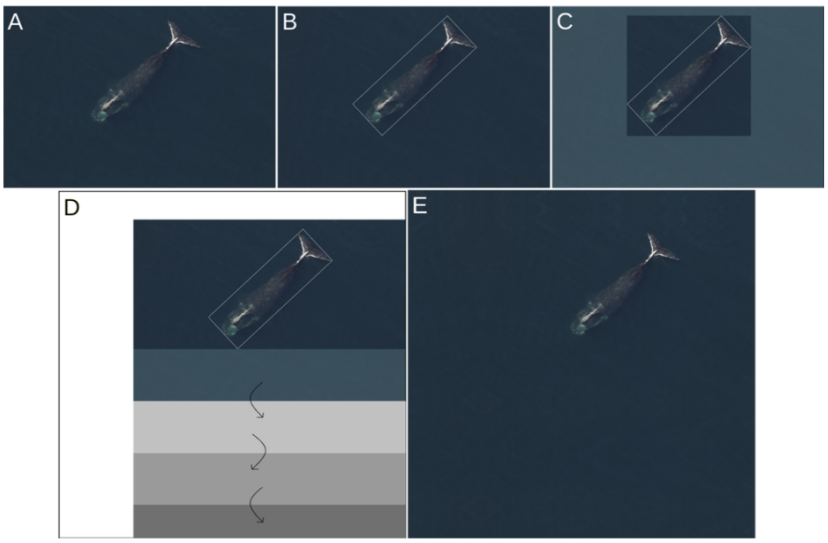

Figure 5.2: The procedure for padding aerial photographs: Starting with the original aerial photographs (A), a rotated bounding box is drawn around the whale (B). Areas outside of this bounding box are considered to contain only water (C). The number of pixels needed to pad out to the correct dimension are calculated, and the areas of only water are sequentially mirrored to achieve the correct dimension in each direction (D), resulting in the finished padded image (E). Center for Coastal Studies NOAA federal permit #19315–01.

NST Satellite-Like Imagery

Neural Style Transfer (NST) is a machine-learning based method for transferring the *style* of one image onto the *content* of another image (Gatys et al. 2015). Popularly, these are used to modify photographs to have the style of famous paintings. Here, NST is used to simulate satellite imagery from aerial photographs, essentially applying the "style" of an actual, rare, satellite observation of a whale to the content of many thousands of aerial photos. Details of the NST method as applied to aerial whale photographs, including an examination of image similarity between actual satellite imagery and NST simulated imagery can be found in Chapter 4; Figure 5.3e shows an example of one such simulation.

Satellite Image Chips

633 satellite imagery chips of whale observations are available from the dataset compiled by Cubaynes and Fretwell (2022). Whales observed include Southern right (463 of the chips), humpback (56), fin (34), and grey (80); each further classified into "Definite", "Probable", and "Possible" observations. Figure 5.4 shows an example of each species. Using southern right whales, as well as other species of whales, as a proxy to train a detector for North Atlantic right whales is an established technique (Davies et al. 2025).

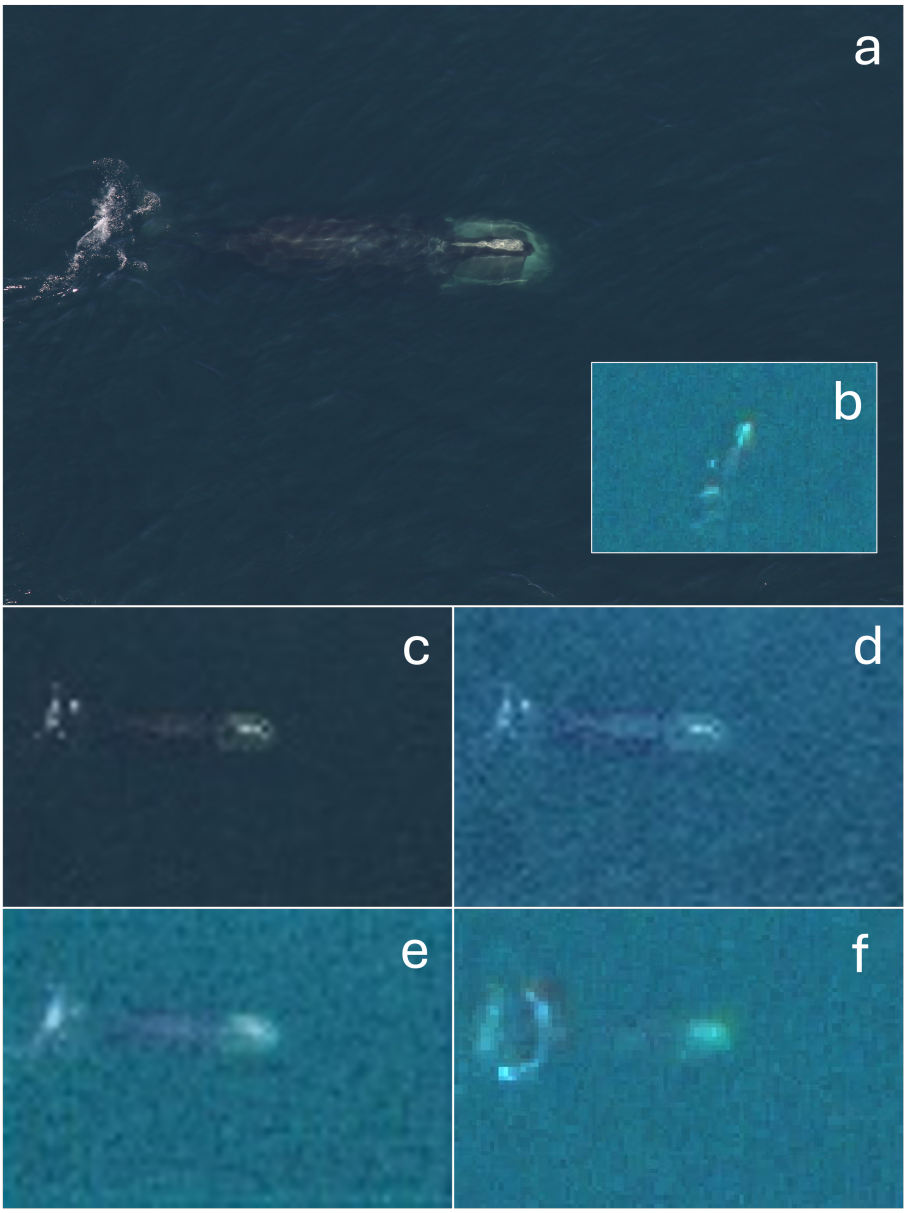

Figure 5.3: An example of the various pre-processing steps used to create the aerial-derived training datasets: a) The original aerial photograph, b) the satellite image used as reference for colour normalization and NST style, c) downsampled aerial, d) colour-normalized, e) NST satellite-like, and f) a similar-looking satellite observation of a whale (see Chapter 4 for explanation on these 'reference pairs'. Center for Coastal Studies NOAA federal permit #19315–01. Satellite image © 2022 Maxar Technologies.

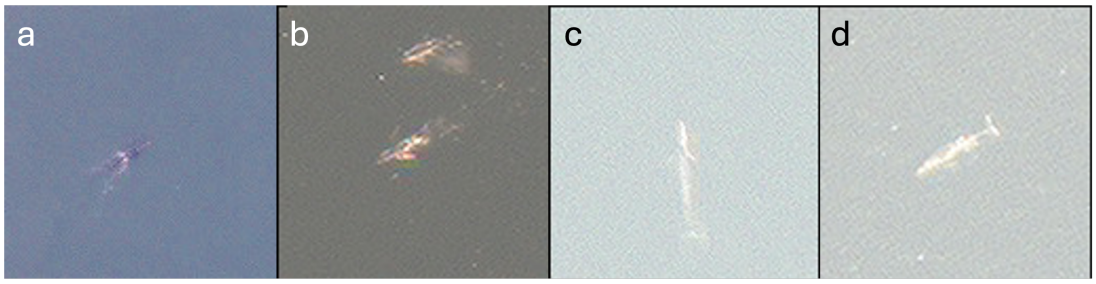

Figure 5.4: Example chips from the Cubaynes and Fretwell (2022) dataset, showing A) Southern right whale, B) humpback whale, C) fin whale, and D) grey whale.

5.2.2 Testing Data: Satelite Imagery

The detector models were tested on 200 km^2 of WorldView-3 imagery (Standard 2A) acquired on 24 April 2021 in Cape Cod Bay; see Hodul et al. (2022) for details on the imagery. A manual scanning approach found 39 whale observations (31 individual whales, some were observed twice a few seconds apart, due to two slightly overlapping swaths being acquired). A concurrent aerial survey by the Center for Coastal Studies (CCS) confirmed all observations as North Atlantic right whales. Imagery used in testing was pansharpened to 30 cm using the Brovey algorithm available in QGIS. Notably, this is different than the 15 cm imagery shown in the previous studies: partly this was done because the field of whale detection has so far *not* been using the 15 cm imagery, likely for cost and computational reasons, using 30 cm imagery for comparison is thus more relevant to common practice in the field.

5.2.3 The Detector Model

An existing, proven deep learning architecture was chosen to reduce the probability that poorly designed architecture would lead to unsatisfactory results. The model used was a VGG16 backbone, due to its proven ability to generalize on small datasets after being pre-trained (Chollet 2018), and its relatively small input size of 224x224 pixels, which may be helpful when dealing with satellite imagery of relatively small objects, as the object takes up more of the frame of the image (Chen et al. 2024).

Pretraining is a critical step in training models when a relatively small amount of training data is available, such as in the case of whale detection (Davies et al. 2025). Pretraining a model on an extensive, but unrelated, dataset allows for *transfer learning* to occur, where the CNN model learns to distinguish generic visual features before being *fine-tuned* on the target dataset — essentially, we are first teaching the model *how* to see with pretraining, and then we are teaching it *what to look for* with fine-tuning. The first layers of a model learn universal geometric features such as edges, and deeper layers learn increasingly abstract combinations of these features and later meaningful shapes. Because basic geometric shapes transfer well across object-based com-

puter vision tasks, pretraining can reduce the number of whale training data examples needed. Here, the model was pretrained on the well-known ImageNet database (Russsakovsky et al. 2015), with over 1.4 million images in 1,000 classes, including a whale class.

Data augmentation was applied to the training data to bolster the relatively small number of images; the same augmentation was applied to each model, which included rotation, zooming, stretching, and flipping. Reasonable values were chosen as ranges for each augmentation type. Of particular note is the zoom augmentation, which stretches or shrinks each training image by up to 15%. During image annotation, whale length was assumed to be 12.5 m for all whales; thus the range of possible whale sizes during augmentation becomes 10.6 m to 14.3 m, which is approximately the correct size distribution for right whales. Hyperparameters were kept constant for all models. The significant lack of testing data made it difficult to perform hyperparameter optimization, so hyperparameters were set to a standard value across all models.

5.2.4 The Experiment

A separate model was trained for each type of training data. For each model, the number of negative (non-whale) tiles was set equal to the number of positive tiles; these negative tiles were randomly selected from the available bank of imagery tiles. For the satellite image chips, a version of the dataset containing *all* data was tested, as well as a version containing only Southern right whales, and of those, only the "Definite" and "Probable" classes, reducing the dataset size from 633 chips to 260.

The testing imagery was divided into 332,307 tiles of 112x112 pixels, separated with a 25% overlap to ensure that each whale would be fully represented on at least one tile. This way, if any one tile encompassing a given whale observation was classified as 'whale', that whale could be considered found, even if other tiles encompassing the same whale did not return a positive classification. A tile size of 122 was used because a right whale, at about 13 m in length, in 30 cm imagery, and with a tile stride of 25%, will always be fully encompassed in at least one tile. Additionally, with the VGG model having an input tile size of 224 pixels, the tiles are easily scaled up to fit the model input. A tile size of 224 was tested but discarded due to quality issues with padding (Figure 5.2) at that size. The tiles were then sent to the models for inference, and the detector assigned each tile a confidence score, or probability, indicating how likely the tile was to contain a whale.

For validation, tiles actually containing whales were manually determined, and each whale was given a whale ID number. Since a given whale could appear in several tiles due to the overlap, this allowed the validation system to mark the whale as correctly found if any of the tiles containing that whale were classified correctly. This is in line with what would occur in an operational context. Model performance was calculated using precision, recall, and F1 score for chips identified as containing whales, using the standard equations for those values (Equations 5.2, 5.3, and 5.4).

$$Precision = \frac{True\ Positive}{True\ Positive + False\ Positive} \tag{5.2}$$

$$Recall = \frac{True\ Positive}{True\ Positive + False\ Negative} \tag{5.3}$$

$$F1 = Precision = 2 * \frac{Precision * Recall}{Precision + Recall} \tag{5.4}$$

Threshold curves for the above metrics were created by calculating the metrics for all tiles above a progressively increasing whale probability threshold, from 0.01 to 0.99 in increments of 0.001.

5.3 Results

The processing needed to create the four datasets varied significantly. Simply downsampling the aerial photographs took a negligible amount of time. Colour normalization took several seconds per photo, but the total computational time was not significant, the entire processing taking only a couple minutes. Additionally, neither preprocessing method requires specialized hardware to run, a simple computer without a dedicated GPU is sufficient. By contrast, the NST simulation for the entire 8,749 photo dataset took about one month of continuous processing using a NVIDIA *GeForce GTX 1660 Super* GPU, at about 3-10 minutes per photo depending on each photo's size. As of 2025, this is outdated hardware, and significantly less computational time might be expected with modern equipment. However, performing the simulation without a GPU would take significantly longer and would thus not be practically feasible. The satellite dataset was used directly in the format that it was downloaded in, so no computational time was spent in preprocessing.

Figure 5.5 shows the progressive threshold curves for each of the four training data methods, and Figure 5.6 shows the same data organized by metric instead of training method. For the satellite training method, dotted lines show the filtered dataset containing only Definite and Probably Southern right whales. The relatively very high precision but low recall of the model trained on satellite imagery is likely explained by the small number of high quality training data in that dataset: the model is very good at finding the types of whale observations that it has been trained on, but due to the small dataset, it hasn't had the opportunity to see many different kinds of right whale behaviour and appearance. With a significantly larger dataset, we might expect these metrics to improve. The filtered dataset has lower values across all performance metrics. This is expected, since we are further reducing an already very limited dataset, and even training data of whales of a different species are valuable to include.

Of the three aerial preprocessing methods, the results for downsampled aerial appear quite a bit different from NST and colour normalization. Peak F1 occurs at a much lower threshold, 0.42, as opposed to the other two which peak around 0.99 (Table 5.1), and the recall scores are lower at their respective F1 peaks

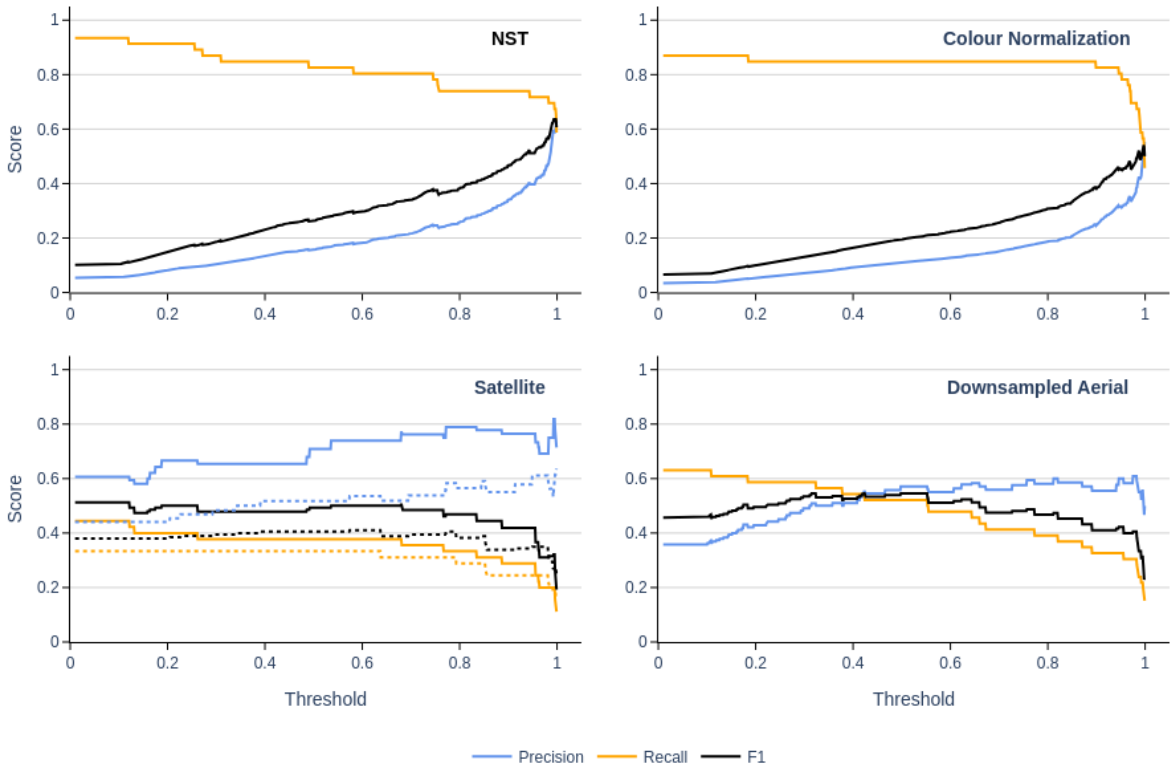

Figure 5.5: Progressive threshold curves showing precision, recall, and F1 score for the four training methods. Curves are created by using all detected points with a whale confidence score above the given threshold to calculate the metrics. A threshold range between 0.01 and 0.99 in increments of 0.001 is used. Dotted lines in satellite plot show the model trained using the filtered satellite dataset.

than NST. Furthermore, precision and recall for the downsampled aerial, at a threshold of around 0.99, is at 0.467 and 0.152 respectively. Given these values, and the understanding that generally, a higher recall is desirable for whale detection to reduce the likelihood of missing whales, some form of aerial photo preprocessing is desirable.

While metric values are slightly better for NST than colour normalization, the increase in detector performance comes at the cost of significantly increased preprocessing time and the requirements for a GPU, though the NST simulation only has to be performed once to generate the data, not each time a detector model is run. In both cases, a very high threshold value would be best to use operationally.

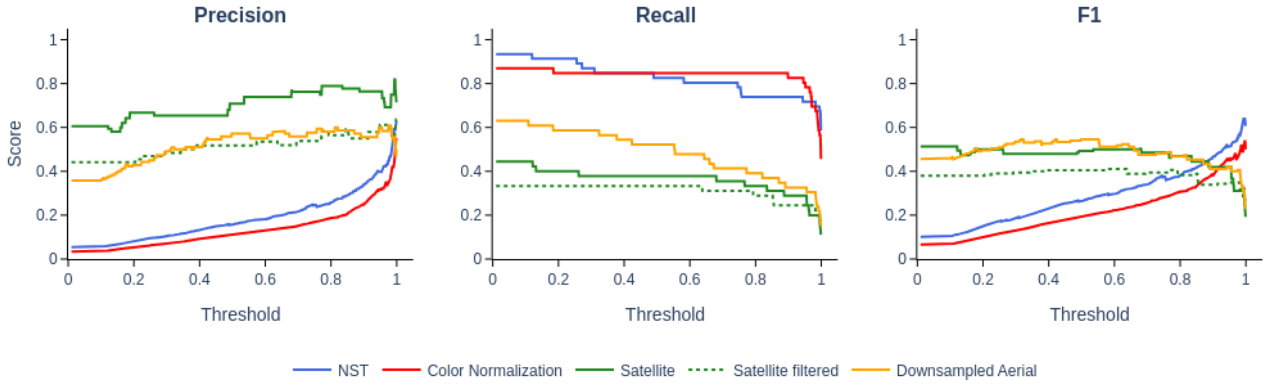

Figure 5.6: Progressive threshold curves, as in Figure 5.5, organized by metric instead of training type.

Table 5.1: Peak F1 score and the corresponding threshold that peak occurs at for each of the four training data methods.

Method	Peak F1	Threshold at Peak F1	Precision at Peak F1	Recall at Peak F1
Downsampled Aerial	0.55	0.423	0.358	0.630
Colour Normalization	0.54	0.997	0.545	0.522
NST	0.64	0.992	0.593	0.696
Satellite	0.51	0.010	0.606	0.434
Satellite Filtered	0.41	0.574	0.536	0.333

5.4 Transferability to Other Sensors

One of the benefits of the NST simulation, and also the colour-normalization method of aerial pre-processing, is the relatively easy transferability to other sensors. Provided that you have an example of a whale observed by the relevant sensor, you can simulate what a whale would look like in that imagery. For instance, Figure 5.7 shows a Pleiades Neo image in Cape Cod Bay, captured on April 9th, 2023, with whale detections shown as yellow dots. The detector used here was trained on a different set of NST images created using a Pleiades Neo whale observation as the style image. As in the results based on the WorldView-2 image, an extremely high threshold of 0.99 also works well for whale detection here, as most of the false-positives are below this threshold.

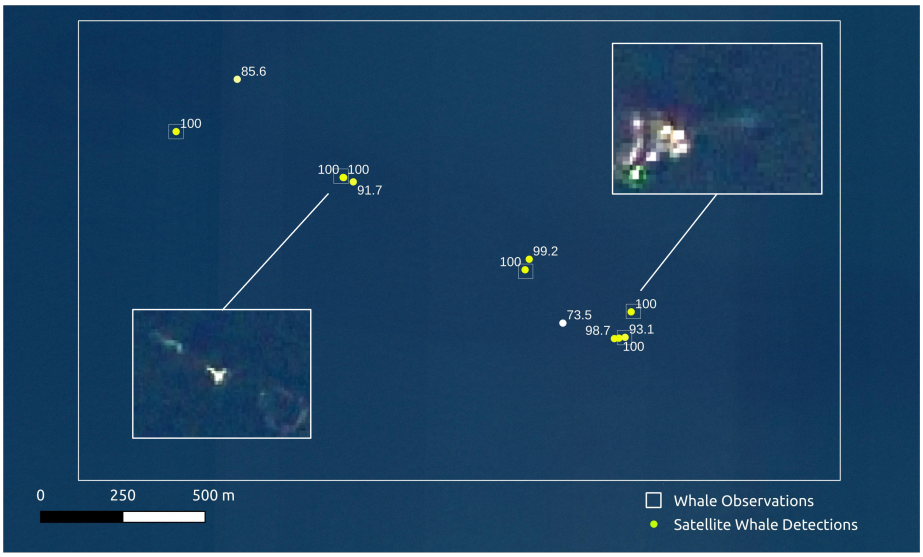

Figure 5.7: Whale detections in a Pleiades Neo image from Cape Cod Bay on April 9th, 2023. Yellow dots indicate detections, white squares indicate actual whale locations, and numbers show the model's whale confidence score. Insets are used to more clearly show the whales in the imagery.

5.5 Discussion

Aside from the model performance differences, there are evident advantages and disadvantages with each type of training data. Conceptually, actual satellite imagery of the target whale species is the best kind of training data, or barring that, imagery of species with a similar appearance. However, the difficulty and especially cost of acquiring such imagery may be prohibitive, which results in a substantially smaller dataset than all other types of training data. A lack of varied examples of whales in the training imagery may lead to whales being missed during detection, because the model may not have been trained on all instances of what a whale may look like. This is shown in the lower recall but higher precision scores seen in the results here. It is important to note here that for the type of human-in-the-loop operations that would be used for right whale detection in an operational context, a high recall is much more desirable than a high precision, since it is considered acceptable for an analyst to sort through and remove false positives while ensuring that no whale goes undetected. Recall values for NST demonstrated in this study are in the same range as those reported for other satellite whale detectors (Davies et al. 2025).

Downsampled aerial photographs, the current non-satellite standard in the field, are typically plentiful, but as demonstrated here, they don't closely resemble satellite imagery, and their use with no preprocessing can worsen model performance. Both NST and colour normalization images improve model performance, with NST being slightly better than colour normalization. Visually,

the NST images do resemble satellite imagery to a greater degree than colour normalization, containing more of the noise and atmospheric effects seen in imagery, and this may be the cause of the small increase in detector performance. Since the NST simulation is only needed to be performed one time, and ensuring right whale safety is of such a high concern, the processing time will likely be acceptable to conservationists intending to train such a model. Regardless of the choice of which to use, it remains clear that using either is better than simply downsampling the imagery, and thus one of these two methods, or a similar preprocessing method, is recommended when developing a whale detector using aerial photographs as the basis for the training data.

This research was limited by the limited testing dataset (one test image under ideal conditions), and so conclusions drawn from these results should be seen as a preliminary exploration into training dataset types, rather than a definitive answer as to which one is best. Confidence bounds on the validation metrics (precision, recall, and F1) are large due to only having 39 test observations of right whales available. While the benefit of using some form of preprocessing on the aerial imagery is large, and so it can be fairly confidently stated that preprocessing is better than not preprocessing, choosing between NST and colour normalization is less clear. The difference in performance between NST and colour normalization is small, and given the small testing dataset, it can't definitively be stated which one would perform better on other test images.

Note that the focus of this work was to compare relative performance of detector models trained with different sets of data, rather than model development and optimization of detector performance. Re-running this comparison on a broader set of images from different locations, and with different environmental conditions, should be an avenue of further research. As such, the research here should be seen as a preliminary exploration of the influence of different training data, and their preprocessing, for satellite whale detection, rather than providing a definitive answer pointing to the best approach. The authors also encourage further research into the use of synthetic (GAN) images for training models.

5.6 Conclusion

Automated detector models used for finding whales in satellite imagery have typically been trained with either downsampled aerial photographs or satellite observations of whales. However, downsampled aerial photographs of North Atlantic right whales don't closely resemble satellite observations, and gathering enough actual observations from satellite imagery to train a model is difficult and expensive. Several methods have been proposed to improve the quality and quantity of training data, including various preprocessing methods intended to make aerial photographs more closely resemble satellite images, as well as the creation of synthetic imagery.

This work compared two of those preprocessing methods, Neural Style Transfer (NST) and colour normalization, against downsampled aerial and satellite

chips, by training detector models on datasets created using each of the methods, and comparing the resultant model performance on a test image of Cape Cod Bay containing known right whale observations. Synthetic imagery was not investigated as part of this study.

The NST method of aerial photograph preprocessing resulted in the best model accuracy, followed by colour normalization. Both of these were significantly better than the un-preprocessed downsampled aerial photographs. The detector trained on satellite imagery chips had excellent precision, but poor recall, suggesting that while the data were of good quality, the relatively small number of available training images limited performance.

Based on the results, it is recommended that, if using aerial photographs for model training, preprocessing should be used to make the photographs look more like satellite imagery; our results show that this will lead to improved model performance. The use of NST-based training data led to a relatively small improvement in model performance compared to colour normalization, while requiring a significantly larger amount of compute resources and time. In an operational setting, this trade-off must be considered when determining the choice of preprocessing method. However, we suggest that considerations of model performance, because of their implications for whale detection and the conservation efforts they contribute to for the endangered North Atlantic right whale, should generally be considered more important than the computing resources required for one-off model training. Further research into other methods of model training, including the use of synthetic images, is recommended by the authors.

5.7 References

Abileah, R. 2002. Marine mammal census using space satellite imagery. U.S. Navy Journal of Underwater Acoustics, 52(3), 709-724.

Bamford, C.C.G., Kelly, N., Dalla Rosa, L., Cade, D.E., Fretwell, P.T., Trathan, P.N., Cubaynes, H.C., Mesquita, A.F.C., Gerrish, L., Friedlaender, A.S., Jackson, J.A., 2020. A comparison of baleen whale density estimates derived from overlapping satellite imagery and a shipborne survey. Sci Rep 10, 12985. https://doi.org/10.1038/s41598-020-69887-y

Borowicz, A., Le, H., Humphries, G., Nehls, G., Höschle, C., Kosarev, V., Lynch, H.J., 2019. Aerial-trained deep learning networks for surveying cetaceans from satellite imagery. PLoS ONE 14, e0212532. https://doi.org/10.1371/journal.pone.0212532

Brodzicki, A., Piekarski, M., Kucharski, D., Jaworek-Korjakowska, J., Gorgon, M., 2020. Transfer Learning Methods as a New Approach in Computer Vision T asks with Small Datasets. Foundations of Computing and Decision Sciences 45, 179–193. https://doi.org/10.2478/fcds-2020-0010

Chen, Y.L., Lin, C.L., Lin, Y.C., and Chen, T.C. 2024. Transformer-CNN for small image object detection. Signal Processing: Image Communication, 129, 117194. https://doi.org/10.1016/j.image.2024.117194

Chollet, F. 2018. Deep Learning with Python. Manning Publication Co. Shelter Island, NY.

Christiansen, F., Dawson, S., Durban, J., Fearnbach, H., Miller, C., Bejder, L., Uhart, M., Sironi, M., Corkeron, P., Rayment, W., Leunissen, E., Haria, E., Ward, R., Warick, H., Kerr, I., Lynn, M., Pettis, H., Moore, M., 2020. Population comparison of right whale body condition reveals poor state of the North Atlantic right whale. Mar. Ecol. Prog. Ser. 640, 1–16. https://doi.org/10.3354/meps13299

Corrêa, A.A., Quoos, J.H., Barreto, A.S., Groch, K.R., Eichler, P.P.B., 2022. Use of satellite imagery to identify southern right whales (Eubalaena australis) on a Southwest Atlantic Ocean breeding ground. Marine Mammal Science 38, 87–101. https://doi.org/10.1111/mms.12847

Cubaynes, H.C., Fretwell, P.T., Bamford, C., Gerrish, L., Jackson, J.A., 2019. Whales from space: Four mysticete species described using new VHR satellite imagery. Marine Mammal Science 35, 466–491. https://doi.org/10.1111/mms.12544

Cubaynes, H.C., Fretwell, P.T., 2022. Whales from space dataset, an annotated satellite image dataset of whales for training machine learning models. Sci Data 9, 245. https://doi.org/10.1038/s41597-022-01377-4

Cubaynes, H.C., Clarke, P.J., Goetz, K.T., Aldrich, T., Fretwell, P.T., Leonard, K.E., Khan, C.B., 2023. Annotating very high-resolution satellite imagery: A whale case study. MethodsX 10, 102040. https://doi.org/10.1016/j.mex.2023.102040

Davies, K.T.A., Brillant, S.W., 2019. Mass human-caused mortality spurs federal action to protect endangered North Atlantic right whales in Canada. Marine Policy 104, 157–162. https://doi.org/10.1016/j.marpol.2019.02.019

Davies, K.T.A., Webster, A., Babu, V., Brillant, S.W., Carlyle, C.G., Lonati, G.L., Sharma, H., Tsui, O.W., 2025. Semi-Automated Detection of Right Whales (Eubalaenaspp.) in Very High-Resolution Satellite Imagery. Marine Mammal Science. https://doi.org/10.1111/mms.70024

Deng, J., Dong, W ., Socher, R., Li, L.-J., Kai Li, Li Fei-Fei, 2009. ImageNet: A large-scale hierarchical image database, in: 2009 IEEE Conference on Computer Vision and Pattern Recognition. Presented at the 2009 IEEE Computer Society Conference on Computer Vision and Pattern Recognition Workshops (CVPR Workshops), IEEE, Miami, FL, pp. 248–255. https://doi.org/10.1109/CVPR.2009.5206848

Fretwell, P.T., Staniland, I.J., Forcada, J., 2014. Whales from Space: Counting Southern Right Whales by Satellite. PLoS ONE 9, e88655. https://doi.org/10.1371/journal.pone.0088655

Gatys, L.A., Ecker, A.S., Bethge, M., 2015. A Neural Algorithm of Artistic Style. Journal of Vision, 16(12). https://doi.org/10.1167/16.12.326

Green, K.M., Virdee, M.K., Cubaynes, H.C., Aviles-Rivero, A.I., Fretwell, P.T., Gray, P.C., Johnston, D.W., Schönlieb, C., Torres, L.G., Jackson, J.A., 2023. Gray whale detection in satellite imagery using deep learning. Remote Sens Ecol Conserv 9, 829–840. https://doi.org/10.1002/rse2.352

Guirado, E., Tabik, S., Rivas, M.L., Alcaraz-Segura, D., Herrera, F., 2019. Whale counting in satellite and aerial images with deep learning. Sci Rep 9, 14259. https://doi.org/10.1038/s41598-019-50795-9

Hausner, A., Samhouri, J.F., Hazen, E.L., Delgerjargal, D., Abrahms, B., 2021. Dynamic strategies offer potential to reduce lethal ship collisions with large whales under changing climate conditions. Marine Policy 130, 104565. https://doi.org/10.1016/j.marpol.2021.104565

Hodul, M., Knudby, A., McKenna, B., James, A., Mayo, C., Brown, M., Durette-Morin, D., Bird, S., 2022. Individual North Atlantic right whales identified from space. Marine Mammal Science mms.12971. https://doi.org/10.1111/mms.12971

Höschle, C., Cubaynes, H.C., Clarke, P.J., Humphries, G., Borowicz, A., 2021. The Potential of Satellite Imagery for Surveying Whales. Sensors 21, 963. https://doi.org/10.3390/s21030963

Karras, T., Aittala, M., Hellesten, J., Laine, S., Lehtinen, J., and Aila, T. Training generative adversarial networks with limited data. 34th Conference on Neural Information Processing Systems (NeurIPS 2020), Vancouver, Canada. https://doi.org/10.48550/arXiv.2006.06676

Khan, C.B., Shashank, W.K. (2015). Right Whale Recognition. https://kaggle.com/competitions/noaa-right-whale-recognition

Pettis, H.M. and Hamilton, P.K. 2025. North Atlantic Right Whale Consortium 2024 Annual Report Card. Report to the North Atlantic Right Whale Consortium.

Rodofili, E.N., Houegnigan, L., Lecours, V., Klarenberg, G., Cuesta, E., 2025. Automated detection of migrating Gray whales and measurement of their bearing in satellite imagery. Marine Mammal Science 41. https://doi.org/10.1111/mms.13213

Russakovsky, O., Deng, J., Su, H., Krause, J., Satheesh, S., Ma, S., Huang, Z., Karpathy, A., Khosla, A., Bernstein, M., Berg, A. C., and Fei-Fei, L., 2015. ImageNet Large Scale Vi-

sual Recognition Challenge. International Journal of Computer Vision, 115(3):211–252. doi: 10.1007/s11263-015-0816-y.

Stewart, J.D., Durban, J.W., Knowlton, A.R., Lynn, M.S., Fearnbach, H., Barbaro, J., Perryman, W.L., Miller, C.A., Moore, M.J., 2021. Decreasing body lengths in North Atlantic right whales. Current Biology 31, 3174-3179.e3. https://doi.org/10.1016/j.cub.2021.04.067

Chapter 6

Conclusion

The North Atlantic right whale, a critically endangered baleen whale living off the eastern coast of North America, is of particular interest to conservationists and scientists due to its extremely low numbers (only around 372 are left alive), public awareness of their plight, and the political, cultural, and economic pressures surrounding their interactions with humans. One of the critical difficulties in rehabilitating the right whales has been knowing their locations at any given time, since much of the conservation efforts centre around dynamically altering protected zones, slowing or diverting shipping around known locations, and closing fisheries when the whales are nearby.

Established survey methods, including aerial and shipborne surveys, and acoustic monitoring, are extremely accurate at pinpointing whale location, but they are costly and resource-intensive to implement and can only cover relatively small areas. To provide wider coverage at a reasonable cost, satellite imaging has been proposed as another method, complementary to these conventional survey methods, allowing for much larger swaths of ocean to be monitored in a short period of time, albeit at reduced accuracy owing to the limitations of the platform (resolution, cloud cover, atmospheric effects, and lower signal-to-noise ratio).

When work began on this thesis, which started with the writing of a funding proposal in late 2019, the field of satellite whale detection was just getting off the ground. There were a few papers out, showing examples of whale detection in satellite imagery, but, at the time, there were none where detections were confirmed using concurrent aerial survey, and the North Atlantic right whale had yet to be observed at all in satellite imagery. During the writing of this thesis, the field accelerated, with many papers and other contributions coming out between 2020 and 2025, including major working groups and seminars at key conferences, such as the Conference on the Biology of Marine Mammals in Perth in 2024. The work which I have presented in this thesis documents some of the key developments in the field during this time, foremost of which is the first confirmed satellite observations of the North Atlantic right whale. The overall goal of this thesis was to investigate the feasibility of detecting North Atlantic

right whales in satellite imagery, and if so, develop an automated method of detecting them in the imagery.

The first step was to attempt to make the first ever satellite observations of the whales, and at the same time have the observation occur during a planned aerial survey by the Center for Coastal Studies, which would be a first in the whale detection field. On April 24$^{\text{th}}$ 2021, on a day when the ocean was very calm and numerous right whales were present in Cape Cod Bay, a series of three satellite images were captured by the WorldView-3 satellite while, at the same time, the aerial survey team was making observations of what would end up being a staggering 80 right whales, which at the time, was nearly one quarter of the entire living population (there having been an estimated 340 right whales in 2021). Since some of the whales observed by the aerial team were under water at the time of satellite overpass, and due to budgetary constraints limiting us to the amount of imagery we were able to purchase, not all of these whales were observed in the satellite imagery; yet still, an impressive 31 right whales were visible in our imagery —nearly 10% of the entire population in one satellite image. Coincidentally, April 24$^{\text{th}}$ would go on to become Massachusetts's official 'Right Whale Day' a few years later.

As luck would have it, the imagery was captured at the *exact* same moment as the survey team was making an observation of the right whale named Halo, giving us the fantastic Figure 3.5 showing Halo and the survey aircraft right next to each other in the satellite imagery. These results allowed us to conclude that North Atlantic right whales were indeed possible to observe in satellite imagery, and further, that they could be identified on a species level based on body markings visible in the imagery, which would be important when making conservation decisions based on their observation. We were also able to identify one whale by name, 'Ruffian' based solely on the extremely large and distinct markings on his back, visible in the satellite imagery.

The second step was to develop an automated detector model. It was immediately clear that the number of right whale observations that we had (39 instances of right whales in satellite imagery —some were captured twice in the span of a few seconds because of swath overlap) would not be sufficient to train a model. Looking to the literature, we saw that the few detector models which had been developed up to that point were trained on aerial photographs, with no preprocessing applied save for downsampling them to satellite resolution.

Any model that uses training data to learn to detect a specific type of object in imagery necessarily learns to detect such objects *as they are presented in the training data*. This means that both the object characteristics (e.g. diving whale vs. whale at the surface) and the imaging modality (e.g. oblique vs. nadir imaging) influence the model's ability to recognize new instances of those objects. As a result, the training data should contain the full range of object characteristics that the model is expected to detect, and those objects should be imaged with the same modality that the model will be applied to for detection. This was a fundamental problem for our work, because existing satellite imagery was limited in quantity and not expected to cover the full range of whale poses and environmental contexts necessary, while a substantial difference exists

between the aerial photographs and satellite imaging modalities, as is obvious when comparing imagery from those two sources.

With the hope that it would improve detector accuracy, we therefore decided to apply some preprocessing to the aerial photographs that we had, before using them as training data, with the goal of making them more similar to the satellite imagery the model would ultimately be applied to for whale detection. At the time, we thought that simulation of satellite imagery from aerial photographs was likely a solved problem because of the somewhat generic nature of the problem (not isolated to use in whale detection), but we discovered that no standardized methods were available to conduct the necessary image processing. Several options were considered, including a physics-based atmospheric 'de-correction' simulating what the aerial photographs would have looked like if the camera had been in space, with the atmosphere in between the sensor and the target; this proved to be quite complicated since we had no metadata for much of the aerial photographs which we had access to.

At some point around this time, the idea struck that trying to make an aerial photograph resemble a satellite image was not too dissimilar to making a photo look like a painting (in essence, reducing the quality in a very specific way), which is where the idea to use Neural Style Transfer began, NST being most commonly represented as a fun way to make pictures look like they were painted by Van Gogh.

Critically, to make a comparison between aerial 'simulated' satellite imagery and actual satellite imagery of right whales, we needed a dataset of aerial-satellite pairs. We developed this dataset of pairs from the aerial survey photos acquired by CCS on that now-famous April 24$^{\text{th}}$ 2021 survey. Implementation of the NST was subsequently fairly straightforward. Using two image similarity metrics, one which measures colour similarity and another which measures shape similarity, we demonstrated that running NST incrementally on the aerial photos resulted in a corresponding incremental improvement in image similarity between each NST-modified aerial photograph and its satellite observation pair. While conceptually a simple task, the real strength of this part of the research were these carefully curated image pairs, which allowed us to directly see the improvements in the similarity between NST simulated images and satellite observations.

The final aspect of the research was to compare this newly developed NST dataset to the types of datasets currently used in the satellite whale detection field to train models: downsampled aerial and satellite images themselves. On the suggestion of a reviewer for the NST paper (Chapter 4), we also included a simpler preprocessing method, colour normalization, in the comparison. We discovered that colour normalization and NST both improved detector performance over simple downsampled aerial, with NST providing just slightly better results than colour normalization, leading to the recommendation that if using training data based on aerial photographs, it is beneficial to first apply some preprocessing step to get the aerial photos to more closely resemble actual satellite imagery.

Because of the rather small difference in performance, the choice of which

preprocessing step to use, between NST and colour normalization, can be left to the end-user to decide based on needs, and willingness and computer resources to implement the lengthy NST simulation process. The model trained on a relatively small amount of satellite imagery saw far better precision, but far worse recall, than the two preprocessing methods, which is to be expected of a high-quality but small dataset. We also suggested that investigating the use of synthetic images of whales for training, such as those produced using a GAN, would be a beneficial avenue of research; a method for creating such images hasn't yet been put forth, and we decided it was out of scope for this research.

Conclusions drawn from these final results were limited by the small amount of test data available, however. It is important to note that the results shown here apply to one test image, in an ideal location under ideal environmental conditions, and that results may differ under different conditions. Indeed, under different conditions, it is possible that NST may not be better than colour normalization. Despite this, it is still very likely that performing some form of preprocessing on aerial photographs before using them for training is better than not doing so, and that having a large number of simulated training data is better than a small number of actual satellite observations.

Overall, the work done in the five years it took to put together this thesis spanned during the years in which some of the fastest progress on satellite whale detection has been made. And, while this thesis represents only a small piece of that larger effort, carried out by a great number of researchers all over the world, many of whom I had the pleasure of meeting in Perth in November of 2024, I believe that it represents a key element of that larger effort. We demonstrated the first ever observation of a North Atlantic right whale in satellite imagery, the first identification of a named individual from satellite imagery based solely on body markings, and the first aerial survey concurrent with satellite observations of whales. We proposed a new method for simulating satellite imagery from aerial photographs, and explained why this might be important in the effort to build automated whale detectors. We tested these new simulated images against other forms of data typically used to train satellite whale detectors, and while it turned out that our new method didn't result in revolutionary new-and-improved model performance, we did show that it was an improvement on existing methods and that preprocessing aerial photos before using them in training satellite detectors is important.

Despite the rapid acceleration in the past five years, the field of satellite whale detection remains in its early years. Still to come will be the study showing us how to train a model using synthetic images (and achieve good performance), the first use of this technology in earnest by the Canadian government, the first right whale saved by a satellite detection, and perhaps even the first evidence of a sustained recovery of the population of the North Atlantic right whale.

Appendix A

Below are all observations from the WorldView-3 imagery from Cape Cod Bay acquired on April 24th 2021, including both the 30 cm pansharpened imagery (left), and the 15 cm HD imagery (middle). Also included are the aerial photographs (right) considered 'reference pairs' to each satellite observation (see Chapter 4). All satellite imagery © 2022 Maxar. All aerial photographs: Center for Coastal Studies NOAA federal permit #19315-01.

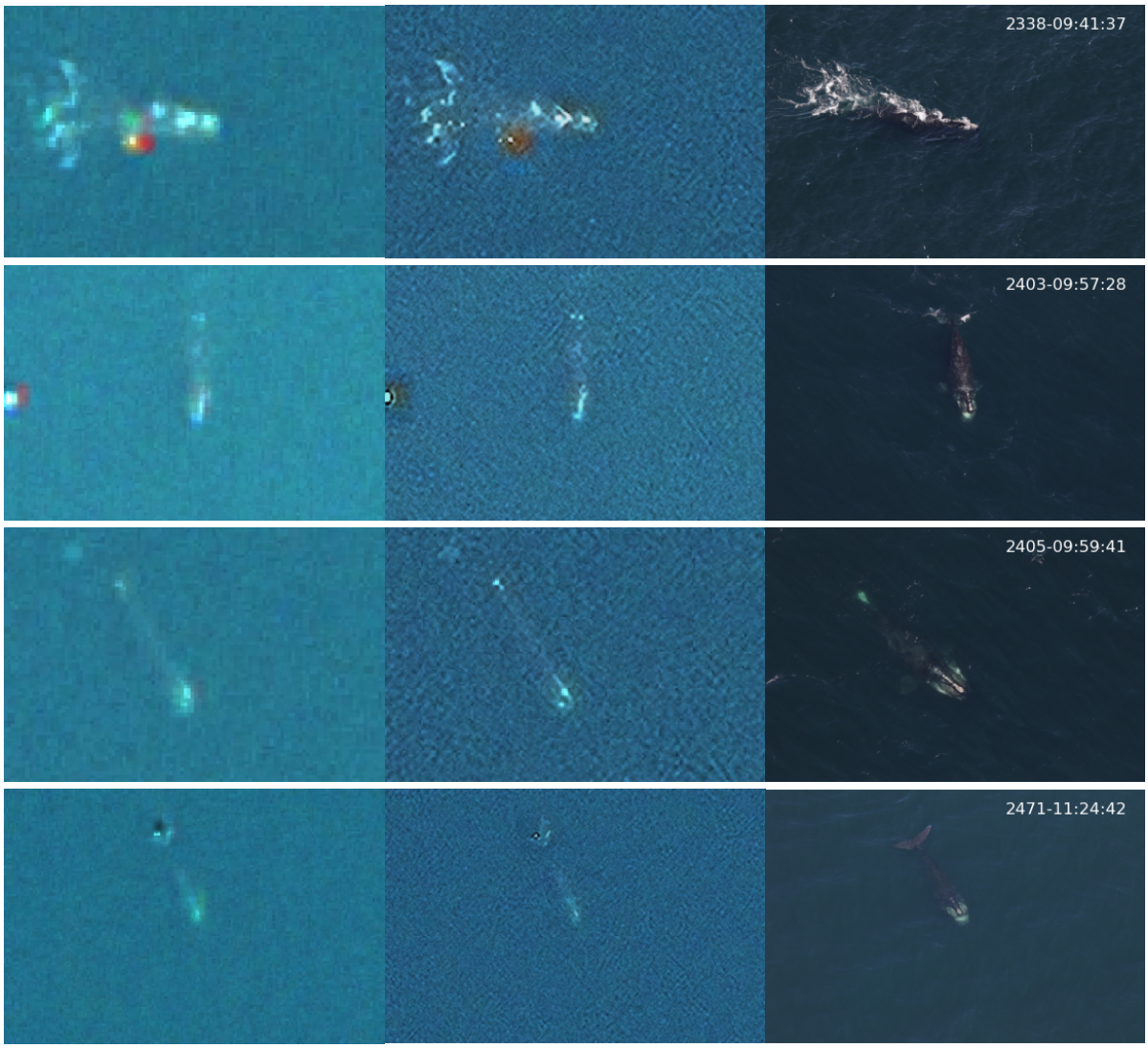


2504-11:39:22
2516-11:39:41
2517-11:39:42
2597-12:05:45
2639-12:10:15


2640-12:10:17
2649-12:10:48
2787-12:31:08
2803-12:32:44
2832-12:34:13


2837-12:34:21
2855-12:35:42
2856-12:35:43
2861-12:36:29
2862-12:36:30

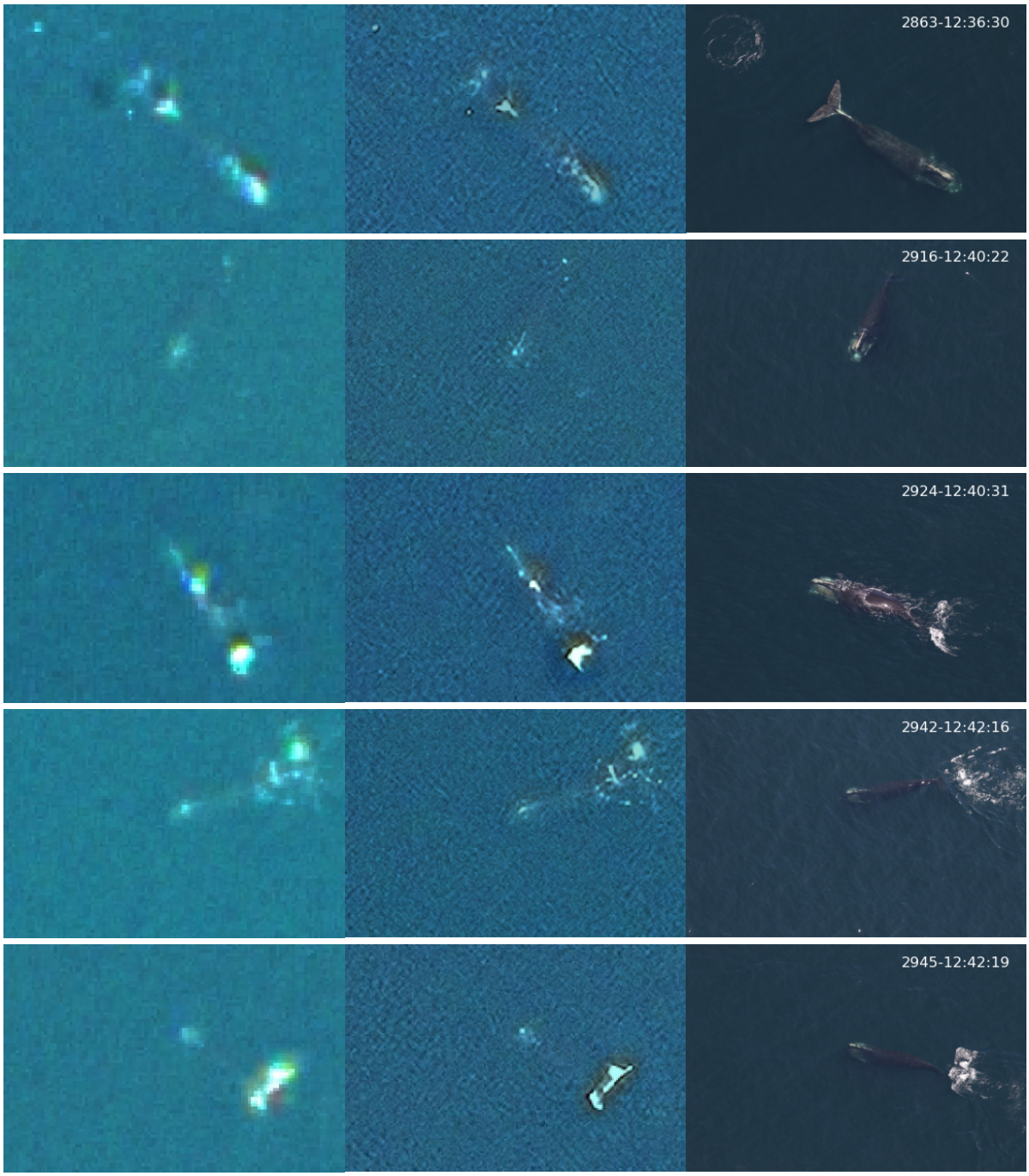
2863-12:36:30
2916-12:40:22
2924-12:40:31
2942-12:42:16
2945-12:42:19


2948-12:42:22
2979-12:53:30
3057-13:00:11
3114-13:19:47
3162-13:26:17


3181-13:33:03
3188-13:36:19
3244-13:54:01
3246-13:54:04
3257-13:55:41


3261-13:56:07
3286-14:06:32
3341-15:11:10
3374-15:15:11
3443-15:21:15